Technical Report Documentation Page

1. Report No. FHWA/TX-09/0-5218-1	2. Government Accession No.	3. Recipient's Catalog No.
4. Title and Subtitle Investigation of the Internal Stresses Caused by Delayed Ettringite Formation in Concrete		5. Report Date November 2008 6. Performing Organization Code
7. Author(s) Bedford Burgher, Arnaud Thibonnier, Dr. Kevin J. Folliard, Tyler Ley, Dr. Michael Thomas		8. Performing Organization Report No. 0-5218-1
9. Performing Organization Name and Address Center for Transportation Research The University of Texas at Austin 3208 Red River, Suite 200 Austin, TX 78705-2650		10. Work Unit No. (TRAIS) 11. Contract or Grant No. 0-5218
12. Sponsoring Agency Name and Address Texas Department of Transportation Research and Technology Implementation Office P.O. Box 5080 Austin, TX 78763-5080		13. Type of Report and Period Covered Technical Report 12/1/2004 – 8/31/2008 14. Sponsoring Agency Code
15. Supplementary Notes Project performed in cooperation with the Texas Department of Transportation and the Federal Highway Administration.		

16. Abstract

Delayed ettringite formation (DEF) in concrete has been identified in recent as a significant cause of deterioration in some of the reinforced concrete infrastructure in Texas. This report is part of a research project, TxDOT project 5218, to investigate the possible long-term structural and durability related effects of DEF in such structures. The focus of this particular report is the determination of the internal stresses caused by DEF which at this point in time are not known. The research presented here began by first looking at past and recent research involving concrete deterioration due to alkali-silica reaction (ASR) and discussing the results of a comparative study between DEF and ASR affected concrete with different dosages of steel fibers to provide restraint. The study then went on to directly study the stresses caused by DEF in a new testing methodology that was developed using a Hoek tri-axial load cell to provide a direct measurement of the confining stress necessary to stop DEF induced expansion. In addition to the steel fiber and Hoek cell testing, reinforced concrete elements were made to study the structural effects of DEF. Lastly, a series of tests performed at the University of New Brunswick were performed to assess the stresses generated by DEF and the requisite levels of confinement needed to resist these stresses. The following report outlines the process, results, and lessons learned from the conducted tests.

17. Key Words	18. Distribution Statement
DEF, delayed ettringite formation, Hoek	No restrictions. This document is available to the public through the National Technical Information Service, Springfield, Virginia 22161; www.ntis.gov.

19. Security Classif. (of report)	20. Security Classif. (of this page)	21. No. of pages	22. Price
Unclassified	Unclassified	114	

Form DOT F 1700.7 (8-72) Reproduction of completed page authorized

Investigation of the Internal Stresses Caused by Delayed Ettringite Formation in Concrete

Bedford Burgher
Arnaud Thibonnier
Kevin J. Folliard
Tyler Ley
Michael Thomas

CTR Technical Report:	0-5218-1
Report Date:	November 2008
Project:	0-5218
Project Title:	Extending Service Life of Large or Unusual Structures Affected by Concrete Deterioration
Sponsoring Agency:	Texas Department of Transportation
Performing Agency:	Center for Transportation Research at The University of Texas at Austin

Project performed in cooperation with the Texas Department of Transportation and the Federal Highway Administration.

Center for Transportation Research
The University of Texas at Austin
3208 Red River
Austin, TX 78705

www.utexas.edu/research/ctr

Disclaimers

Author's Disclaimer: The contents of this report reflect the views of the authors, who are responsible for the facts and the accuracy of the data presented herein. The contents do not necessarily reflect the official view or policies of the Federal Highway Administration or the Texas Department of Transportation (TxDOT). This report does not constitute a standard, specification, or regulation.

Patent Disclaimer: There was no invention or discovery conceived or first actually reduced to practice in the course of or under this contract, including any art, method, process, machine manufacture, design or composition of matter, or any new useful improvement thereof, or any variety of plant, which is or may be patentable under the patent laws of the United States of America or any foreign country.

Engineering Disclaimer

NOT INTENDED FOR CONSTRUCTION, BIDDING, OR PERMIT PURPOSES.

Project Engineer: David W. Fowler
Professional Engineer License State and Number: Texas No. 27859
P. E. Designation: Researcher

Acknowledgments

The research team greatly appreciates the financial support from the Texas Department of Transportation (TxDOT) that made this project possible. The research team would like to acknowledge the technical support provided by the TxDOT Project Director, Program Coordinator, and Project Monitoring Committee Members. Lastly, the team greatly appreciates the hard work and dedication of the Concrete Durability Center staff members who assisted on this project.

Table of Contents

List of Figures

List of Tables

Chapter 1. Introduction

A great deal of research has been conducted to identify, as well as understand the mechanisms of alkali-silica reaction, ASR, and delayed ettringite formation, DEF, in concrete structures. ASR and DEF are culprits causing durability issues in concrete structures around the globe. Both ASR and DEF can be avoided if proper measures are in place during mixing and curing, and much research has been conducted in identifying methods of avoiding such problems. However, a number of questions remain; particularly the question of rehabilitating a structure that is in service that is showing signs of ASR or DEF distress. A number of methods have been implemented in an effort to stop the chemical reactions from occurring in the first place; however, doing so after the reactions have begun has not received the attention in the research or practitioner arenas that it deserves – this is the focus of this study and report.

The idea of external mechanical confinement is under investigation because, if successful, it will provide designers the ability to economically rehabilitate concrete structures and subsequently prolong the service life of those structures. Fiber-reinforced plastics wraps, post-tensioning and steel jacketing are all methods of externally rehabilitating concrete structures; however, the use and success of each individual method is beyond the scope of this report. This report concentrates on the means of quantifying the stresses that are generated by DEF affected concrete and providing that information to designers for the rehabilitation of concrete structures in the field.

Chapter 2. Literature Review

This chapter briefly discusses the mechanisms of DEF and mechanical confinement testing conducted on specimens affected by ASR. There have been a number of projects dealing with the effects of mechanical confinement on ASR; however, there has been little to no work conducted on the effects of mechanical confinement on DEF. Much of the literature to date on mechanical confining methods has examined ASR only, and therefore this project has examined specimens affected by ASR, DEF, and a combination thereof.

2.1 Mechanisms of DEF

In simple terms, DEF is defined as the formation of ettringite after the concrete has hardened (Taylor et al. 2001). Normally, ettringite forms during the curing process where the concrete is still plastic and can accommodate the growth of ettringite without cracking. The seeds for DEF-induced distress are planted when the heat of hydration is so high that ettringite becomes unstable, leading to incongruous dissolution and the "trapping" of aluminate and sulfate ions in rapidly forming calcium silicate hydrates (C-S-H). Subsequent long-term exposure to moist environments leads to the release of these aluminate and sulfate ions, which then react with monosulfate compound to form ettringite. However, formation of ettringite in small pores in hardened concrete cannot be accommodated by the rigid microstructure, and expansion and subsequent cracking results.

Previous literature strongly suggests that DEF occurs in steam cured concrete that has been cured at excessive temperatures. However, a number of DEF cases in non-steam cured concrete have been reported (Diamond 1996; Thomas et al., 2008). This is of particular importance to structures in Texas because during the summer months the ambient mid-day temperatures are elevated enough to exacerbate the internal temperatures that occur in mass pours, thus making DEF a legitimate concern.

DEF can easily be prevented through proper material selection and construction operations. Keeping curing temperatures below 158 F will ensure that DEF will not occur. Using sufficient dosages of suitable SCMs can also prevent DEF, even if excessive temperatures (greater than 158 F) are encountered (Folliard et al., 2006). It is much more difficult to mitigate DEF in existing concrete structures. One potential method is to reduce access to moisture through improved drainage or through the application of waterproofing sealers or coatings (e.g., coatings). Another method, which is the topic of this report, is to confine the expansions triggered by DEF. This is discussed next.

2.2 Mechanical Confinement

Turanli showed that the addition of micro steel fibers, MSF, to mortar was able to reduce the effects of ASR (Turanli et. al. 2001). The experiment used a mortar composition known to exhibit large expansions due to ASR and included various doses of MSF ranging from zero to seven percent by volume. The experiments showed that each increase in dosage of MSF was able to effectively reduce the overall expansion of the mortar specimens. Prior to the current TxDOT project, there was no previous reported testing on the effects of steel fibers on DEF. Chapter 3 discusses the fiber restraint tests that were conducted to examine the effects of internal restraint on DEF and to provide a direct comparison between specimens affected by ASR and DEF.

Multon showed that the application of an axial load was effective in reducing the strain experienced by ASR (Multon et al. 2005). In his experiments specimens were subjected to various axial loads for 450 days and the resulting strains were plotted over time. He observed that the increase in axial load reduced axial strains, however, increased lateral strains as one would expect due to Poisson's ratio. As a follow-up to Multon's work, the current project examined the effects of tri-axial states of stress on specimens affected by DEF. The tri-axial testing is further discussed in Chapter 4 of this report.

Multon also examined the effects of ASR on reinforced concrete beams (Multon et al. 2005). He showed that reinforcement on ASR induced strains in the longitudinal direction was significant; however, reinforcing stirrups were insignificant in reducing transverse deformations and strains (Multon et al. 2005). Chapter 5 and 6 of this report examine the effects of DEF on reinforced columns subjected to axial loads. The specimens used in Chapters 5 and 6 of this report attempt to compare the findings found by Multon for ASR affected structures and see if any similarities exist with structures affected by DEF.

Sahu examined the deterioration experienced by railroad ties and discovered that DEF was the primary culprit of the premature deterioration of the ties (Sahu et al. 2004). The ties were steam cured at elevated temperatures; however, what was observed was that DEF occurred at lower than expected DEF curing temperatures. Sahu suggests that other factors such as high cement content, high alkali content, high sulfate content, high magnesium oxide content in the cement and high reactivity of the ferrite phase in the cement are responsible for a lower than normal DEF curing temperature.

The above discussion briefly highlights some of the research performed to date on ASR and DEF as it relates to stress and strain generation; unfortunately, there is a general shortage of information in literature with regard to the requisite confinement needed to control ASR and essentially no published work on the levels of confinement needed to control DEF. It is hoped that the work described in this report will help to address some of the inherent shortcomings in published literature.

Chapter 3. Evaluation of Steel Fibers for Internally Confining ASR and/or DEF

The use of steel fibers in ASR affected concrete has been shown to significantly reduce levels of expansion, as discussed in section 2.2. Although it is difficult to derive an exact value of internal restraint from the use of steel fibers, their use does provide a simple method of qualitative comparison. Since at this point in time there is a fair amount of research on the internal stresses generated by ASR but none on those due to DEF, a test using steel fibers presents a simple method of comparing the level of restraint necessary to slow or stop ASR and that necessary to slow or stop DEF. Therefore a test was done to monitor the level of expansion of different concrete mixes affected by ASR, DEF and a combination of both, with various dosages of steel fibers.

3.1 Test Setup

3.1.1 Materials

Concrete cylinders measuring 4 inches in diameter by 8 inches in height were initially made from two different concrete mixes. A third mix was cast later on to support the findings from the first reactive mix as well as investigate a modification of the heat curing cycle. This difference will be discussed later in this report. The "non-reactive" or NR mix consisted of a fine aggregate that is non-reactive for ASR in ASTM C 1260 testing (Drimalas 2004). Both "reactive," RA1 and RA2, mixes included siliceous sand that is reactive for ASR (Drimalas 2004). All mixes consisted of a non-siliceous coarse aggregate and Type III Portland cement. The mixes were also "doped" with sodium hydroxide solution to bring the sodium hydroxide (NaOH) equivalent to 1.25% by mass. Table 3.1 lists the various mixes with their constituent materials.

Table 3.1: Concrete Mix Proportions and Materials

NR Mix		RA1 Mix		RA2 Mix	
lbs/yd^3	Material	lbs/yd^3	Material	lbs/yd^3	Material
800	Cement *PC - Type III*	800	Cement *PC - Type III*	800	Cement *PC - Type III*
1390	Coarse Aggregate *¾" crushed limestone*	1390	Coarse Aggregate *¾" crushed limestone*	1500	Coarse Aggregate *tan dolomite limestone*
1395	Fine Aggregate *manufactured limestone sand*	1450	Fine Aggregate *mixed quartz/feldspar siliceous sand*	1287	Fine Aggregate *mixed quartz, chert, feldspar sand*
0.36	w/c	0.36	w/c	0.36	w/c

A high water reducing admixture (HWRA) was used for all three concrete mixes to create highly flowable concrete with initial slumps between 9 and 11 inches, into which high dosages of

fibers could be mixed. The fibers used were hooked steel fibers 1.188 inches long by 0.022 inches in diameter (aspect ratio of 55).

3.1.2 Testing Matrix

A total of 32 concrete cylinders were cast from each of the NR and RA1 mixes. A total of 72 concrete cylinders were cast from the RA2 mix. Half of the NR and RA1 cylinders, 16 each, were held at elevated temperatures during curing, while the other half cured at 72ºF. A third of the RA2 cylinders, 24 cylinders, cured at 72ºF while the rest, 48 cylinders, were held at elevated temperatures during curing. Eight cylinders were cast for each of the four dosages of steel fibers for the NR and RA1 mixes. Eighteen cylinders were cast for each of the four dosages of steel fibers for the RA2 mix. The dosages of steel fibers were 0% (no fibers), 0.5%, 1.0%, and 1.5% by volume. After curing and placement of demec points for measurements, the cylinders were placed in one of two different storage environments. Table 3.2 summarizes the testing matrix for all of the fiber reinforced mixes.

Table 3.2: Testing Matrix

Fiber dosage by volume %	NR Concrete Mix		RA1 Concrete Mix		RA2 Concrete Mix	
	Non-Heat Cured	Heat Cured	Non-Heat Cured	Heat Cured	Non-Heat Cured	Heat Cured
0.00%	3 (L) + 1 (A)	3 (L) + 1 (A)	4 (A)	4 (A)	6 (A)	6 (A) + 6 (L)
0.50%	3 (L) + 1 (A)	3 (L) + 1 (A)	4 (A)	4 (A)	6 (A)	6 (A) + 6 (L)
1.00%	3 (L) + 1 (A)	3 (L) + 1 (A)	4 (A)	4 (A)	6 (A)	6 (A) + 6 (L)
1.50%	3 (L) + 1 (A)	3 (L) + 1 (A)	4 (A)	4 (A)	6 (A)	6 (A) + 6 (L)

(L) = Limewater storage, (A) = Above water in sealed container at 100°F

3.1.3 Concrete Mixing

The concrete mixes were mixed in a six cubic foot drum mixer and according to the guidelines of ASTM C 1293 for mixing of concrete. During mixing, the steel fibers were progressively added to the same batch of concrete. After the batch of concrete had been appropriately mixed in the drum-mixer, enough concrete was removed to cast the 0% fiber cylinders. The amount of concrete removed from the drum-mixer was weighed to determine the amount of concrete still left in the mixer so that steel fibers equivalent to 0.5% by volume of the concrete still left in the drum could be added. This process was repeated for each 0.5%, 1.0% and 1.5% steel fiber concrete. Through this process of subtracting the necessary concrete and then adding steel fibers to the remaining concrete, we were able to cast cylinders for all four steel fiber dosages from the same batch of concrete for all mixes.

3.1.4 Curing Treatment

The heat-cured cylinders were placed in an oven approximately 1 hour after casting. The temperature of the oven was then raised from 72^{o}F to 203^{o}F over one hour according to the Fu regime[2] for accelerating DEF in concrete. After 18 hours the cylinders were removed from the oven, demolded, and placed in a water bath. After 6 hours in the water bath the de-molded

cylinders were again placed in the oven for the heat-drying phase of the Fu Method. This extreme drying event is done to trigger micro-cracking in the concrete and thereby accelerate the time to expansion in the test. Figure 3.1 illustrates the Fu cycle. The non-heat cured cylinders remained in a controlled 72°F room and were demolded after approximately 24 hours.

The NR and RA1 mixes were subjected to the Fu regime and heat-drying phase. It was later suspected that the heat-drying phase pre-engaged the fibers due to the micro-cracking. Thus the RA2 mix was subjected to the Fu regime without the heat-drying phase in order to capture the expansion prior to the engagement of the fibers.

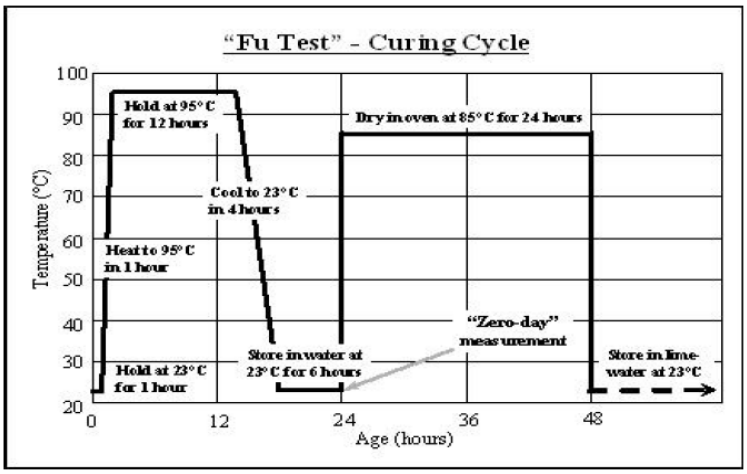

Figure 3.1: Fu curing cycle for DEF (Thomas 2003)

3.1.5 Demec Gauge, Gauge Pins and Measurements

To measure the expansion of the cylinders, two sets of demec points were glued to opposite sides of a cylinder using a ceramic epoxy. The gauge length between the demecs is approximately 5.9 inches (150mm). A digital demec gauge with a precision of ±0.00005 inches was used to measure the sets of demec points. The NR and RA1 mixes were measured by the surface laid demec points. Over time the demec points were prone to falling off and therefore the RA2 mix were measured by utilizing end placed gauge pins. The ends of the RA2 cylinders were drilled for the placement of gauge pins that were also glued to the cylinders by the above mentioned ceramic epoxy. These cylinders were measured by the use of an 8 inch comparator with a precision of ±0.0001 inches.

Measurements of the NR and RA1 cylinders began three days after the cylinders were cast. Measurements for the RA2 cylinders began seven days after the cylinders were cast because the drilling of the ends proved to be more difficult than expected. The first measurements were taken prior to placing the cylinders in their storage environment. At the time of the first measurements the cylinders had been in a 72°F room at 50% RH for 2 days. Therefore some of the initial expansion recorded reflects water gain of the cylinders once they were placed in storage. Measurements were done every week for the first few months and then every two weeks thereafter.

3.1.6 Storage

The cylinders were stored in one of two storage environments. Most of the cylinders from the NR and some of the RA2 mix were stored in a limewater bath with a volumetric ratio of water to concrete of approximately 3.5. The limewater bath remained at room temperature or about 75°F. All of the RA1, most of the RA2 and some of the NR mix cylinders were stored in sealed five gallon buckets seated above approximately one inch of water and placed inside a 100°F chamber. Each sealed bucket contained four concrete cylinders. The above water at 100°F storage setup is similar to that used for ASTM C 1293.

3.2 Expansion Measurements

To measure the cylinders stored in sealed buckets above water, the buckets were first removed from the 100°F oven a day prior so the cylinders could cool to about room temperature prior to measuring. The cylinders stored in the limewater bath were removed from the bath and allowed to dry for about 10 minutes prior to measuring. Occasionally it was found that discovered that a demec point had been knocked loose from a cylinder and a measurement would be missed. When this happened the demec was immediately re-glued to the cylinder. The missed expansion data was estimated by calculating an assumed strain gradient based on an average of the strain rates immediately before and immediately after the demec was lost. This method produced reasonably accurate estimates with a maximum observed error of about ±0.02% per reset value.

3.2.1 Expansion Measurements: NR Concrete Cylinders

Figure 3.2 shows that the NR mix cylinders that were non-heat treated showed no significant levels of expansion, about 0.05% or less. Since the concrete was not heat cured and did not contain siliceous aggregates, one would not expect any significant expansion to occur.

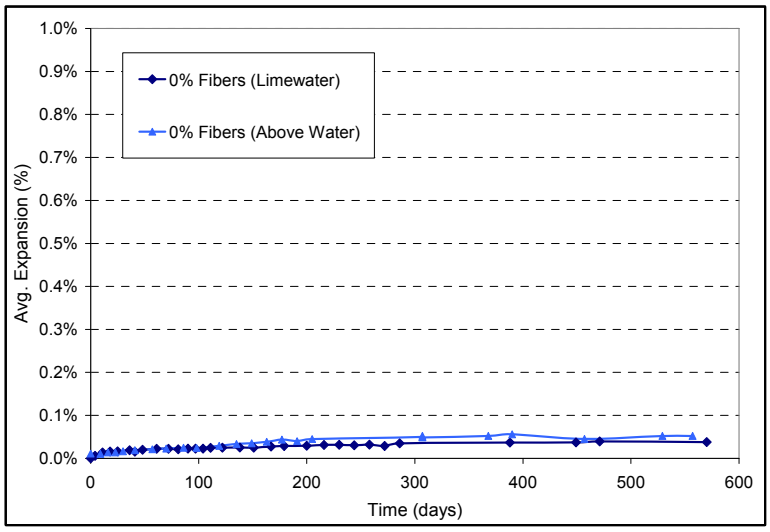

Figure 3.2: Expansion of non-heat cured NR Mix cylinders

However, the heat cured cylinders did show high levels of expansion as illustrated in Figures 3.3 and 3.4. The cylinders without steel fibers (0% fibers) expanded about 1.0% and 0.4% in limewater and above water, respectively.

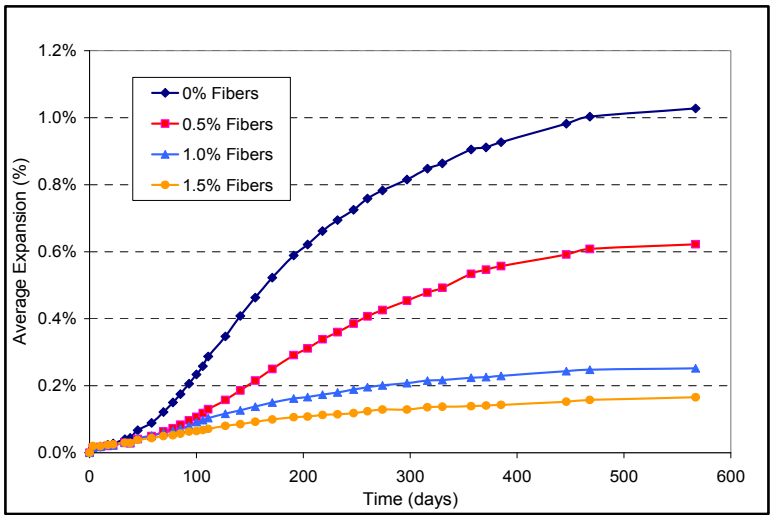

Figure 3.3: Expansion of heat cured NR Mix cylinders stored in limewater solution

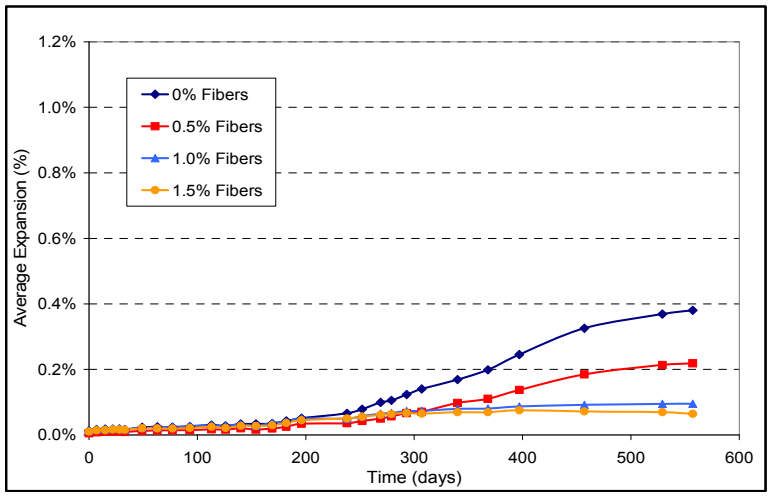

Figure 3.4: Expansion of heat cured NR Mix cylinders stored above water at 100°F

The higher level of expansion observed with the cylinders stored in limewater over those stored above water seems to indicate how the level of saturation drives the level of DEF expansion. In addition the delayed expansion of the above water cylinders versus the early expansion of the limewater cylinders could be an indication of how leaching of alkalis and the subsequent lowering of pore solution pH within the concrete can be an important factor in the triggering of DEF. High pH favors the presence of monosulfate rather than ettringite (Taylor et al 2001), so a concrete with a high initial pore solution pH must undergo alkali leaching to drop the pH before DEF will initiate. Since a limewater bath would lead to a more rapid leaching of alkalis from the concrete, this could be a plausible explanation for the difference of DEF initiation in the two environments. Most importantly Figures 3.3 and 3.4 indicate a strong

correlation between the dosage of steel fibers and the reduction in DEF induced expansion. The measurements show that DEF induced expansions can be restrained by the use of steel fibers and provide potentially useful information for comparing DEF and ASR.

Table 3.3 shows the level of variability in expansion measurements between cylinders of similar fiber dosage. There was only one cylinder per fiber dosage kept above water at 100°F so no measure of variability could be determined.

Table 3.3: Heat Cured NR Mix: Final Average Expansion and Variability

Fiber Dosage	LIME WATER		ABOVE WATER	
	Final Average Expansion	Standard Deviation	Final Average Expansion	Standard Deviation
0.0%	1.03%	0.14%	0.38%	*Only one cylinder was measured per fiber dosage so no level of variability could be determined.
0.5%	0.62%	0.08%	0.22%	
1.0%	0.25%	0.06%	0.10%	
1.5%	0.17%	0.03%	0.06%	

3.2.2 Expansion Measurements: RA1 Concrete Cylinders (Test 1)

The non-heat cured and heat cured cylinders from the RA1 mix both showed high levels of expansion. The expansion of the non-heat cured cylinders, illustrated by Figure 3.5, were due to ASR induced strains given the siliceous fine aggregate present, the high alkaline content of the concrete (Na_2O_{eq} of 1.25%), and the fact that the concrete was not heat cured so DEF was not a possibility. Also Figure 3.5 shows a progressive decrease in expansion with increasing levels of steel fiber dosage.

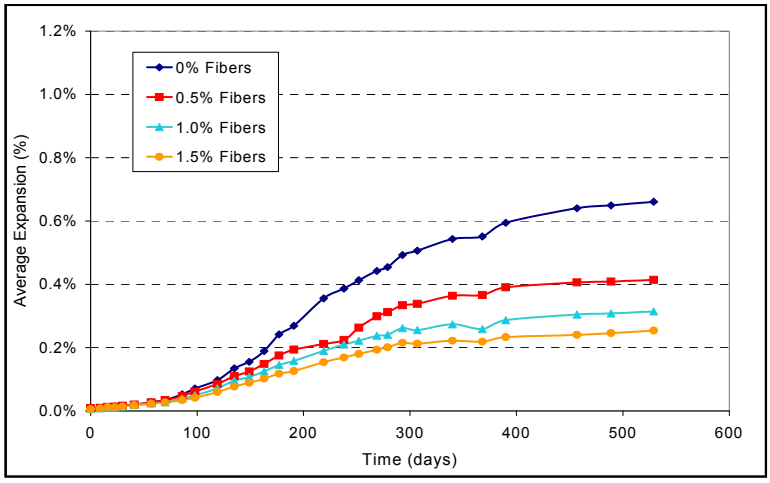

Figure 3.5: Expansion of non-heat cured RA1 Mix cylinders stored above water at 100 °F.

The heat cured RA1 Mix cylinders however did not show the same progression of decrease in expansion with increased fiber dosage. As Figure 3.6 shows, the average expansion of the non-fiber reinforced (0% fiber) cylinders surpassed 1.4% but none of the fiber reinforced concrete cylinders expanded beyond 0.10%.

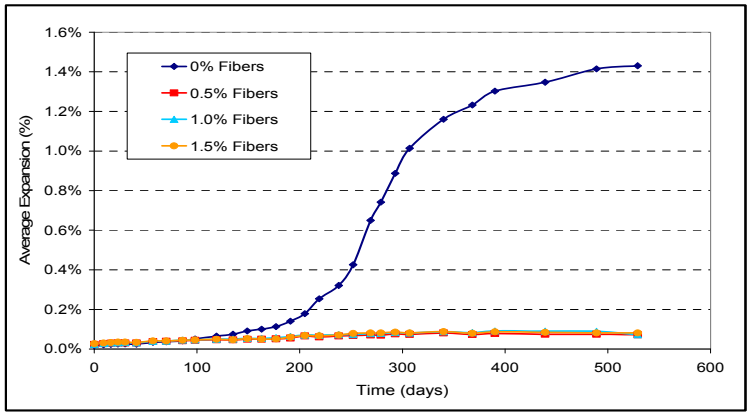

Figure 3.6: Expansion of heat cured RA1 Mix cylinders stored above water at 100°F.

In the non-fiber reinforced cylinders that showed large levels of expansion, it is possible that the combined effects of ASR and DEF could be responsible for the very high level of expansion. It is postulated that ASR could have occurred initially and then been followed by DEF induced expansion as the pH of the pore solution dropped due to a drawing out of the alkalis by leaching in the above water storage environment and/or the occurrence of ASR. However no work was done to confirm this assertion.

Table 3.4 shows the level of variability in expansion measurements between cylinders of similar fiber dosage.

Table 3.4: TRA1 Mix: Final average expansion value and variability

Fiber Dosage	NON-HEAT CURED RA1 MIX		HEAT CURED RA1 MIX	
	Final Average Expansion	Standard Deviation	Final Average Expansion	Standard Deviation
0%	0.66%	0.12%	1.43%	0.08%
0.50%	0.41%	0.05%	0.07%	0.01%
1.00%	0.31%	0.07%	0.07%	0.02%
1.50%	0.25%	0.04%	0.08%	0.01%

The results shown in Table 3.4 are quite encouraging, suggesting that steel fibers are very effective in confining and reducing expansions due to DEF. However, because the results from the expansion of the heat cured RA1 Mix cylinders in Figure 3.6 differed so drastically from the NR mix concrete and the non-heat cured RA1 mix concrete, it raised a number of questions about the test, particularly the question of how heat curing of the RA1 mix concrete might have affected the action of the fibers.

It was noted that after removing the heat cured RA1 cylinders a number of the cylinder mold caps had come loose, and after de-molding the cylinders, the heat-cured RA1 cylinders appeared very dry and cracked on the surface. This same drying and cracking was not evident with the heat-cured NR cylinders. Also, both the RA1 and NR heat-cured cylinders had also been subjected to a dry heat cycle of the Fu-regime (Figure 3.1), where the de-molded cylinders are placed in an oven at 185°F for 24 hours for the purpose of micro-cracking the concrete to accelerate future DEF expansion.

In section 2.2.1 the supposed mechanical action of fibers in concrete is discussed. In summary of that section, fibers provide internal restraint to concrete expansion by bridging the

micro-cracks and restraining further propagation of those cracks. Therefore if the fiber reinforced concrete has already experienced micro-cracking prior to experiencing additional micro-cracking due to ASR or DEF or both, the concrete will likely be more resistant to additional cracking since the initial cracks have "engaged" a number of fibers and effectively "pre-tensioned" the concrete to some degree. It was postulated therefore that the drying of the RA1 cylinders during curing, the Fu drying cycle, or both could have introduced significant levels of micro-cracking that could have "pre-engaged" the fibers in the fiber-reinforced cylinders. If this was the case then the fiber-reinforced cylinders would be much more resistant to any additional micro-cracking due to ASR or DEF induced expansion. To examine the potential effect that drying and cracking of fiber-reinforced concrete during curing and immediately after curing, could have on the subsequent restraint provided by the fibers a second series of RA1 mix concrete cylinders were cast and measured.

Figure 3.7: Concrete cylinder from heat cured RA1 Mix; surface drying and cracking after curing.

3.2.3 Expansion Measurements: RA1 Concrete Cylinders (Test 2)

The second RA1 concrete mix was done using similar materials and mixing procedure as the first mix. A non-heat cured and a heat cured set of cylinders with different steel fiber dosages, similar to the non-heat cured cylinders in test 1, were cast. Also a second set of heat cured cylinders were cast and cured in the oven according to the Fu regime, but they were not subjected to the second dry heat cycle of the Fu regime. An effort was made to ensure that none of the cylinder mold caps came loose during curing in the oven to prevent the drying of the concrete that had occurred during test 1. All of the cylinders were stored in the above water at 100^{o}F environment.

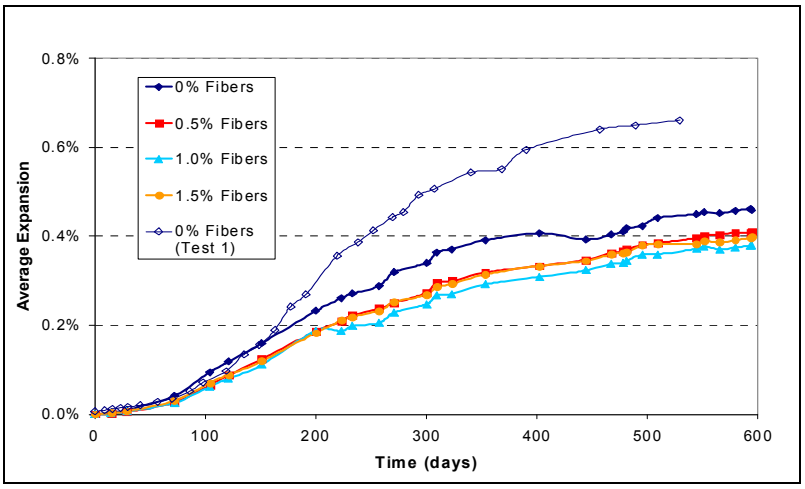

Figure 3.8: Expansion of non-heat cured RA1 Mix cylinders stored above water at 100°F (also the 0% Fibers average expansion from test 1 shown).

Figure 3.8 illustrates the expansion levels to date of the non-heat cured cylinders. The cylinders are following a similar trend of expansion for each fiber dosage as test 1. The test 1 cylinders have a pronounced difference in expansions between the different fiber dosages; however, all the test 2 cylinders have very similar expansions and vary only by a small amount. Another point of interest is the 1.5% fiber cylinders of test 2 that are showing noticeably larger levels of expansion than in test 1.

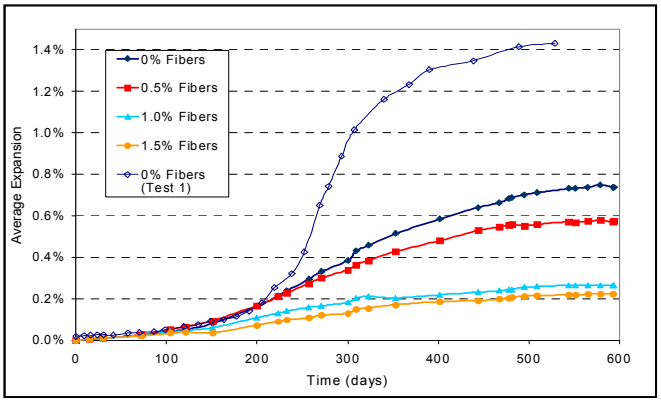

Figure 3.9: Expansion of heat cured RA1 mix cylinders stored above water at 100°F (also the 0% Fibers average expansion from test 1 shown).

The expansions of the heat cured cylinders are shown in Figures 3.9 and 3.10. The heat cured cylinders shown in Figure 3.9 were subjected to the full Fu regime like the cylinders in test 1 but are showing very different results. The fiber reinforced cylinders in test 2 are experiencing significant expansion levels unlike the fiber reinforced cylinders in test 1 (Figure 3.6) that never surpassed 0.10% expansion. These results strongly suggest that the drying of the heat cured RA1 mix cylinders during curing that was evident by the dried and cracked surface of the cylinders did in fact introduce significant micro-cracks that effectively "pre-engaged" the steel fibers.

The expansion of the second set of heat cured RA1 mix cylinders that were not subjected to the drying heat cycle of the Fu regime, are also expanding as shown in Figure 3.10. Since

these cylinders did not go through the drying cycle of the Fu regime, they are not expanding at the rate of the cylinders in Figure 3.9. What is interesting to note is that the 0.5% fiber cylinders exhibit virtually the same expansion as the 0% fiber cylinders in Figure 3.10. This is different from the cylinders in Figure 3.9 where each increase in dosage of fibers has a distinct reduction in expansion. The removal of the drying cycle for the test 2 cylinders has a definitive reduction in the rate of expansion of the cylinders; however, more time is needed in order to assess the effect on the overall expansion of the cylinders.

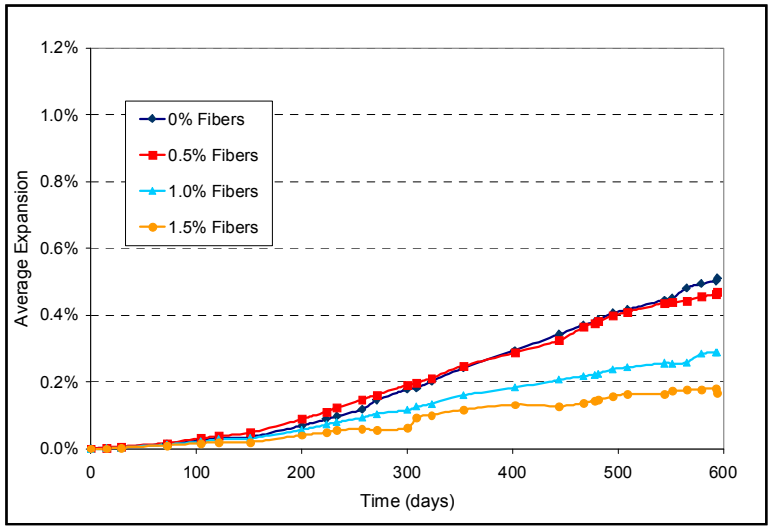

Figure 3.10: Expansion of heat cured RA1 mix cylinders not subjected to drying cycle stored above water at 100°F.

3.2.4 Expansion Measurements: RA2 Concrete Cylinders

The RA2 mix was done using similar materials and mixing procedure as the NR and RA1 mixes. Both heat-cured and non-heat cured cylinders were cast from the RA2 mix. The heat cured cylinders were subject to the Fu regime without the heat-drying phase. All of the non-heat cured and half of the heat-cured cylinders were placed in the above water 100°F environment. The other half of the heat-cured cylinders was placed in a limewater bath. The goal of the RA2 mix was to validate the findings of the RA1 mix as well as directly compare the expansions due to ASR, DEF and a combination of the two based on their storage environments.

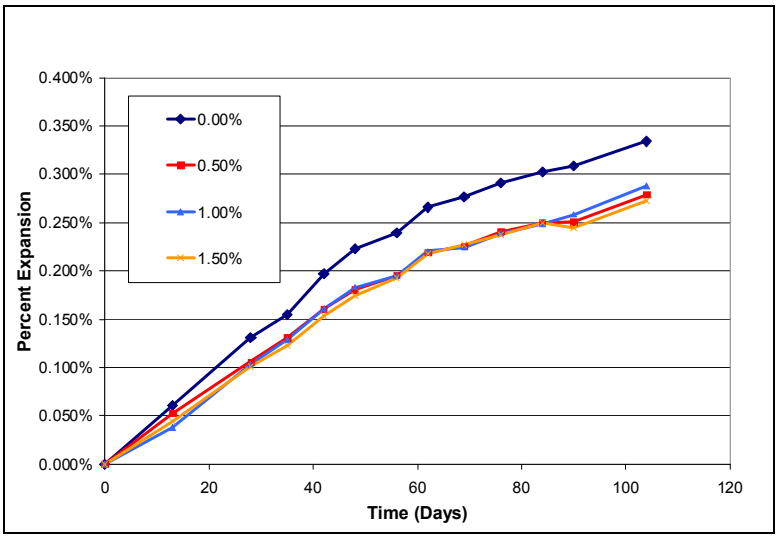

Figure 3.11: Expansion of non-heat cured RA2 mix cylinders not subjected to drying cycle stored above water at 100°F.

Figure 3.11 shows the expansions to date of the non-heat cured cylinders of the RA2 mix. The expansion of the non-heat cured cylinders is attributed to the reactive aggregates and thus expands due to ASR only. Currently it is too early in the testing to determine with any certitude the effects of the Fu regime without the heat-drying phase or even the effects of differing fiber dosages. Continued testing will answer these questions.

Figure 3.12 shows the expansions to date of the heat-cured cylinders of the RA2 mix that were stored in a limewater bath. The expansion of the heat-cured cylinders stored in limewater is attributed to DEF only because the limewater will leach all the alkalis out of the cylinders to effectively stop any expansion due to ASR.

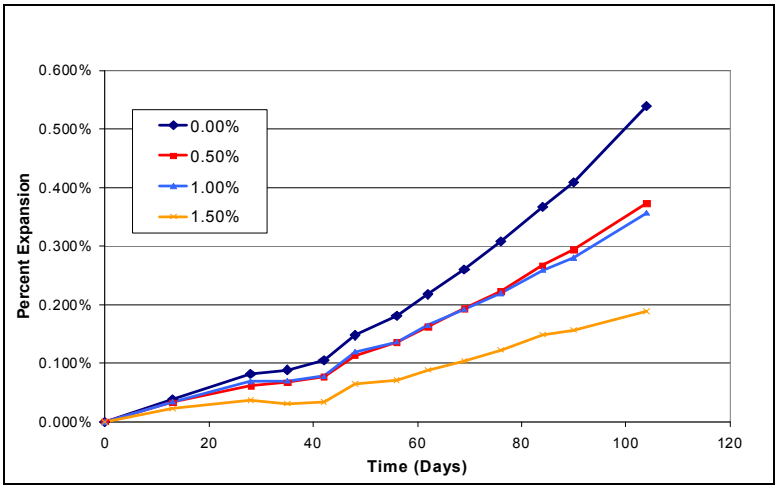

Figure 3.12: Expansion of heat cured RA2 mix cylinders not subjected to drying cycle stored in limewater bath.

However, the leaching of the alkalis from the cylinder will lower the pH within the system and create a favorable environment for the formation of ettringite, or DEF. These

cylinders are following the general trend of the NR cylinders that were stored in limewater in Figure 3.3. The 0.5% and 1.0% cylinders of the RA2 mix do not have a pronounced difference as the same cylinders in the NR mix; however, it is fairly early in the testing and we expect to see similar trends as those of the NR mix over time.

Figure 3.13 illustrates the expansions to date of the heat-cured cylinders of the RA2 mix that were stored in the above water environment. The expansion of these cylinders is attributed to a combination of ASR and DEF. The initial expansion of the cylinders is attributed to ASR due to the high alkali content within the concrete. Over time the high humidity environment will leach some of the alkalis creating a favorable environment for DEF. As seen before the different dosages of fibers have a distinct effect on the expansions of the cylinders; however, the 0.5% cylinders are exhibiting smaller expansions than the 1.0% cylinders. As stated before the RA2 cylinders are still in the early stages of testing and full conclusions will only be drawn after more time has passed.

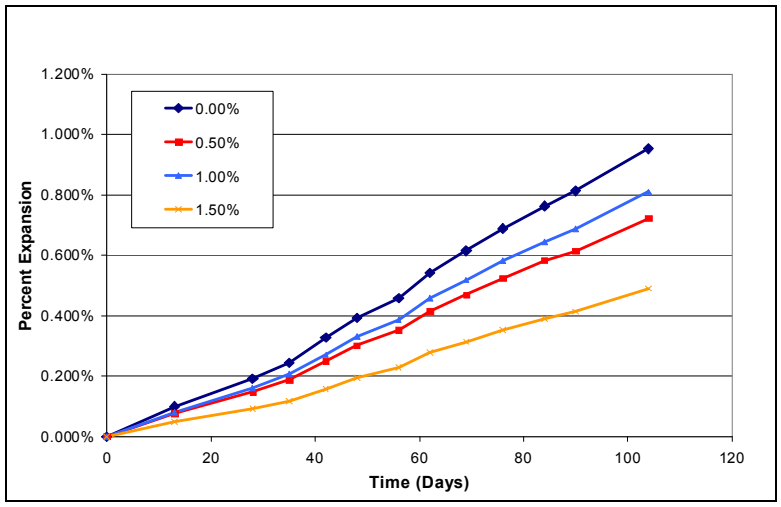

Figure 3.13: Expansion of heat cured RA2 mix cylinders not subjected to drying cycle stored in the above water 100°F environment.

3.2.5 Summary

This section summarized extensive testing performed on steel fiber-reinforced concrete and its ability to internally restrain ASR, DEF, or a combination thereof. The test results seem to point out that DEF is at least as easy to confine as ASR, and in some cases, it appears easier to confine DEF. Although it is not possible to extrapolate these results to estimate the requisite amount of external confinement needed to suppress DEF, it does provide a useful, side-by-side comparison to ASR. These results, which show the promise in being able to confine DEF, despite its expansions being much higher than those triggered by ASR, coupled with data presented later in this report, help to shed some light on stresses generated by DEF and potential remedies for confining DEF in field concrete elements.

Chapter 4. Hoek Cell Tri-Axial Confinement Test

The Hoek cell provides a simple but innovative approach for determining the level of confining stress necessary to stop delayed ettringite formation (DEF) or alkali-silica reaction (ASR) in concrete. The Hoek cell is a tri-axial load cell apparatus that was first designed by Franklin E. Hoek (Hoek 1968) for multi-axial testing of rock cores. The Hoek cell has also been utilized for multi-axial testing of concrete specimens (Ganjian et al 2006, Hyett et al 1995).

The Hoek cell consists of a cylindrical steel body that is hollow and into which a rubber membrane is inserted. The cavity formed between the body of the Hoek cell and the membrane acts as a reservoir for hydraulic oil which can be pressurized up to 10,000 psi. The steel caps seal the ends of the cells but are hollow in the center to allow for load platens to be inserted so an axial load can be applied to the specimen contained within the membrane. Figure 4.1 illustrates the typical Hoek Cell design.

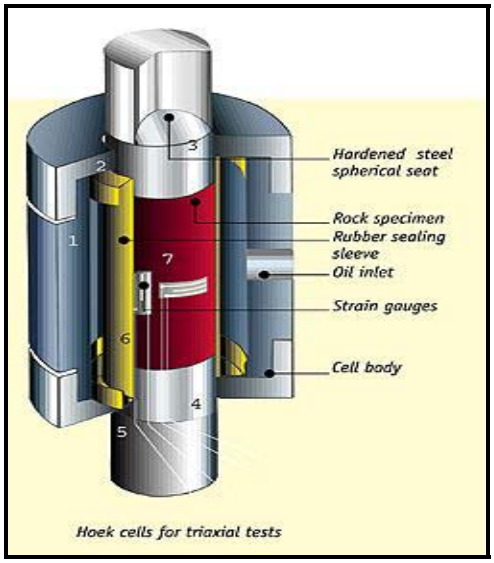

Figure 4.1: Typical Hoek Tri-Axial Cell.

As discussed in chapter 2, the majority of past research has only looked at confinement of ASR affected concrete in a single (uni-axial) direction. However, such uni-axial testing does not provide information about the restraint necessary to halt expansions in the transverse directions which are unconfined. In the field, an element such as a reinforced concrete column that is affected by ASR and/or DEF typically expands in the horizontal or transverse direction since in the vertical direction the column is partially or fully confined by the axial loads it is supporting. Therefore to effectively stop the expansion and deterioration of such an element, it is necessary to determine the level of confinement required to stop expansion in all directions.

The goal of this study is to utilize the Hoek cell to determine this level of tri-axial confining pressure necessary to stop DEF or ASR induced expansion in concrete. In theory if a concrete cylinder affected by DEF or ASR is placed inside a Hoek cell and continues to try to expand the confining pressure of the hydraulic oil will increase until it reaches a level of confining pressure at which the internal kinetics driving the expansion of the concrete cannot

overcome the external pressure. For the first series of testing we looked at concrete primarily affected by DEF.

4.1 Test Setup

4.1.1 Hoek Cell Design

In order to use the Hoek cell to confine concrete affected by DEF, some significant modifications had to be made, bearing in mind that this apparatus was initially developed for short-term testing of rock samples, not long-term testing of concrete specimens undergoing internal expansion. The first modification was the design of rubber gaskets to provide long-term protection against oil leakage at the interface between the Hoek cell cap and the ends of the rubber membranes. The second modification was the creation of a water supply system through the end platens to supply a continual circulation of water to the ends of the concrete cylinders. The following section describes the water supply system. Figure 4.2 provides a cross-section profile of the inside of the modified Hoek cell setup used in the testing.

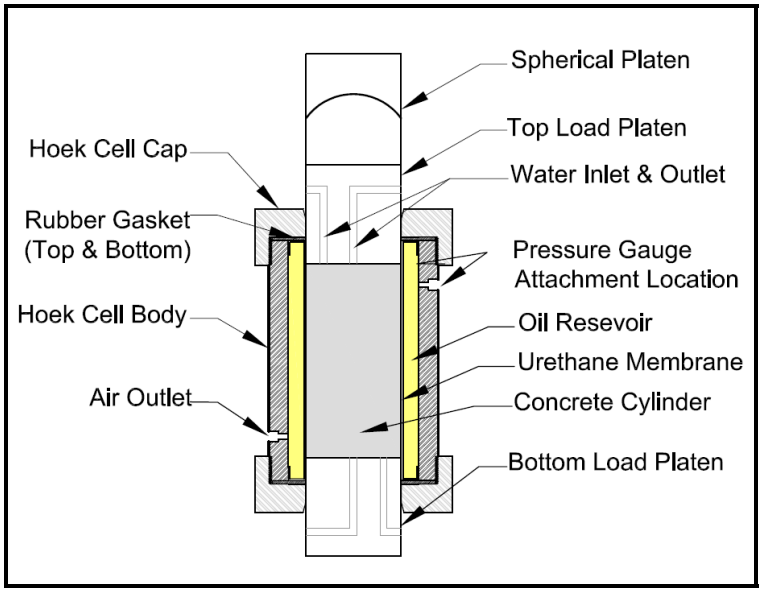

Figure 4.2: Cross-Section View of Hoek Cell with concrete test cylinders and load platens shown.

4.1.2 Water Supply System

In order for expansions due to DEF to progress in concrete, the concrete must be exposed to a continual supply of water. For this purpose modified load platens were created that would allow for water to circulate to and from the ends of the concrete cylinders while they were subjected to tri-axial loads inside the Hoek cell. Small grooves were machine cut into one side of the top and bottom load platens to allow the water to circulate along the end surfaces of the concrete cylinder. Two holes less than ¼ inch diameter carry the water in and out of the load platens to provide continual water circulation. Water is pumped to the platens by a submerged water pump through vinyl tubing. Figure 4.3 illustrates the design of the load platens.

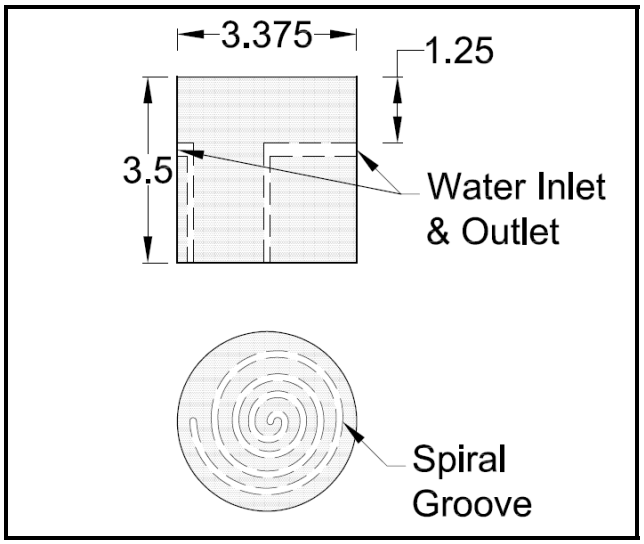

Figure 4.3: Load Platens with water supply system shown from Profile view (top) and bottom view (bottom).

4.1.3 Load Frame

The load frame used for applying the axial confinement load is a frame typically used for creep frame testing. The frame consists of 3 inch thick load plates that are supported by three - inch diameter threaded rods. To gauge the applied axial load, aluminum cylinders of 3.375 inch diameter, similar to the spherical heads and load platens, were placed in the load assemblage. Three strain gauges were placed 120^{o} apart on the aluminum cylinders from which the axial load applied by the frame could be determined based upon the strain in the aluminum cylinders and effective modulus of elasticity of the aluminum. The aluminum cylinders were calibrated prior to testing to determine the effective modulus, which was about $11x10^{6}$ psi. Figure 4.4 illustrates the load frame arrangement.

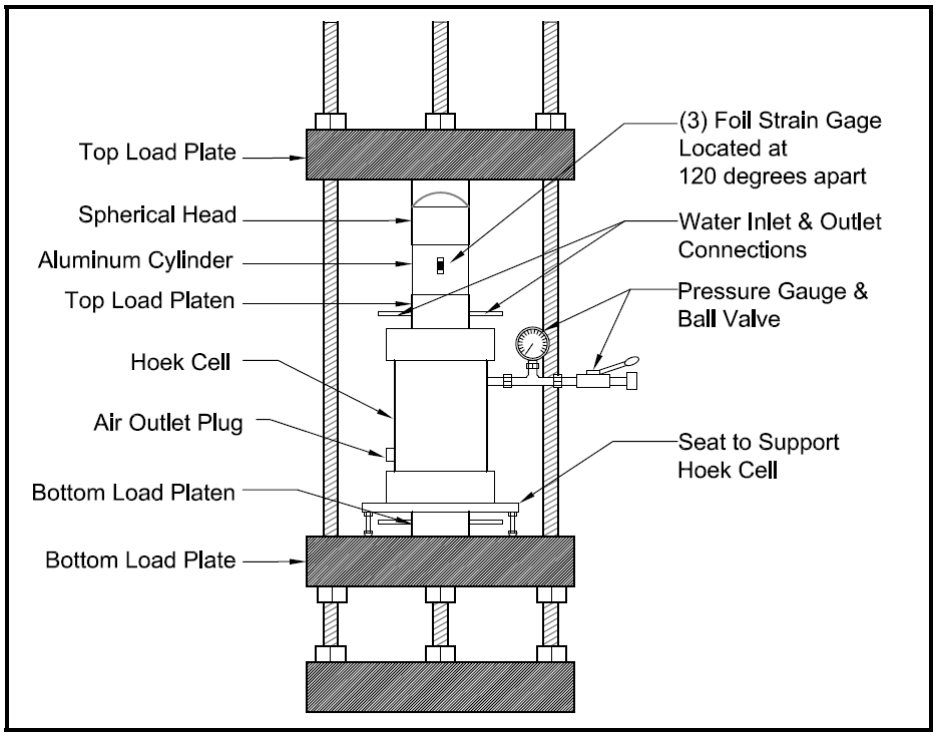

Figure 4.4: Load Frame arrangement with Hoek cell and supporting components. (Note: the vinyl tubing connected to the water pump is not shown)

4.1.4 Concrete Test Cylinders

The concrete cylinders to be tested in the Hoek cell had to be made using custom-made molds because of the unique dimensions of the Hoek cell. The cylinders were 3.375 inches in diameter by 7.0 inches in length. The first molds used to cast the cylinders were made using typical 4 inch by 8 inch plastic molds and pouring a two part urethane sleeve that upon hardening reduced the diameter of the mold to 3.375 inches in diameter. It was later found that the two part urethane sleeve did not perform well during repeated heat cycles and therefore a second set of molds were made. The second set of molds was made from light gauge sheet metal that was rolled and secured by hose clamps with circular plywood end caps. See Appendix B for details on how to make custom molds using light gauge sheet metal.

The concrete cylinders which were created for this test came from the same concrete mix design that was used to cast the model columns, see section 5.2, and therefore have been labeled as MC cylinders for Model Column. A total of 16 cylinders were cast and 12 of the cylinders were heat treated according to the same time-temperature regime that was used for the model column cylinders, shown in Figure 5.1. The remaining non-heat cured cylinders were allowed to cure at 73 ^{o}F. After a day of curing the cylinders were demolded and two sets of demecs were placed on the cylinders for expansion measurements. At three days age the cylinders were placed in limewater for long-term storage at 73 ^{o}F.

Expansion measurements of the cylinders were taken every two weeks. Figure 4.5 illustrates the rate at which the concrete cylinders expanded. At approximately 110 days two of the heat cured cylinders and one of the non-heat cured cylinders were removed from the limewater and prepped for testing in the

Hoek cells. The expansion levels of the three cylinders immediately prior to Hoek cell testing are shown in Table 4.1.

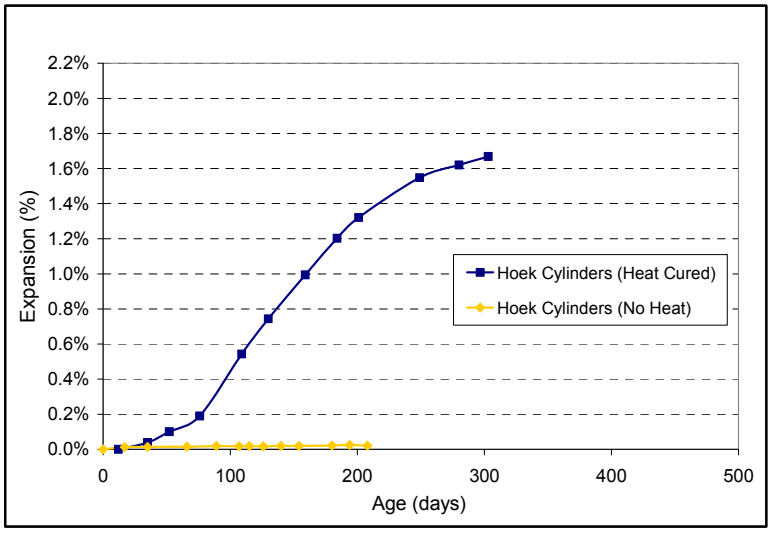

Figure 4.5: Expansion of Hoek cell cylinders in Limewater.

Table 4.1: Expansion level of Hoek Cylinders prior to testing.

MC Concrete Cylinders	Expansion (%)
#1 – Heat Cured	0.61
#2 – Heat Cured	0.51
#3 – Non-Heat Cured	0.02

The cylinders were prepared for confinement testing by carefully sanding the ends to a plainness of $^{1}/_{32}$ inch or less and perpendicularity within $^{1}/_{16}$ inch. Mortar was then used to fill in small voids in the surface of the cylinders. The cylinders were stored in a fog room for one day to allow the mortar to cure and then placed in a limewater again for two days before placing them in the Hoek cells.

4.1.5 Initial Confinement Load

The three concrete cylinders were placed inside a Hoek cell and each was loaded with similar levels of axial and confining pressure. The setup of the Hoek cells typically requires about one hour per cell. The actual process of setting up the Hoek cells and providing initial axial and confinement loading is detailed in Appendix A.

Figure 4.6: Hoek Cell inside Load Frame.

Cylinders were removed from the limewater bath immediately prior to being inserted into the Hoek cell in order to minimize drying of the concrete. Once a cylinder had been placed inside the Hoek cell, the Hoek cell was positioned inside the load frame. After checking the alignment of the frame and cell, and axial load was applied to the concrete cylinder by first lowering the top plate of the frame and then tightening the bolts. By monitoring the strain in the aluminum load platens with the 3 foil strain gauges, it was possible to calculate the level of load being applied and also the distribution of the applied load to insure that the load was applied as uniformly as possible.

Once an axial load of approximately 100 psi had been applied to the cylinder, a hydraulic pump was used to apply a load of about 400 psi of confining pressure in the Hoek cell. The 400 psi is used to help initially seal the interfaces between the body of the cell and rubber gaskets with that of the rubber membrane. Once the confining load was applied the axial load increased to about 160 to 180 psi due to Poisson effects. Once the axial and confining loads have been applied the water inlet valve is open to allow water to begin to circulate to the ends of the cylinders.

After one day the confining load is lowered to about 50 psi, and consequently the axial load decreased to about 100 psi. After a second day the confining pressure increased slightly, about 10 to 20 psi. It was assumed that this slight increase might be due to water absorption by the concrete so the confining load was adjusted a second time back to about 50 psi. After this point the axial and confining loads were not adjusted. The pressure gauges were read once a day for the following 33-days of the test. Strain gauge readings from the aluminum cylinders were tabulated on a data-logger system and were then converted into load readings based upon the calibrated modulus for each cylinder. Some technical difficulties with the data-logger system led to the loss of data during the first seven days of the test and also between days 10 and 14 of the test as can be seen from the results in the following section.

4.2 Test 1 Results

The testing period lasted about 33 days during which the confining pressure in the Hoek cells and the axial load applied by the frames were measured. There were technical difficulties

that arose with regards to the tabulation of the axial load data and an oil leakage problem that impacted the results of one Hoek cell test. Again, it should be reiterated that this test set-up was not intended for long-term testing, and problems such as the aforementioned leakage are not surprising.

4.2.1 Confining Pressure Change with Time

The confining pressure inside the Hoek cells for both of the reactive cylinders, MC #1 and #2, did increase with time. However on day 17 a suspected hydraulic oil leak seems to have affected the resulting pressure in the Hoek cell containing MC #1. The leak was stopped by tightening the thread connection. The non-reactive cylinder, MC #3 showed no significant build up in confining pressure with time. Figure 4.7 illustrates the change in confining pressure with time for each of the Hoek cells. The pressure gauges from which the measurements were read are accurate to ± 3 psi, but they have graduation marks only every 20 psi. Therefore the level of potential error is likely around ± 10 psi. Despite these inaccuracies it still seems apparent that the reactive cylinders increased the level of confining pressure up to at least 120 psi and as high as 200 psi in the case of MC#2. This increase in confining pressure for the reactive specimens and lack thereof for the non-reactive specimen reflects the promise that this innovative testing approach holds.

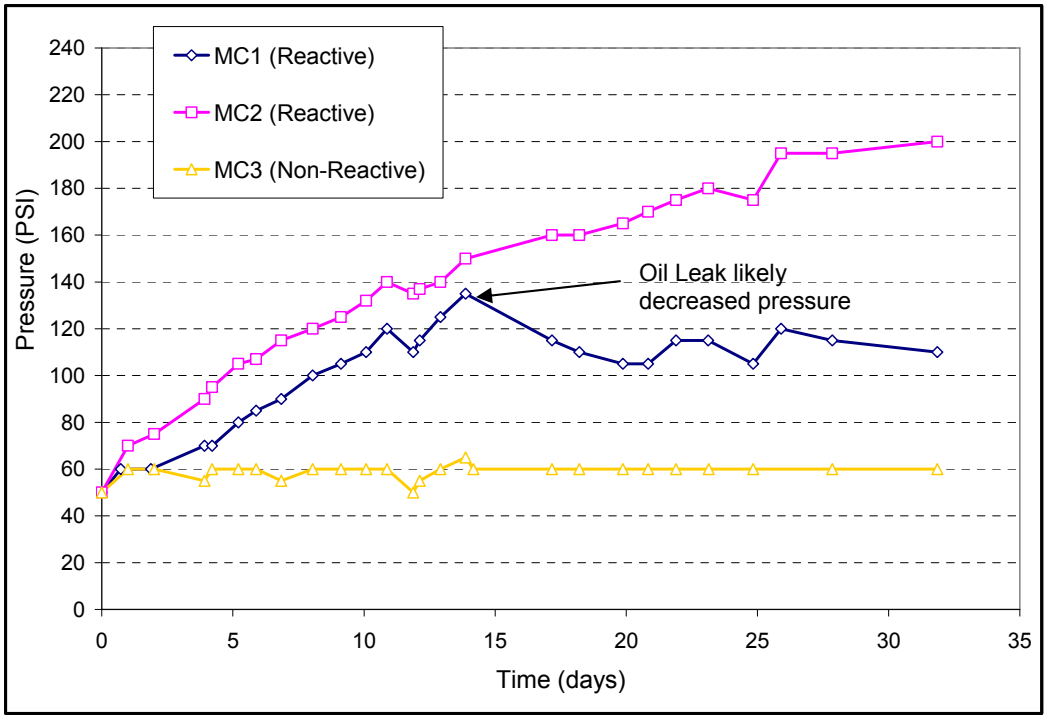

Figure 4.7: Confining Pressure versus time for each of the Hoek cells.

4.2.2 Axial Pressure Change with Time

The axial load like the confinement pressure also increased with time for the reactive cylinders and remained at about the same level for the non-reactive cylinder. However there

were some technical difficulties encountered with the datalogger system that led to lost data, and there were also fluctuations in strain due to temperature change. Figure 4.8 illustrates the change in axial load with time for the three different cylinders. The missing periods of data were due to datalogger errors as mentioned. It was determined that the large daily fluctuations in calculated load were due to thermal effects. Though the testing room remained at 72°F ± 1.5°F constantly, it was determined that even a small fluctuation in temperature of one degree Fahrenheit could result in a change of 5 to 10 microstrain of the threaded rods in the load frame. For a highly rigid system like the steel load frames 10 microstrain would increase the applied axial load by as much as 60 psi. Figure 4.9 presents the same axial load data but plotted as a daily average.

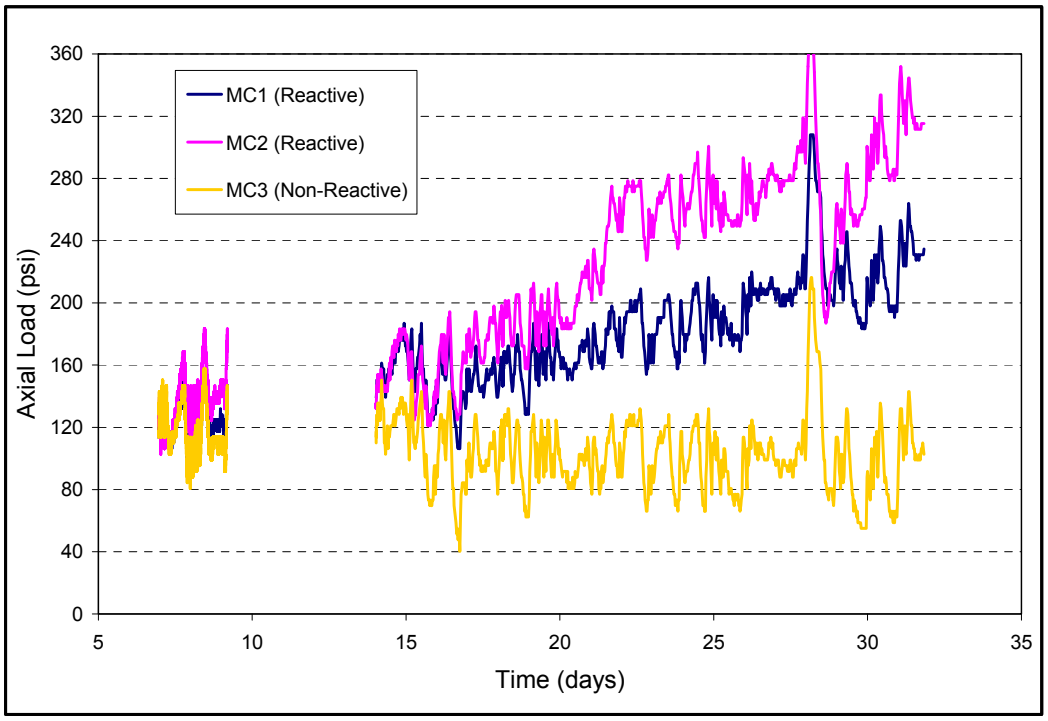

Figure 4.8: Axial Load versus time for each of the Hoek cells.

For the Hoek cells that contained the two reactive cylinders, MC1 and MC2, the axial load increased to as much as 230 and 320 psi respectively. The non-reactive cylinder showed no significant gain in axial load.

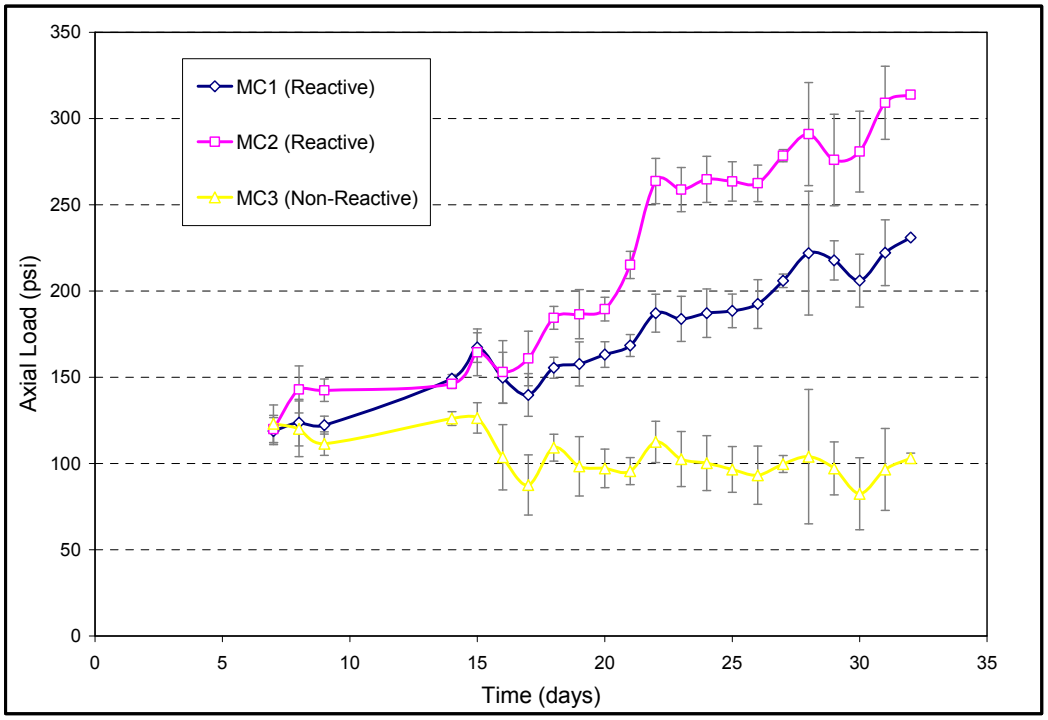

Figure 4.9: Axial Load versus time for each of the Hoek cells where the load is represented as a daily average. (The error marks represent ± one Average Deviation).

4.2.3 Confining and Axial Pressure Change with Time

Figures 4.10, 4.11 and 4.12 illustrate the change in confining pressure and axial load for each of the three cylinders that were tested.

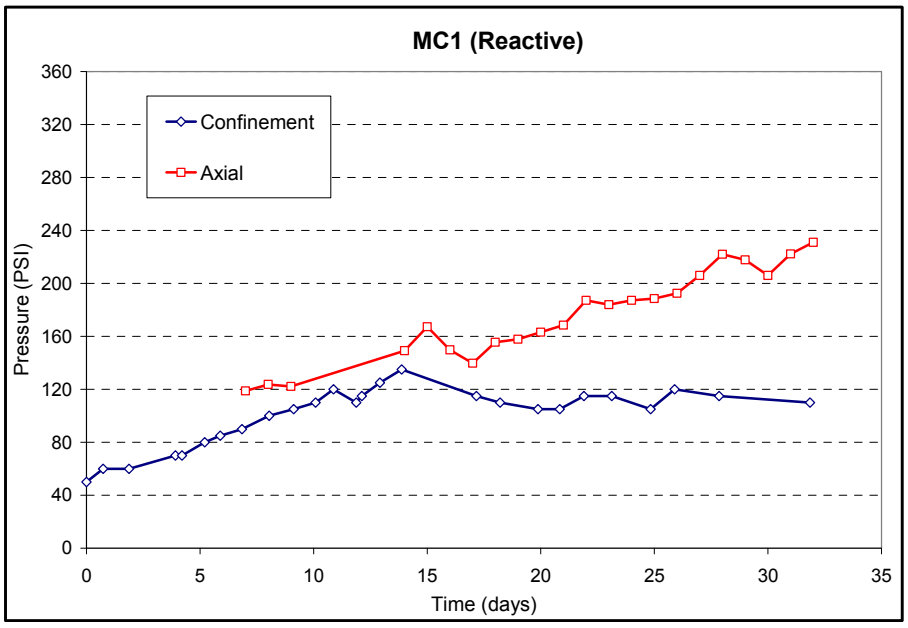

Figure 4.10: Total confining pressure changes with time for MC1 (Reactive) cylinder (The axial pressure data points represent daily averages).

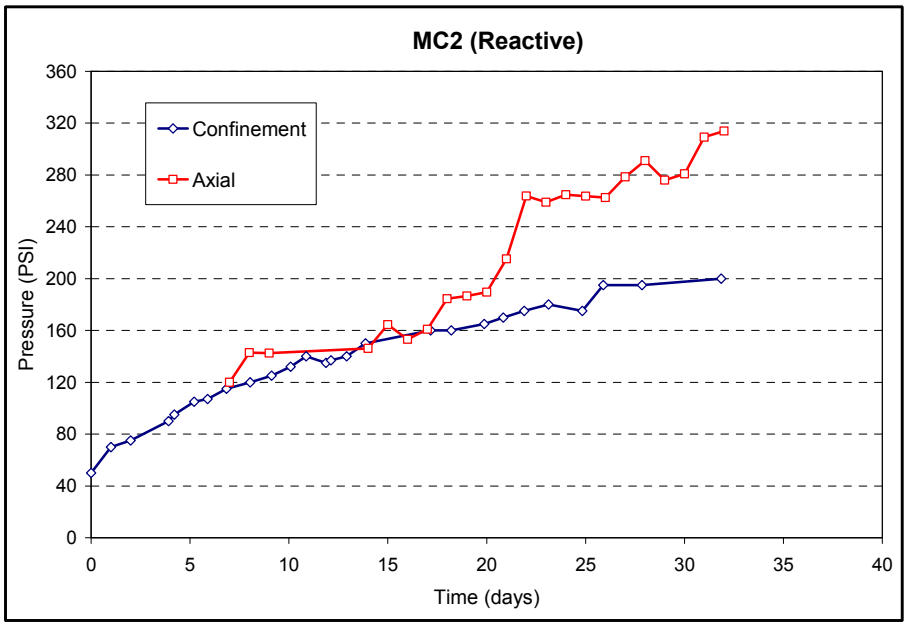

Figure 4.11: Total confining pressure changes with time for MC2 (Reactive) cylinder (The axial pressure data points represent daily averages).

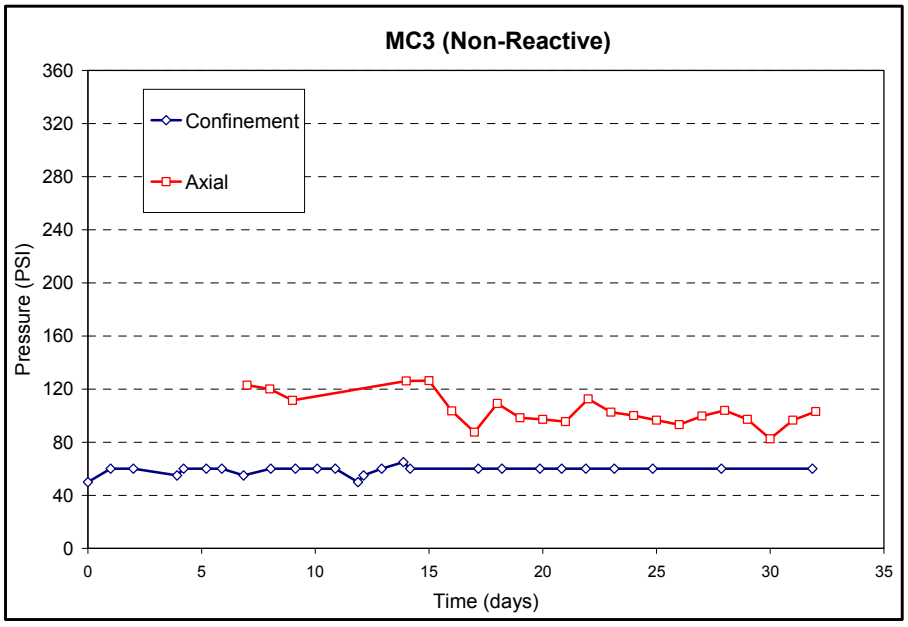

Figure 4.12: Total confining pressure changes with time for MC3 (Non-Reactive) cylinder (The axial pressure data points represent daily averages).

4.2.4 Observations

After about 2 days, the confinement pressure began to immediately increase for both cylinders #1 and #2. Meanwhile the non-reactive cylinder, #3, remained at a nearly constant pressure during the entire period of testing.

Once the confining pressure reached about 100 psi for setups #1 and #2 at about day 15, the axial pressure began to also increase. The axial pressure in fact increased to higher levels than the confining pressure. Both the axial and confining pressure seemed to level off after about 32 days, at which point the test was stopped. The non-reactive cylinder, MC #3, showed no change in confining pressure and actually lost axial pressure likely due to creep.

4.3 Hoek Cell Modifications

After the conclusion of the first test a few modifications to the cells were made in order to minimize system leaks and simplify pressure readings. In the first test the use of a highly rigid system to apply the axial load led to significant fluctuations in load due to small thermal changes. For subsequent testing it was decided to modify the axial load mechanism by using a hydraulic ram to apply a constant axial load. A constant axial load of about 400 psi would more accurately replicate the state of stress of a concrete column under typical dead loads. By connecting the hydraulic ram to a hydraulic accumulator it provides a less rigid system that will not fluctuate as much with temperature increase, and the pressure in the system can be easily monitored and adjusted. Figure 4.13 illustrates the modified Hoek Cell test arrangement.

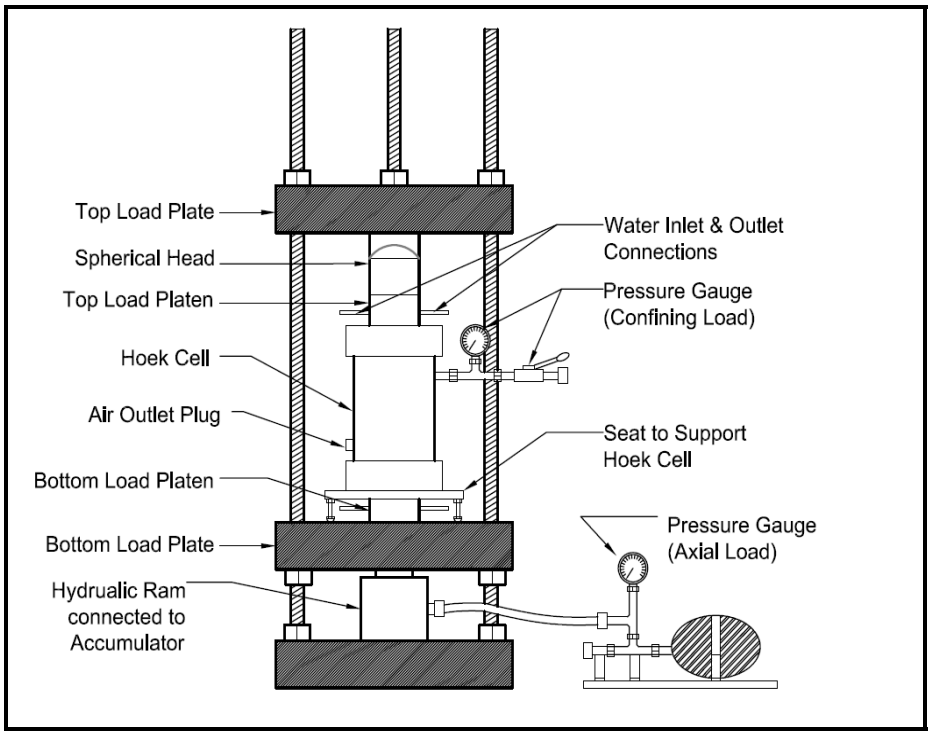

Figure 4.13: Hoek Cell Confinement setup with a constant axial load, to be applied using a hydraulic ram with accumulator.

Also note that in Figure 4.13 the dial pressure gauges that are depicted in the diagram were replaced by digital gauges to minimize reader errors and improve the accuracy of the overall test. The original dial gauges had 5 connection points each while the digital gauges only had three, thus minimizing the risk of hydraulic leaks.

4.4 Test 2 Development and Results

The concrete cylinders created for this test came from the same concrete mix design that was used to cast the reinforced columns, see section 6.1, and therefore have been labeled as RC cylinders for Reinforced Column. These cylinders were cast at the same time the MC cylinders from test 1 were being tested, thus when the RC cylinders reached a percent expansion close to 0.10%, the cylinders were frozen to effectively stop the DEF reaction. Initial expansions below 0.10% are attributed to water absorption not necessarily DEF, thus to speed the testing the RC cylinders were placed in the Hoek cells when they reached 0.10% expansion. The expansion levels of the three cylinders immediately prior to Hoek cell testing are shown in Table 4.2.

Table 4.2: Expansion level of Hoek Cylinders prior to testing.

RC Concrete Cylinders	Expansion (%)
200 #4 – Heat Cured	0.091
200 #6 – Heat Cured	0.091
75 #4 – Non-Heat Cured	0.015

The cylinders were prepared by the same method described in section 4.1.4 prior to placement in the Hoek cells. What is important to note is that the heat cured cylinders were placed into the Hoek cells at a lower percent expansion in an effort to capture the effects of a full range of expansion of those cylinders in the Hoek cell test.

The testing period lasted 187 days during which the confining pressure in the Hoek cells and the axial load applied by the frames was measured. There were interesting results that were obtained during testing that will be discussed later on; however, these results were able to reveal an interesting phenomenon that occurs during long term Hoek Cell testing of DEF induced cylinders. As stated above test 2 was conducted using 2 reactive cylinders, RC 200 #4 and #6, and one non-reactive, RC 75 #4.

4.4.1 Confining Pressure Change with Time

Figure 4.14 shows the confining pressure over time of RC 200 #4 and #6 and RC 75 #4 cylinders. RC 200 #4 and #6 were both subjected to heat treatment during curing while RC 75 was cured at normal temperatures in a fog room. All three cylinders experienced an initial loss of pressure due to the removal of air from the system followed by pressure stabilization. The stabilized pressure for each cell is considered as the initial zero pressure reading. RC 200 #4 stabilized around 50 psi prior to expanding to a high pressure of 285 psi for a net pressure gain of 235 psi. RC 200 #6 stabilized near 30 psi prior to expanding to a high pressure of 195 psi for a net pressure gain of 165 psi. The initial confining pressure seems to have a large impact on the final pressure attained at the end of each test. RC 200 #4 began at a higher initial confining pressure and was observed to have a larger final pressure than RC 200 #6. Also what is interesting to note is towards the end of testing both cylinders began to cycle through pressure losses with subsequent increases. This led to the observation that the pressure loss from the

suspected hydraulic leak, observed in the first test, may actually have been attributed to the actual behavior of the specimens in the cells. A number of ideas have been generated to explain the cycling of the reactive cylinders; however, none are capable to explain in full this behavior with any certitude at this time.

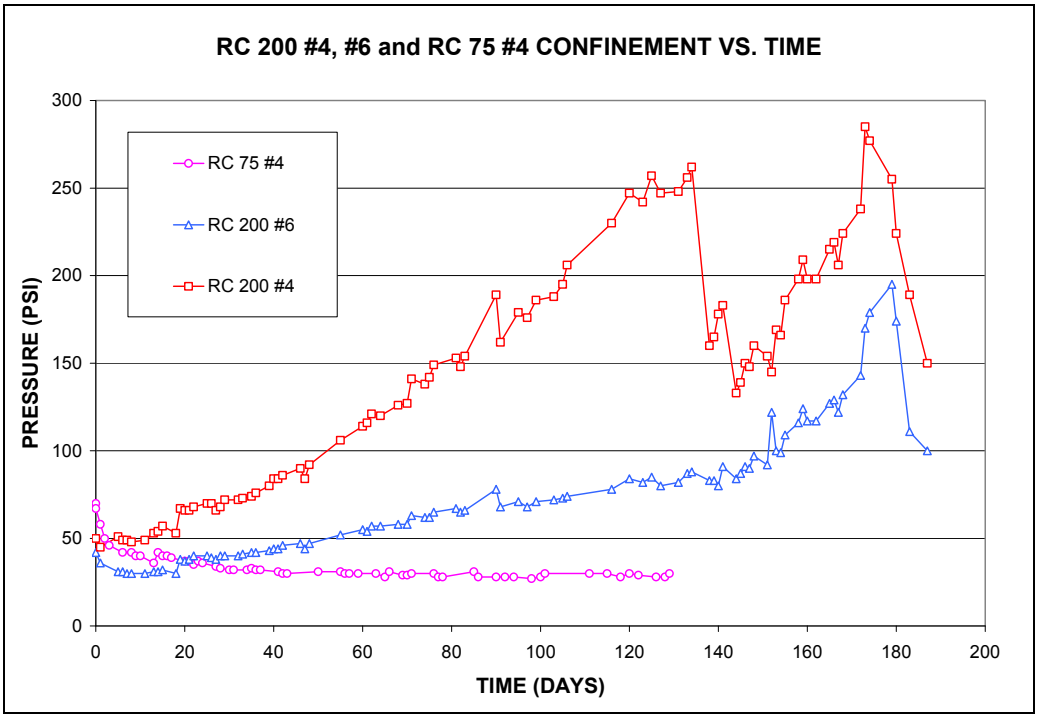

Figure 4.14: Confining Pressure versus time for each of the Hoek cells.

The RC 75 #4 cell in Figure 4.14 did not expand during testing as expected. This cylinder was not subjected to heat treatment and thus no mechanisms were in place to cause the cylinder to expand. The cylinder was seated properly and thus the pressure of the cell stabilized near 30 psi and did not see any subsequent pressure increases. The test was terminated after 129 days because there were no significant pressure changes for the final 100 days of testing as well as to allow for the start of a third round of tests.

4.4.2 Axial Pressure Change with Time

Figure 4.15 shows the axial pressure versus time of the RC 200 #4, #6 and RC 75 #4 cylinders. The axial pressure like the confining pressure did increase over time; however, the accumulators were able to keep the cell pressures fairly constant. The RC 200 #4 and #6 cell held an average pressure of 410 psi and 441 psi respectively while the RC 75 #4 cell held an average pressure of 400 psi. The RC 75 #4 cylinder showed no significant increases in pressure due to the fact that the cylinder was non-reactive and thus did not expand. The RC 200 #4 and #6 did see a slight increase in pressure which is attributed to Poisson's effect; however the increase in pressure was minimized by the accumulators.

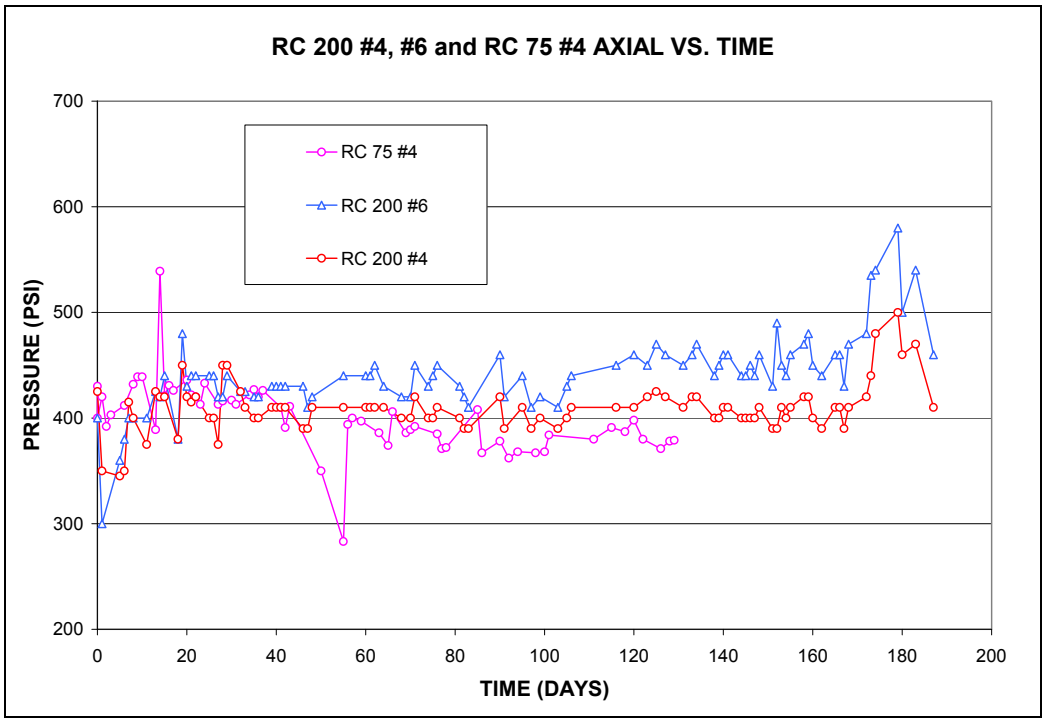

Figure 4.15: Axial Pressure versus time for each of the Hoek cells.

4.4.3 Confining and Axial Pressure Change with Time

Figures 4.16, 4.17 and 4.18 show the confining pressure and axial pressure versus time for the RC 200 #4, #6 and RC 75 #4 cylinders respectively. What is important to note is the addition of the accumulators to the testing setup was critical in maintaining a fairly constant axial pressure on the cylinders. This allowed for a better replication of the nominal dead loads that a structure would experience in the field.

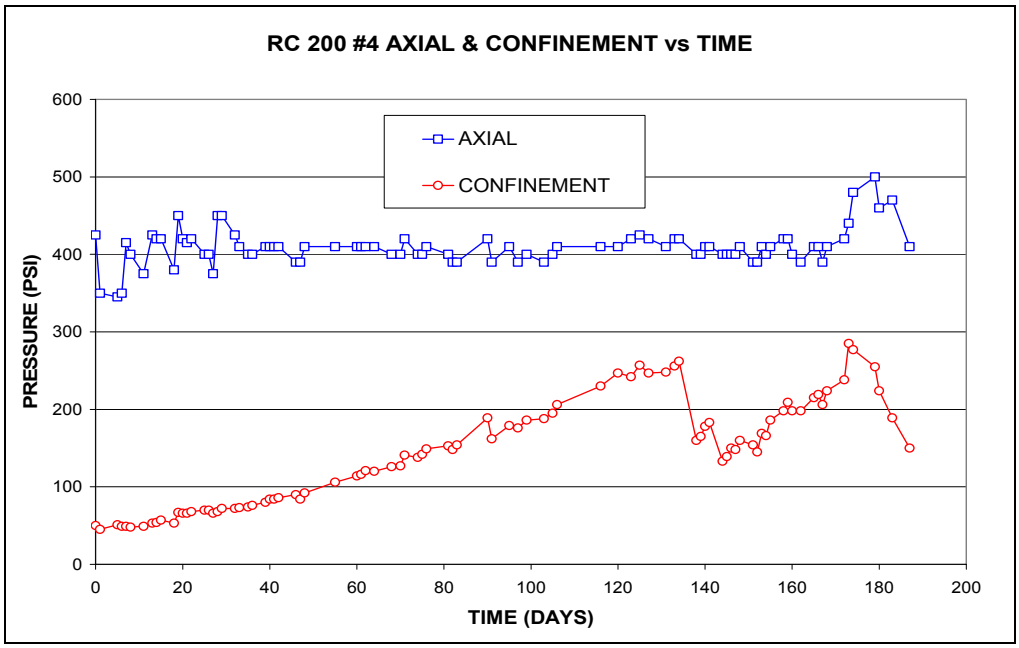

Figure 4.16: Axial and confining pressure versus time for RC 200 #4 cylinder.

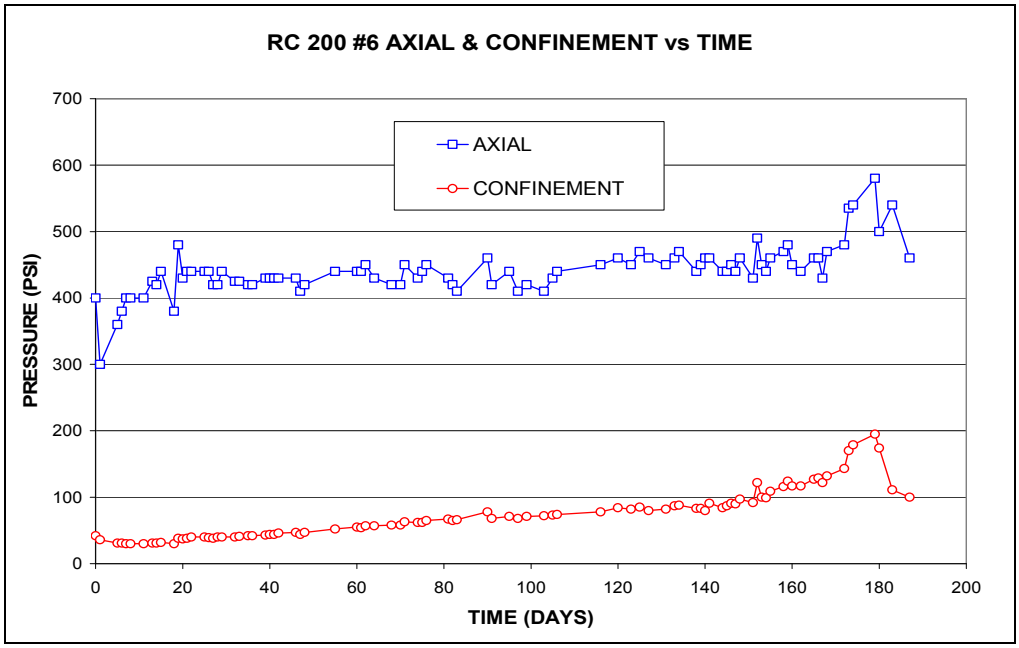

Figure 4.17: Axial and confining pressure versus time for RC 200 #6 cylinder.

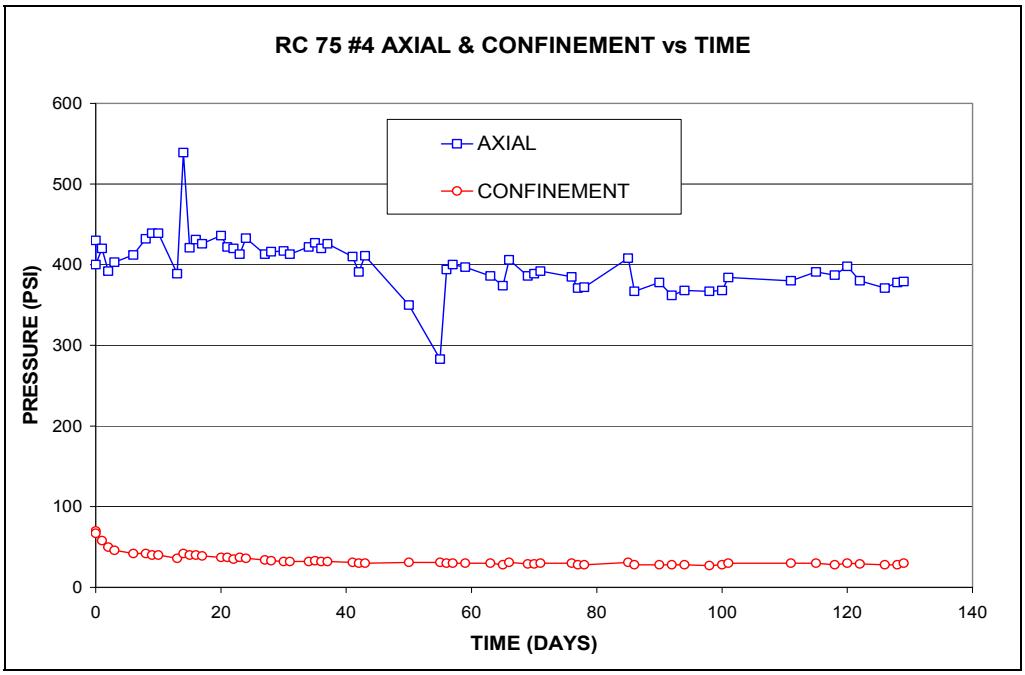

Figure 4.18: Axial and confining pressure versus time for RC 75 #4 cylinder.

4.4.4 Observations

After placement in the Hoek cells, all the cylinders required a few days in order for the confining pressure to stabilize. Once the confining pressure had stabilized the value was recorded and used as a zero pressure reading to obtain a net pressure increase at the end of the test. Both reactive cylinders, RC 200 #4 and #6, had different stabilization pressures, 50 psi and 30 psi, respectively. The initial stabilization pressure seemed to affect the final pressure as well as the rate of confining pressure over time. Towards the end of testing both reactive cylinders exhibited cyclic pressure behavior. This was originally attributed to suspected hydraulic leaks; however, this idea was nullified by the subsequent gain in pressure of the cylinders. As stated before the exact reason for this cyclic behavior is not known with any certitude at this time.

The RC 75 #4 cylinder, a non-reactive cylinder, performed as expected. After the initial pressure stabilization period this cylinder did not expand throughout the duration of testing and maintained a fairly constant pressure of 30 psi during the last 100 days of the 129 day test. This cylinder did validate the idea that non-reactive cylinders would not expand and thus no pressure gains would be experienced in the Hoek Cell test.

4.5 Test 3 Development and Testing

After the completion of test 2, two major questions were raised; first, is the cyclic behavior typical of this Hoek Cell setup? And second, does the initial confinement pressure affect the termination pressure of the test? With these questions in mind a third test was developed in order to answer these questions and is currently underway in the Hoek Cell setup.

4.5.1 Materials

A separate mix design, Hoek Cell 1 or HC 1, was developed specifically for the third round of Hoek cell tests. Concrete cylinders measuring 3.375 inches in diameter by 8 inches in height were made from a single mix that was subjected to the Fu heat treatment without the heat drying phase. The HC 1 consisted of a non-siliceous coarse aggregate, a mixed sand fine aggregate and a type III Portland cement. The mix was also doped with sodium hydroxide solution to bring the sodium hydroxide (NaOH) equivalent to 1.25% by wt. Table 4.3 lists the constituent materials of the HC 1 mix.

Table 4.3: Concrete mix proportions and materials.

HC 1 Mix	
lbs/yd^3	Material
752	Cement *PC - Type III*
1650	Coarse Aggregate *tan dolomite limestone*
1085	Fine Aggregate *mixed quartz, chert, feldspar sand*
0.45	w/c

4.5.2 Concrete Test Cylinders

The HC 1 cylinders were cast by using the same method described in section 4.1.4 using the light gauge sheet metal molds. A total of 20 cylinders were cast from the HC 1 mix. A total of 15 cylinders, HC 1 1-15, were subjected to the Fu heat treatment without the drying phase while the final 5, HC 1 16-20, were cured under normal conditions in a fog room. HC 1 cylinders 12-13 were stored continuously in the limewater storage environment and HC 1 cylinders 14-15 were stored continuously in the Hoek cell water environment. The water circulated through the Hoek cell setup has a small amount of Clorox in order to prevent the clogging of the water lines by mildew. HC 1 cylinders 12-15 served as a basis for direct comparison of the effects of the Clorox on the expansion of the cylinders and as can be seen in Figure 4.19 the amount of Clorox in the water circulated through the Hoek cells has no effect on the expansion of the cylinders.

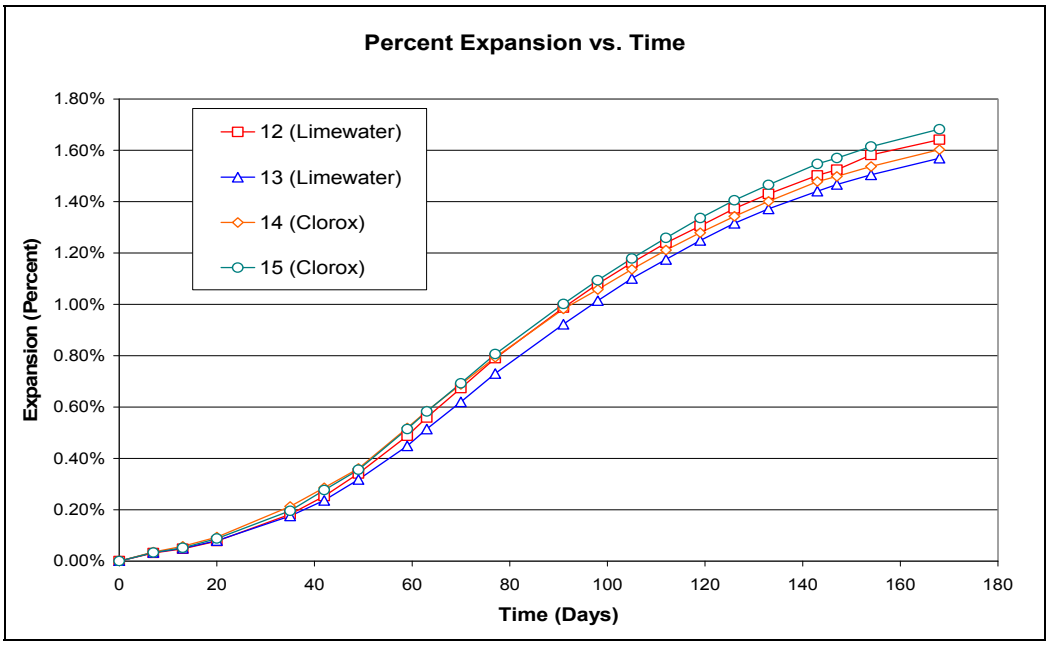

Figure 4.19: Percent expansion of HC 1 cylinders 12-15, 12 and 13 were stored in the limewater storage environment, 14 and 15 were stored in the Hoek cell water containing Clorox.

HC 1 cylinders 1-11 were initially stored in the limewater storage environment and then frozen once they surpassed 0.10% expansion. This was done to ensure that subsequent Hoek cell tests could be performed with cylinders that had minimal initial expansion to capture the full range of expansion within the Hoek cell test. HC 1 cylinders 10 and 11 were later unfrozen and put back into the limewater storage environment to validate that freezing the cylinders has no effect on the expansion of the cylinders after they have been frozen and then unfrozen. As can be seen in Figure 4.20 HC 1 cylinders 10 and 11 continue to expand normally once they have been unfrozen and put back into the limewater storage environment. Table 4.4 summarizes the testing matrix for the HC 1 mix.

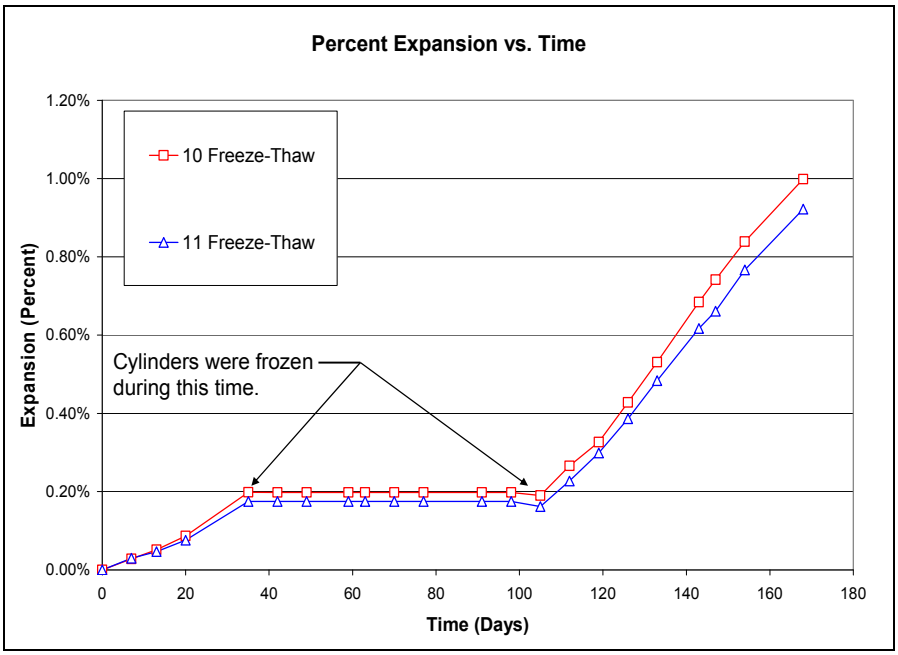

Figure 4.20: Percent expansion of HC 1 cylinders 10 and 11 stored in limewater, then frozen, then stored back in limewater.

Table 4.4: HC 1 testing matrix.

HC 1 Concrete Mix		
Cylinder #	Curing Treatment	Storage Environment
1 - 9	H	L, F
10 - 11	H	L, F, L
12 - 13	H	L
14 - 15	H	C
16 - 20	N. H.	L

H = Fu heat treatment without drying phase
N.H. = No heat treatment, fog room cured
L = Limewater storage
F = Freezer storage
C = Clorox water storage

After the termination of test 2, HC 1 cylinders, 1, 2, and 3 were placed in the Hoek cells to begin testing. The cylinders had been frozen due to the fact that test 2 was still ongoing when the HC 1 cylinders had surpassed 0.10% expansion. Prior to placement in the Hoek cells the HC 1 cylinders 1, 2 and 3 were allowed to thaw, measured, prepped and then stored in limewater for 48 hours prior to placement in the Hoek cells. Figure 4.21 shows the expansion of all three

cylinders before and after freezing and Table 4.5 summarizes the expansion of each cylinder prior to placement in the Hoek cells.

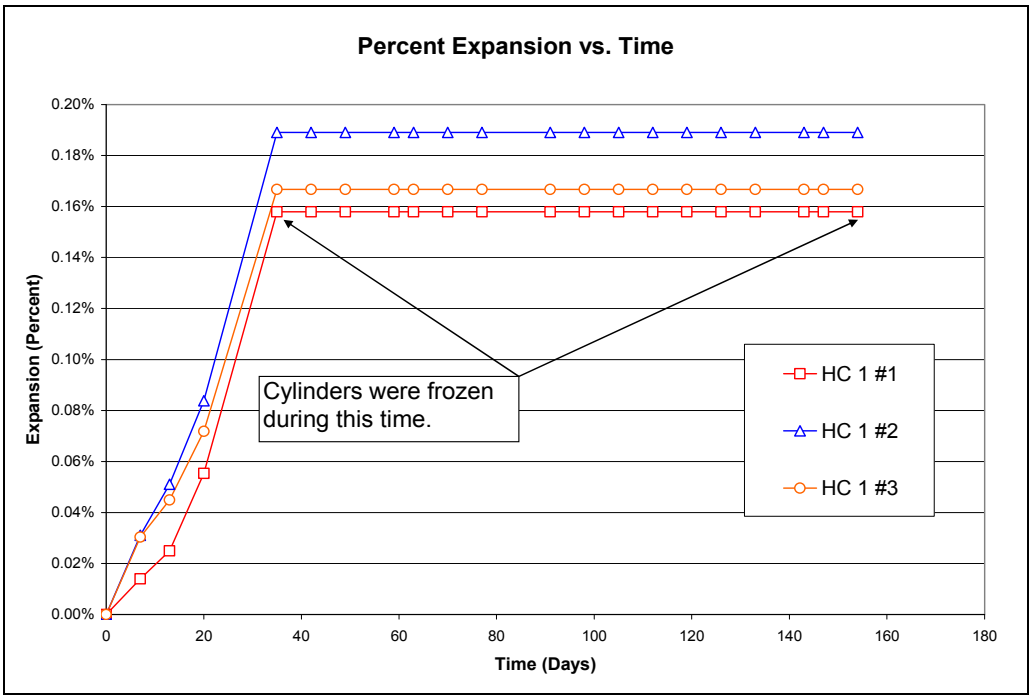

Figure 4.21: Percent expansion of HC 1 cylinders 1, 2, and 3 stored in limewater, then frozen, then placed in Hoek cells.

Table 4.5: Percent expansion of HC 1 cylinders prior to testing.

HC 1 Concrete Cylinders	Expansion (%)
#1 – Heat Cured	0.16
#2 – Heat Cured	0.19
#3 – Heat Cured	0.17

As stated before the HC 1 cylinders of test 3 are in the preliminary stages of testing and more time is needed to generate data and therefore any conclusions. The cylinders are following the same initial trends of test 2 and are entering the confinement stabilization period. The HC 1 cylinders seem to expand at a faster rate in limewater than the MC cylinders of test 1 or the RC cylinders of test 2, therefore the cylinders of test 3 are expected to reach a maximum confining pressure sooner than the previous two tests.

4.6 Hoek Cell Observations and Future Testing

Numerous trials were needed to modify and refine the Hoek cell testing apparatus for successful long term concrete DEF testing. After conducting two successful tests and starting a third, the modifications that were made for the test are effective. The results to date show that DEF requires at least 200-300 psi to laterally confine the expansive stresses that are generated, and the results show that this innovative technique shows great promise. More tests should be

run to validate the previous findings as well as investigate the final cyclic behavior that was seen in test 2. This section describes a couple potential avenues for future research, which are beyond the scope and resources of the current project. A greater number of tests with similar results will statistically validate the Hoek cell as a concrete DEF testing apparatus. Table 4.6 summarizes a future testing regime designed to confirm the findings of the first 3 Hoek cell tests.

Table 4.6: Future testing matrix to validate tests 1 - 3

Mix Design	Same as HC 1 (Table 4.3)
# of Cylinders	35, 30 heat cured, 5 non-heat cured
# of Hoek cell tests	10 (11 if using a non-heat cured cylinder)

Another testing regime worth investigating is the effect of the cyclic behavior on the design strength of the cylinder. The Hoek cells model what a structure would experience in the field if rehabilitated by an external mechanical confining method. However, as observed in tests 1 and 2 the cylinders have a tendency to cycle through expansions and contractions even under confinement. Initially cylinders would be tested in axial compression and splitting tensile to examine the effects of various levels of expansion on overall design strength. 10 cylinders, 5 in axial compression and 5 in splitting tensile, would be tested for each expansion increment of 0.1% from 0.0% up to 1.6% expansion for a total of 170 cylinders. Then cylinders would be placed in the Hoek cells and then tested in axial compression after a number of expansion and contraction cycles starting after the first decline in pressure and then in increments of 5 cycles. Each round of cyclic tests would require 3 cylinders and therefore if the cylinders were tested up to 15 cycles a total of 12 cylinders would be needed to complete the tests. More cylinders would be needed if various increments were to be repeated. Also a number of non-heat cured cylinders would be needed to act as controls. Overall this testing regime would require over 200 cylinders for testing. Table 4.7 summarizes the testing regime.

Table 4.7: Future testing matrix to examine cyclic expansion behavior.

Mix Design	Same as HC 1 (Table 4.3)
Total # of Cylinders	200+, 185+ heat cured, 15 non-heat cured
Total # of Hoek cell tests	4+ (0, 5, 10, 15 cycles)

Chapter 5. Model Columns

As part of Project 5218 two model columns were created to study the combined effects of ASR and DEF induced expansion on reinforced concrete elements. The columns were modeled after column DD7 in San Antonio and scaled down by a factor of 1/3.67. Four previous model columns were constructed by Jake Kapitan and mechanically cracked to create cracks similar to those observed in column DD7 (Kapitan 2006). The columns of this study are structurally similar to those tested by Kapitan, but have been made from concrete susceptible to ASR and DEF and placed in an environment favorable for accelerating ASR and DEF induced expansions. The following chapter describes the methods used to make the model columns and their expansions to date.

5.1 Concrete Trial Batching

The first step in creating the model columns was to design a concrete mix that would be most susceptible to ASR and DEF expansion. In addition, the concrete needed to be of a similar compressive strength as the previous model columns tested by Jake Kapitan which had 28-day strengths of about 4900 psi and ultimate strengths of about 5800psi. The concrete also needed to be fluid enough to be poured through the small spacing of the rebar cage. For this purpose a $^{3}/_{8}$ inch pea gravel was used as the coarse aggregate in the mix.

1. To create a concrete mix that would be highly susceptible to ASR and DEF the following measures were taken:
2. High content of Type III cement used to promote both ASR and DEF reactivity.
3. Sodium hydroxide added to the concrete mixture to increase the alkalinity of the cement paste and promote ASR and DEF reactivity.
4. Siliceous fine and coarse aggregate were used to promote ASR.
5. The concrete was heat cured at temperatures of up to about 205^{o}F to promote DEF.

To obtain the desired 28-day concrete strength of 4900 psi, a series of mixes with different water-to-cement ratios were tested. For each test mix an eight sack load of cement (752 lb/yd^3) and 1650 lb/yd^3 of coarse aggregate were used; the quantity of fine aggregate was adjusted depending on the amount of water used. Sodium hydroxide was added to each mix to raise the alkalinity of the mix to a sodium hydroxide equivalent level of 1.25%. The materials were pre-heated to 140 ^{o}F prior to mixing to help boost early curing temperatures. During mixing varying dosages of high-water-reducing admixture (HWRA) were used to achieve the desired fluidity – seven to nine inch slump. Concrete cylinders were cast from each mix and then heat cured in an oven that followed the temperature profile shown in Figure 5.1. The cylinders were then tested at 7-days and 28-days. Figure 5.2 shows the results from the trial concrete batches. Based upon these compressive strengths it was decided to use a water-to-cement ratio of 0.45 as this would provide a strength level similar to that of the previous model columns. Table 5.1 provides the materials and proportions used in the model column concrete.

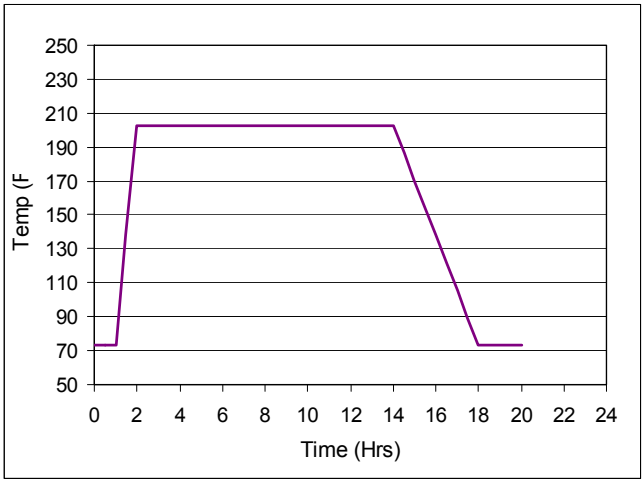

Figure 5.1: Oven curing temperature profile

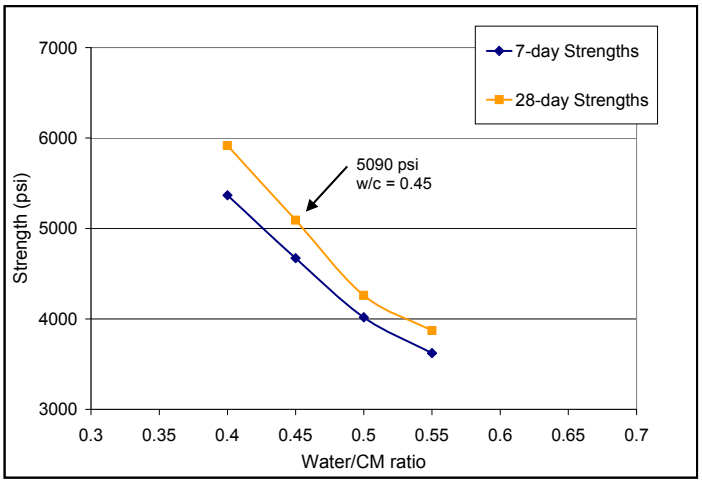

Figure 5.2: Compressive strengths of trial concrete batches

Table 5.1: Model column concrete mix.

	Material	Weight *(lbs.)*	Volume *(Cu. Ft.)*	BSG *(OD)*
Cement	Allentown Type III	752	3.83	3.15
Rock (OD)	3/8" Pea Gravel (TXI)	1650	10.37	2.55
Sand (OD)	Mixed quartz/feldspar siliceous sand (Wright)	1112	6.85	2.6
Water		338.4	5.42	1
Air*			0.53	-------
HWRA**	Glenium 3200 HES		varied	

* Assumed about 2% air content; ** Approx. 8 to 10 oz/cwt of HWRA was used

5.2 Casting the Model Columns

5.2.1 Tent Enclosure for Heat Curing

For the casting of the concrete columns a temporary outside enclosure was built to provide a large enough space for the heat curing of concrete. The enclosure shown in figure 5.3 was a metal frame structure with a plastic tarp covering and plywood siding along the base of the sides. The enclosure had slots where kerosene powered heaters were inserted to provide heating, illustrated in figure 5.4.

Figure 5.3: Heat curing enclosure for model columns

Figure 5.4: Kerosene heater used to heat tent enclosure

With the use of two kerosene heaters the temperature inside the enclosure could be raised to over 200^{o}F in about 15 minutes. During the actual heat curing of the model columns the temperature of the enclosure was adjusted depending on the internal temperature of the columns.

5.2.2 Concrete Mixing Procedure

To pour the columns a total of two 6 cubic foot batches of concrete were required per column, so four batches were done to pour the two columns plus one extra batch was made to make test cylinders. The two columns are referred to as column A and column B. To prepare for the pour the aggregates were first spun in a drum mixer to create uniform moisture levels for

accurate moisture correction calculations. Then all of the concrete materials—cement, aggregates and water—were weighed out and stored in sealed 5-gallon buckets that were placed inside a 140 ^{o}F oven for 18 to 24 hours prior to mixing. The preheating of the aggregate helped provide high initial placement temperatures of the concrete.

On the day of mixing two 9-cubic foot drum mixers were used simultaneously to ensure the columns were poured as quickly as possible. It was important that the columns be poured rapidly so that the temperature of the pre-heated materials would not be lost, and also to guard rapid setting of the concrete prior to pouring. During mixing HWRA was added to increase the fluidity of the concrete to a slump of at least 7 inches. Once the concrete was well-mixed and of a desirable fluidity, it was placed in wheelbarrows that were then lifted up by a fork lift so the concrete could be poured into the column forms. Column B was cast first and then column A was cast about 45 minutes afterwards. Figures 5.5 through 5.8 illustrate the pouring process.

Figure 5.5: HWRA used to increase concrete fluidity

Figure 5.6: Temperature of concrete during mixing

Figure 5.7: Pouring of the concrete into column forms

Figure 5.8: Tent enclosure wheeled over top of columns

The columns were poured in three layers and the concrete was vibrated with each layer. After the columns had been poured they were wrapped with plastic tarp, and the tent enclosure was wheeled over top of the columns. The sides of the tent were then closed and the heat curing process began.

5.2.3 Heat Curing

The temperature of the concrete at placement was about 120^{o}F. The columns were instrumented with thermocouples at the top, center, and bottom. The columns were enclosed within about 30 minutes after pouring, however due to technical difficulties the kerosene heaters used to heat the enclosure were not fully operating until 2 hours after pouring. Still the temperatures at the top and middle sections of the columns reached very high levels of up to 210 ^{o}F after about 5 hours of curing. Figures 5.9 and 5.10 illustrate the temperature profiles of the columns during curing. The kerosene heaters were turned off at about 6 hours for fear that the heat might boil the water in the columns. At about 10 hours the heaters were again turned on to keep the high internal temperature of the concrete at about 200 ^{o}F.

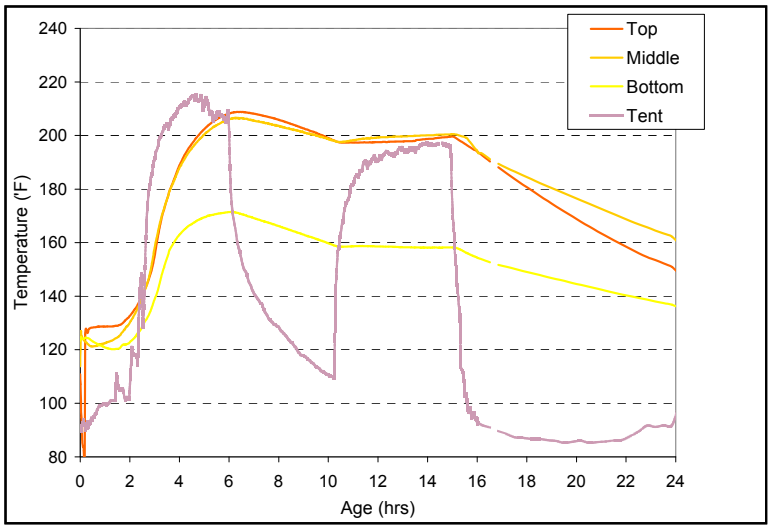

Figure 5.9: Internal temperature profile for Column A

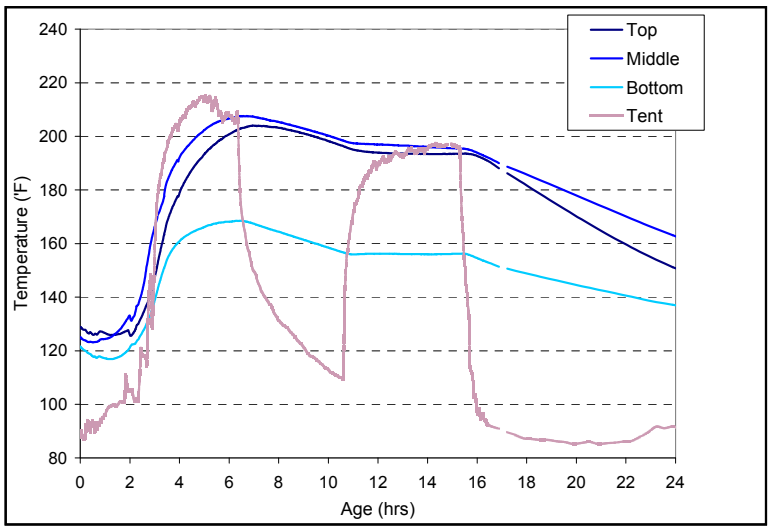

Figure 5.10: Internal temperature profile for Column B

As illustrated by the above Figures the internal temperature of the top and middle sections of the columns reached about 200°F or greater; however the lower section, which was located about 6 inches from the base of the column, did not reach the same high temperatures. This was due to the large concrete footing beneath both columns which acted as a heat sink. Still the lower section of the columns reached temperatures above the 160°F necessary to promote DEF.

5.2.4 Concrete Cylinders

Concrete cylinders were taken from three of the five batches of concrete made for the casting of the model columns. The concrete came from batch number 2 which was used to cast column B, batch number 4 which was used to cast column A and batch number 5 which was used to make a number of test cylinders.

From each of the three batches sampled, 6” diameter by 12” cylinders were made for strength testing at 28-days and ultimate. The 6” by 12” cylinders were caped and placed inside the tent with the model columns during curing. These cylinders are to be used for comparison with the previous testing done by Jake Kapitan. The cylinders have been left in their plastic molds until testing and have not been subjected to an accelerated environment that might deteriorate the concrete.

From batch 4 and 5 a number of 4” diameter by 8” cylinders were made for the purpose of subjecting the concrete to various storage environments to determine the potential for ASR and DEF induced expansion and also the ultimate effects such expansion would have on the modulus and strength of the concrete. The 4” by 8” cylinders were heat cured in the oven according to the temperature profile shown in Figure 5.1. Table 5.2 details the quantity and storage environment of the cylinders.

Table 5.2: Concrete Test Cylinders made from column pour batches

Concrete Batch	6" dia. by 12" Cylinders *(cured with columns)*	4" dia. by 8" Cylinders *(Oven heat curing, Fig. 5.1)*
Column B (2nd mix)	[3] compressive strength testing at 28-days and prior to column load testing	----------
Column A (4th mix)	[3] compressive strength testing at 28-days and prior to column load testing	[4] Expansion measurements and testing at 28-days and ultimate
5th mix	[6] compressive strength testing at 28-days and prior to column load testing	[12] Expansion measurements and testing at 28-days and ultimate

5.3 Instrumentation for Expansion Measurements

5.3.1 External Instrumentation

To measure the horizontal and vertical expansion of the column, demec points were mounted at various heights. To mount the demec points, holes were first drilled to insert $^{3}/_{8}$” threaded rod to which the demecs could be mounted securely at the ends using a two part epoxy. The threaded rods were inserted up to about ¾” or the depth of the cover and secured with a similar two part epoxy. A 19.69” (50cm) Mayes gauge was used to take measurements of vertical and horizontal distances on the long faces of the column, as illustrated in Figure 5.11. The 19.69” gauge was also used to take vertical measurements on the short faces of the column; however a shorter, 5.9” (15cm) Mayes gauge was used to measure the horizontal distances, as illustrated by Figure 5.11. The gauges are precise to ± 0.00005 inches.

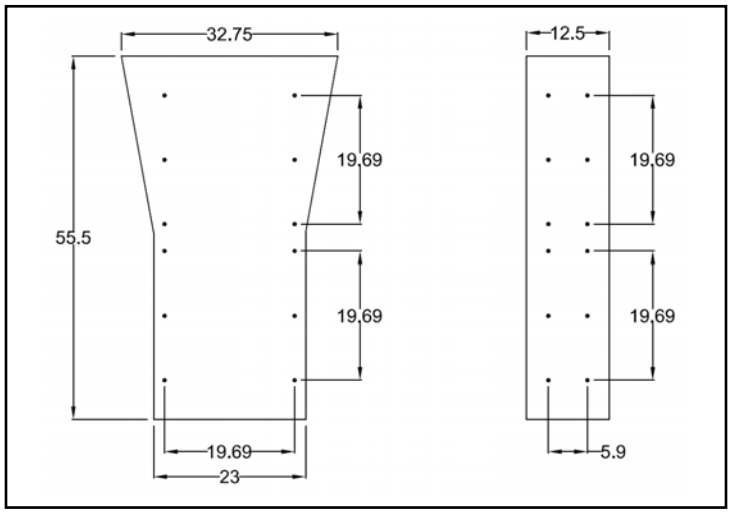

Figure 5.11: Demec point layout for measuring external expansion.

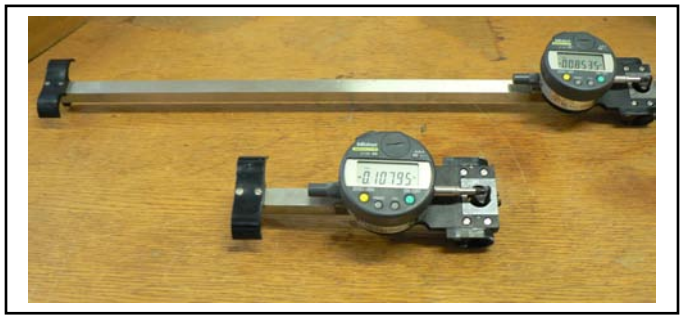

Figure 5.12: Mayes Gauges; 19.69" (50cm) and 5.9" (15cm) respectively.

5.3.2 Internal Instrumentation

To measure the expansion inside the column, vibrating wire gauges 7 inches long were placed at the top of the columns where the greatest amount of expansion was expected to occur. Three gauges were placed in each of the columns at the center of the column about 6 inches from the top. One gauge was oriented vertically to measure vertical expansion and the other two gauges were oriented parallel to the long and short faces of the column to measure horizontal expansions.

5.4 Long-term Environment

To accelerate ASR and DEF in the concrete columns a water supply system was installed. A soaker hose was placed around the top of the column to act as a shower head, as illustrated by Figure 5.13. The column was then wrapped with a two sided material called "burlene" that has a felt interior with a plastic exterior. The burlene wrap is held to the surface of the column by nuts and washer attached to the threaded rod inserts, as illustrated by Figure 5.14. The burlene wrap helps retain moisture and keep the surface of the concrete wet and from drying out. The soaker hose runs four times a day at 8:00am, 12:00pm, 4:00pm, and 10:00pm for about 1 minute.

Figure 5.13: Soaker hose watering system.

Figure 5.14: Burlene Wrap to hold in moisture.

5.5 External Post Tensioning System

A post-tensioning system incorporating the use of springs and Dywidag tie bars was used to place an axial load on the columns similar to the estimated service load of the full-scale columns in San Antonio. Details of the post tensioning system will be provided in future work by Kim Grau.

The loading of the concrete columns did introduce some longitudinal strain in the columns which was measured immediately after loading the columns. Table 5.3 shows the axial strain introduced into the columns and the estimated load placed on both columns. With this information it is possible to calculate an effective modulus of the column and also the modulus of the concrete by assuming a ratio of steel of about 1% with a modulus of 29,000 ksi. Table 5.3 shows the estimated effective modulus of the column and of the concrete.

Table 5.3: Estimated elastic modulus of the columns.

Column	A	B
Strain *(in./in.)*	0.02%	0.02%
Load *(kips)*	196	178
Area *(in.2)*	306	306
Load *(ksi)*	0.64	0.581
E-Mod *(ksi)*	3621	3476
E-Mod* *(concrete, ksi)*	3365	3218

* Assuming about 1% steel

Figure 5.15: Post-tensioning system for simulating service load conditions.

5.6 Expansion Measurements

External expansion measurements began 21 days after casting the columns at about the same time the watering system was installed to provide moisture to the concrete. However it should be noted that the time shown on the plots begins with the actual day of casting. Measurements have been taken every two to three weeks over the past year and a half. The measurements have also been corrected for loss of demec points.

Occasionally demec points would be lost and expansion data would be lost for that time period. To correct for the missed data an estimated expansion rate for that period of time was calculated as an average of the rates from the measurement periods immediately prior to and after the period of missed data. This correction method was shown to produce results consistently within ±0.03% of the actual expansion value.

5.6.1 External Transverse Measurements: Column A

Figures 5.16 and 5.17 illustrate the transverse expansion with age of column A. Both sides of the column have shown high levels of expansion after 617 days of testing.

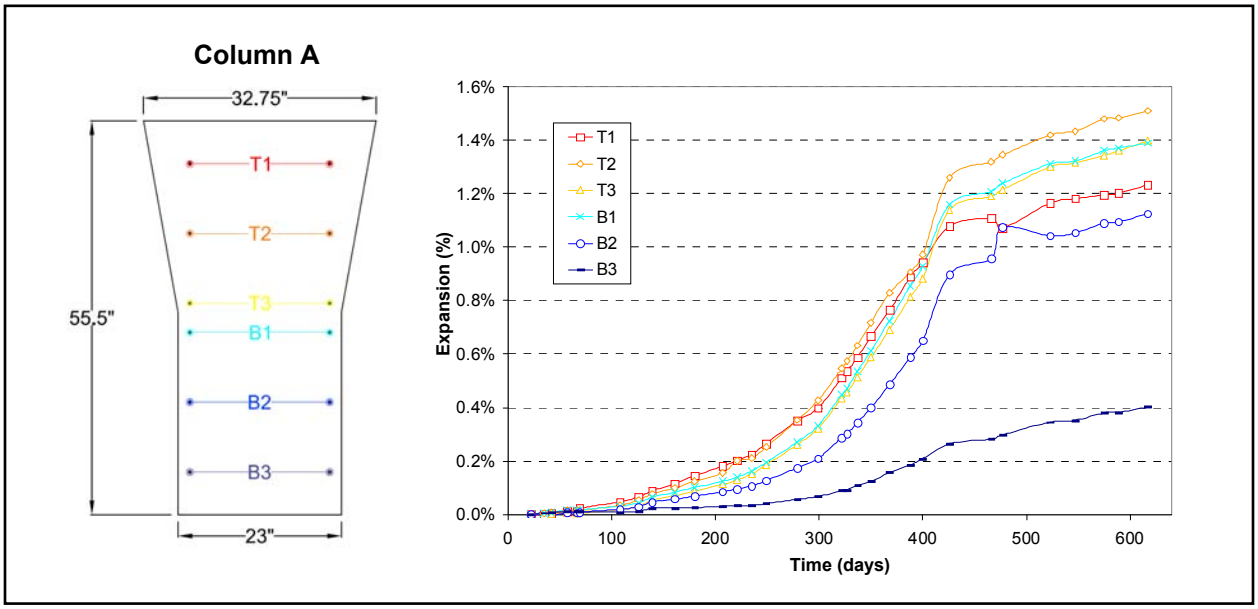

Figure 5.16: Average transverse expansion of the long side of column A.

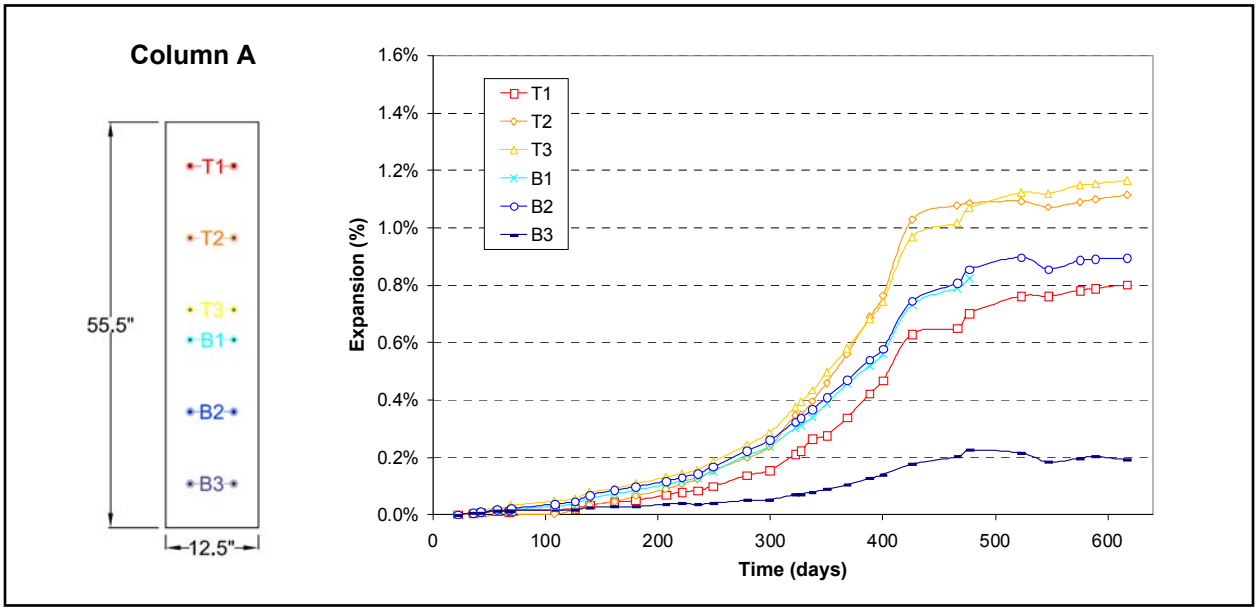

Figure 5.17: Average transverse expansion of the short side of column A.

Figures 5.18 and 5.19 provide a profile view of the expansion based on the location of the measurement relative to the height of the column. Figures 5.18 illustrates how the column is expanding most near the top and middle section of the column which is likely due to the higher curing temperatures that the upper sections of the column experienced. However, in Figure 5.19, the short sides of the column are expanding less near the top of the column. This is likely due to the restraint of the bearing surface along the top of the short side.

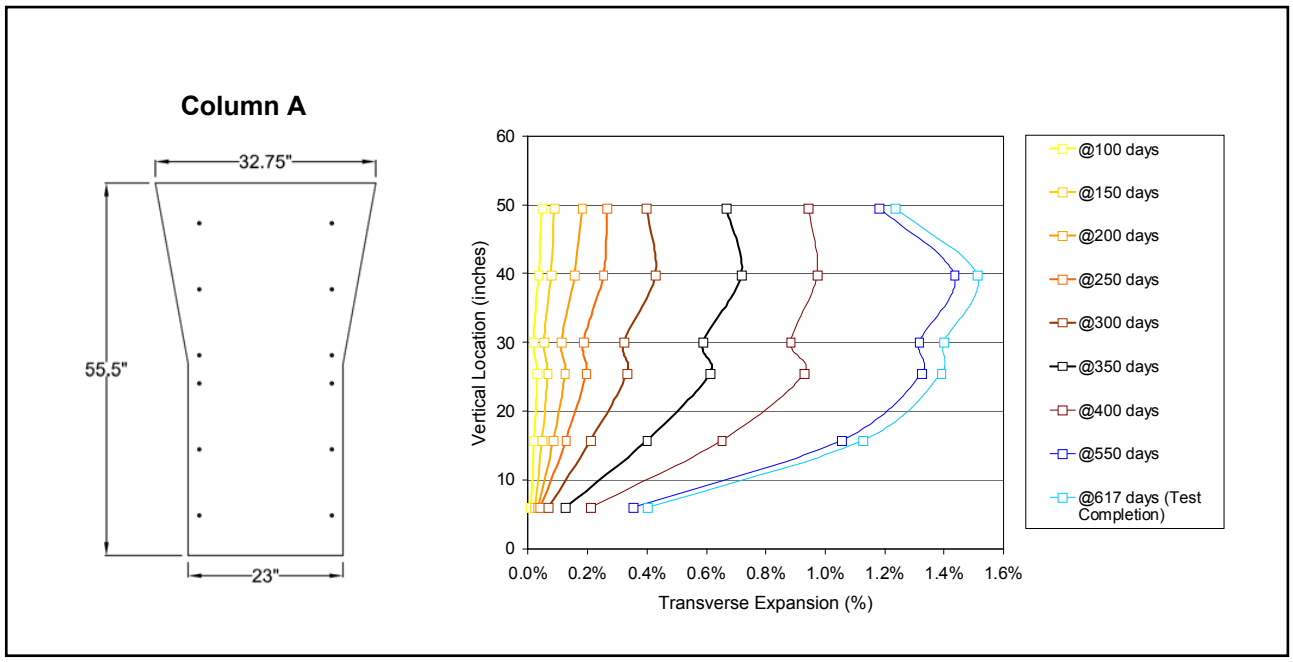

Figure 5.18: Profile plot of transverse expansion of the long side of column A.

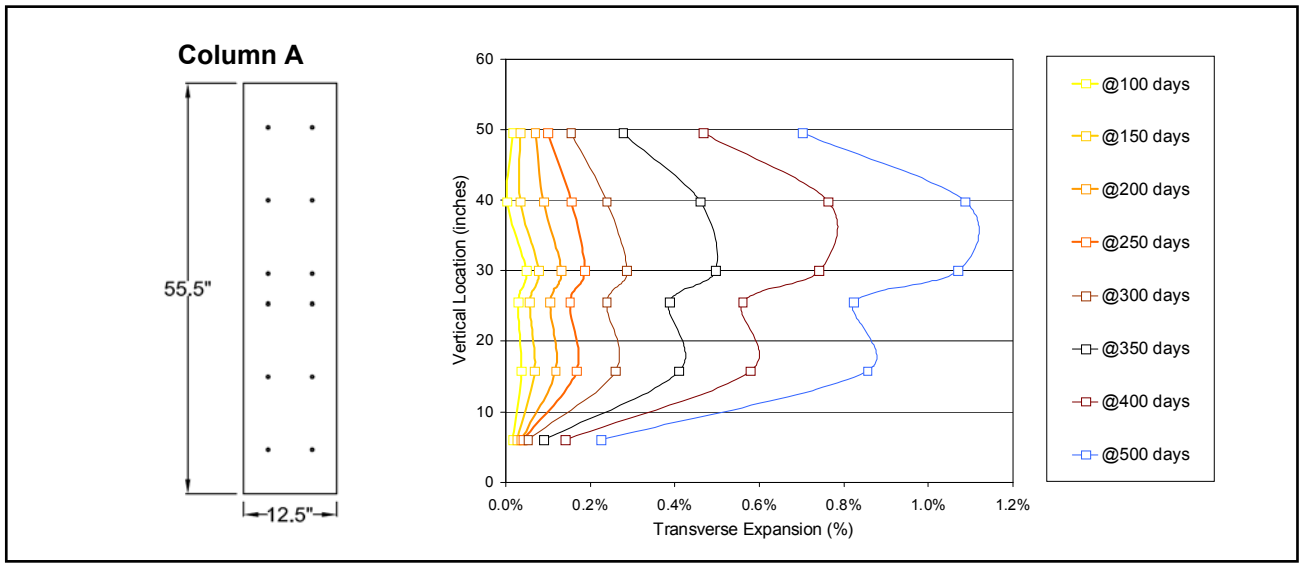

Figure 5.19: Profile plot of transverse expansion of the short side of column A.

5.6.2 External Transverse Measurements: Column B

Figures 5.20 and 5.21 illustrate the transverse expansion with age of column B. Both sides of the column are showing high levels of expansion at about 380 days.

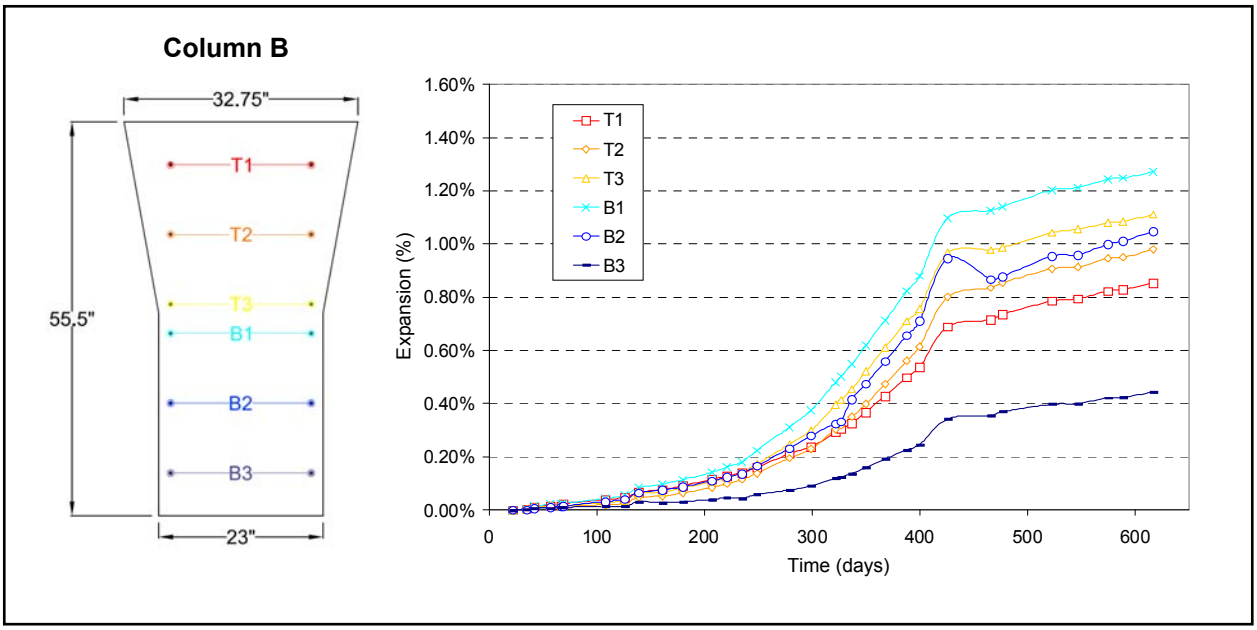

Figure 5.20: Average transverse expansion of the long side of column B.

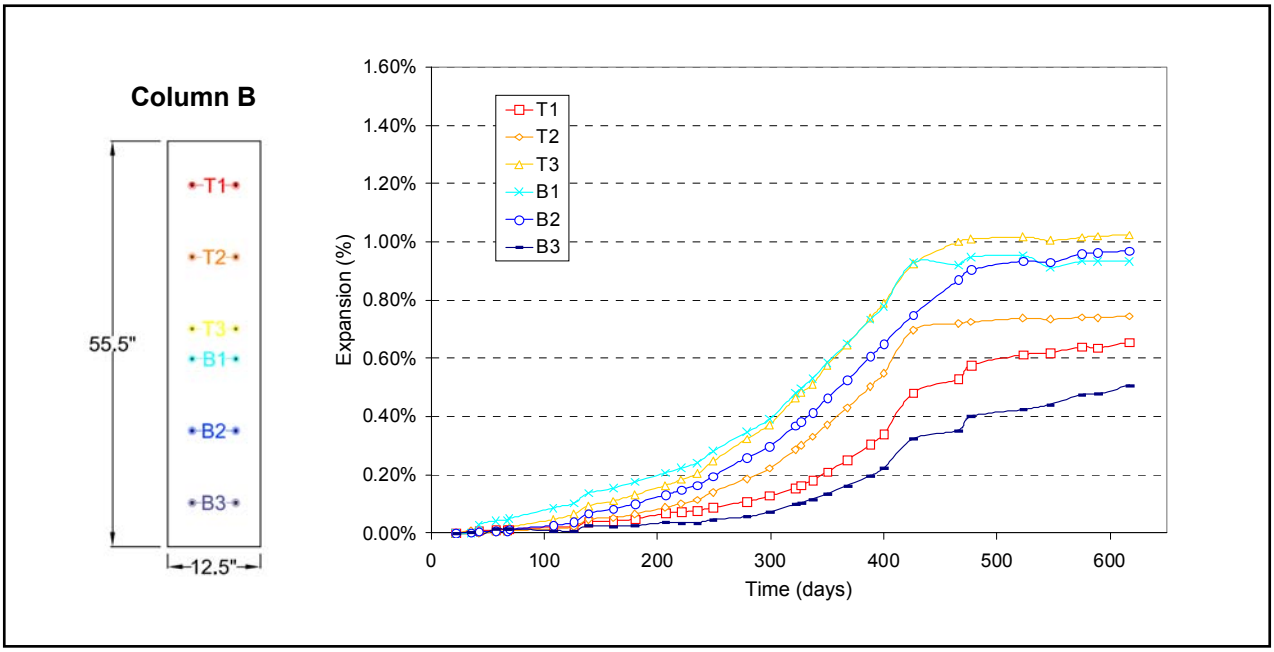

Figure 5.21: Average transverse expansion of the short side of column B.

Figures 5.22 and 5.23 provide a profile view of the expansion based on the location of the measurement relative to the height of the column. Unlike the expansion of column A near the top of the column (Figure 5.18), the expansion of the top measurements on column B is not nearly as great. One possible explanation for this phenomenon is that the measurements are closer to transverse reinforcement ties that are providing more local restraint. However it is difficult to determine if location of the external measurements in relation to the transverse rebar ties because the spacing of the ties is less than 3 inches.

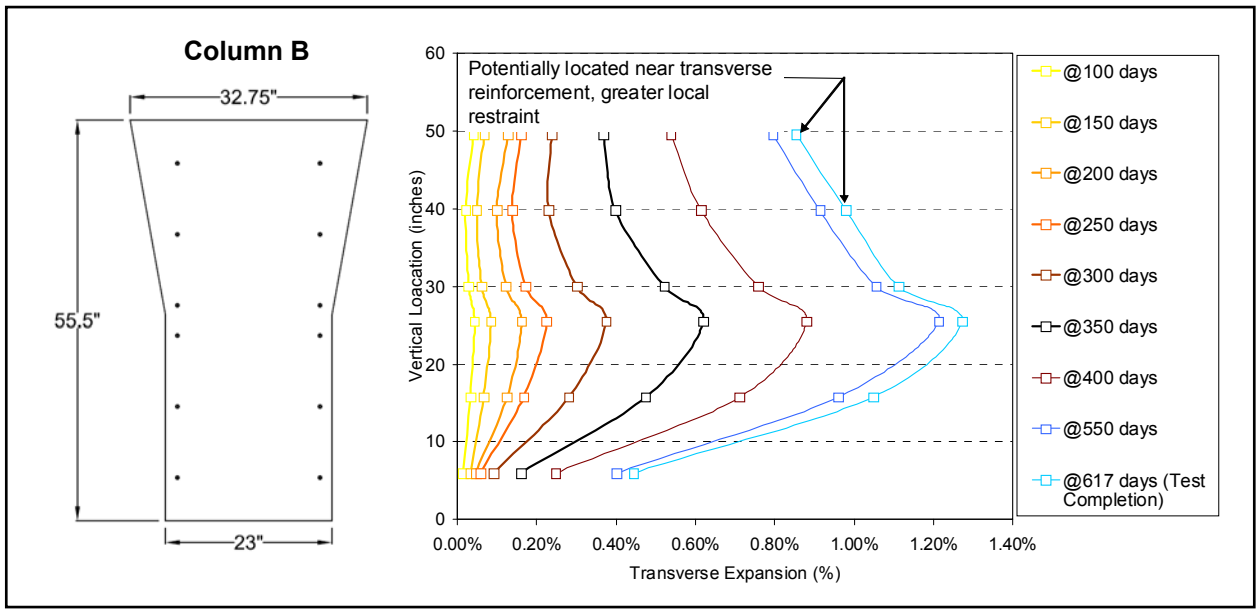

Figure 5.22: Profile plot of transverse expansion of the long side of column B

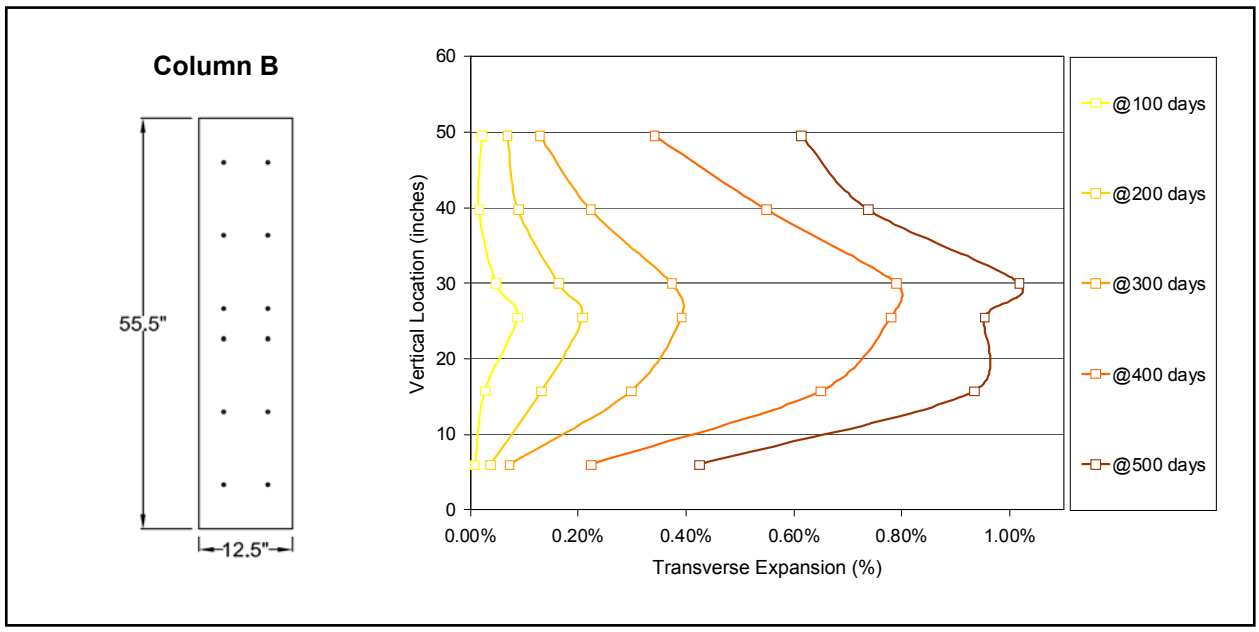

Figure 5.23: Profile plot of transverse expansion of the short side of column B.

Similar to column A, the short side of column B is expanding the most near the center of the column. It is postulated that the bearing restraint at the top of the column is likely restraining the top from expanding.

5.6.3 External Longitudinal Measurements

The columns experienced some initial longitudinal expansion due to water absorption from the watering system that was installed at about 21 days after casting. At 56 days the

columns were loaded using an external post tensioning system which caused some degree of elastic shortening as evident by Figure 5.24. Then after about 150 days the columns both began to expand vertically. It seems apparent that despite the 600 psi of applied load, the ASR and/or DEF induced stresses are still able to cause vertical expansion of the concrete elements.

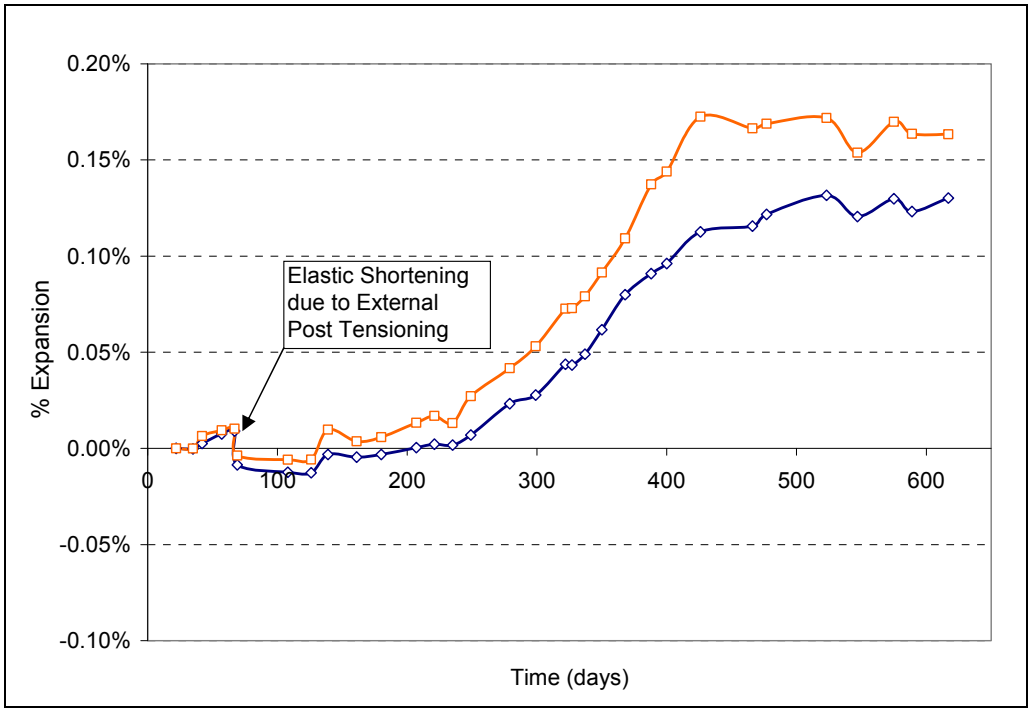

Figure 5.24: Longitudinal Expansion Measurements of the Model Columns.

5.7 Testing of Concrete Cylinders

A number of concrete cylinders were made during the casting of the model columns as discussed in section 5.2.4. The 4" diameter by 8" cylinders were heat cured according to the temperature profile illustrated in Figure 5.1. These cylinders were stored in a fog room at 72°F until 28-day testing. After 28-day testing the remaining cylinders were placed in either limewater solution or above water in sealed 5 gallon buckets that were placed inside a 100°F oven (similar to ASTM C 1293 storage). Demec points were initially placed on the cylinders that were stored long-term and expansion measurements were taken about once a month.

In addition to the cylinders taken from the batches used to pour the model columns, another similar batch of concrete was made a few weeks after pouring the columns and was used to make cylinders that were match cured according to the actual temperature-time profile of the columns. Since the cylinders made from the actual column batches were not cured along the same temperature-time profile as the columns, the match-cured cylinders were made to provide a more similar comparison with the columns. The two different temperature-time profiles used for the column batch cylinders and the match cured cylinders is shown by Figure 5.25. The match cured cylinders were stored in the fog room until 28-day testing and then the remaining cylinders were placed in limewater or above water storage similar to the column cylinders. Expansion measurements were taken along with the column cylinder expansion measurements.

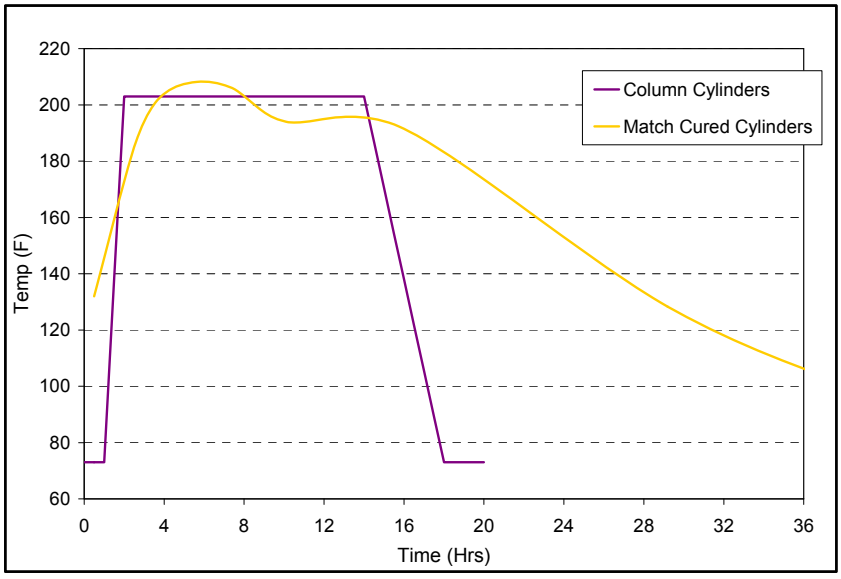

Figure 5.25: Temperature-Time Profile for Column Cylinders and Match Cure cylinders.

The column cylinders and the match cured (MC) cylinders expanded rapidly in both the limewater and above water environments. In the limewater environment the column cylinders and MC cylinders expanded at very similar rates as illustrated by Figure 5.26. In the above water at 100°F storage environment the column cylinders expanded more rapidly than the MC cylinders, illustrated by Figure 5.27; though both sets of cylinders expanded to very high levels of expansion. Severe surface cracking appeared at about 0.5% expansion and continued to grow in severity and crack size with expansion.

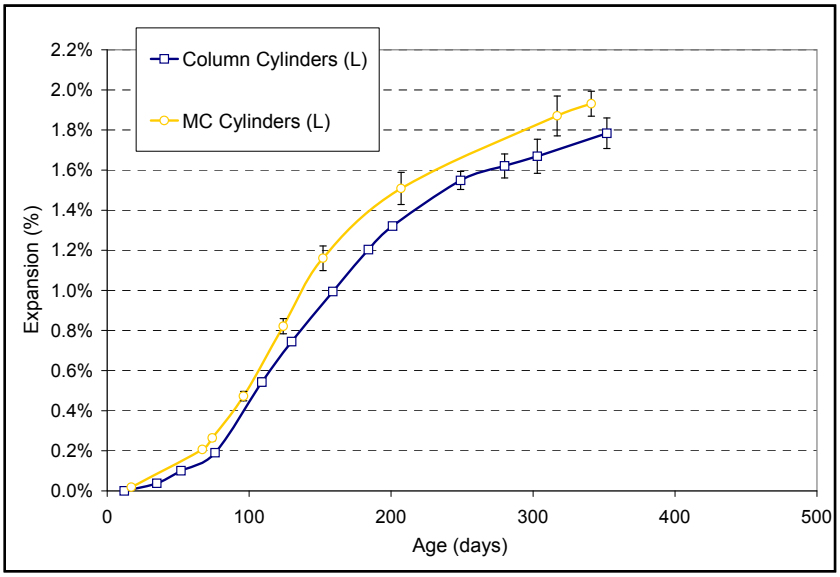

Figure 5.26: Expansion of Cylinders stored in Limewater (L).

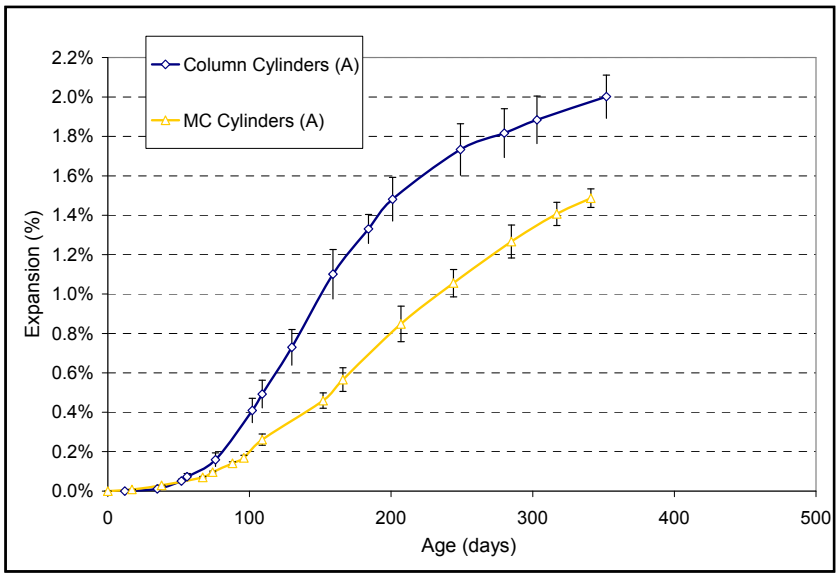

Figure 5.27: Expansion of cylinders store Above Water at 100°F (A).

5.8 Summary

This chapter summarized large-scale evaluation of concrete elements subjected to ASR and DEF. Significant information was gathered on the generation of expansive strains and the interplay between expansion and structural confinement. This study represents the first time that specimens of this size were cast and subjected to heat curing to trigger DEF – a similar approach has since been followed in other TxDOT-funded projects. The structural impact of ASR and/or DEF was not discussed herein but was and is the subject of various projects ongoing in Texas.

Chapter 6. Reinforced Columns

In an effort to answer some of the questions raised with regards to the results of the model column testing, another set of reinforced concrete elements have been created to look at how the DEF-induced strains are distributed within a reinforced concrete element.

6.1 Reinforced Column Purpose and Design

The purpose of the reinforced blocks is to determine how transverse reinforcement in a reinforced-concrete element will be affected by DEF induced strains and how it might affect the distribution of DEF induced strains within the concrete element. Two similar blocks were made and an external post-tensioning system was used to apply an axial load of about 400 psi in order to mimic the service state of a concrete column. A number of different types of strain measurement gauges and methods have been employed to measure both the internal and external expansion of the concrete and transverse reinforcement.

6.1.1 Design of the Reinforced Columns

The reinforced columns are not meant to model an actual structural element but rather to mimic a typical section from a structural element such as a column that supports a constant axially applied dead load. The columns were designed to have #3 closed stirrups at 6 inch spacing with 2” cover from center-of-rebar. The longitudinal reinforcement consists of four #7 bars located at the four corners of the block. Figure 6.1 illustrates the reinforcement layout.

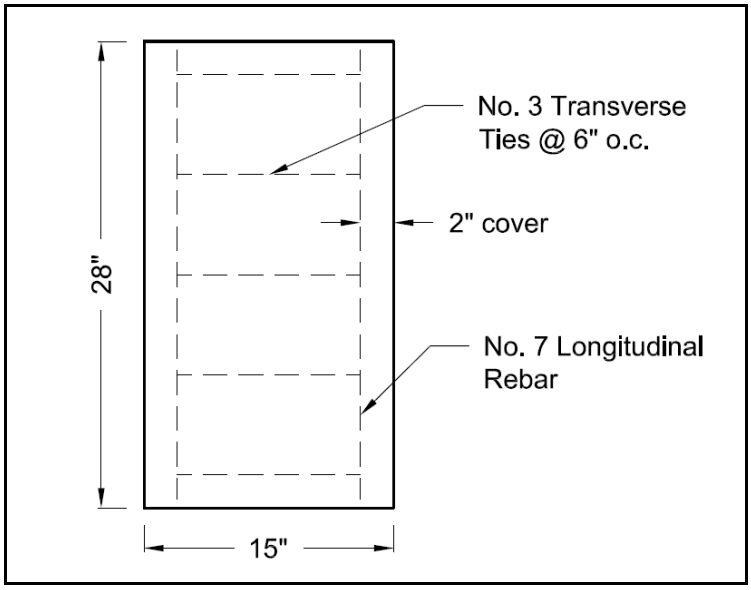

Figure 6.1: Reinforcing Layout for Blocks

6.1.2 Concrete Mix Design

The Reinforced Column or RC mix used the same materials as the mini columns mix mentioned in section 5.1. The reinforced columns were also subject to a heat curing regime that is later described in section 6.1.4. The RC consisted of a non-siliceous coarse aggregate, a siliceous fine aggregate and a type III Portland cement. The mix was also doped with sodium hydroxide solution to bring the sodium hydroxide (NaOH) equivalent to 1.25% by wt. Table 6.1 lists the constituent materials of the RC mix.

Table 6.1: Concrete mix proportions and materials.

RC Mix	
lbs/yd^3	Material
752	Cement *PC - Type III*
1650	Coarse Aggregate *tan dolomite limestone*
1085	Fine Aggregate *mixed quartz, feldspar siliceous sand*
0.45	w/c

6.1.3 Pouring the Reinforced Columns

Both columns were cast and placed at the same time to ensure similar curing regimes, and both were subjected to high temperatures to ensure the triggering of DEF.

6.1.4 Heat Curing Regime

The heat curing regime was similar to the one used for the Mini Columns. However, the Reinforced columns were cast in standalone molds, not on large footings, and cured in an oven. Without a large footing to act as a heat sink the Reinforced Columns were able to reach identical temperatures throughout the entire depth of the section avoiding what was observed in the temperature profiles of the Mini Columns in section 5.2.3.

6.1.5 External Post Tensioning

A post-tensioning system incorporating the use of springs and Dywidag tie bars was used to place an axial load on the columns similar to the system used for the mini columns as described in section 5.5. Both Reinforced Columns were placed in the same loading frame and separated with a bearing pad. This was done to ensure that both columns were subjected to the same loading. A 400 psi load was applied to the Reinforced Columns to simulate a nominal service load. Demec points were also placed on both Dywidag bars and springs to measure any stress changes that occurred. Prior to the placement of the reinforced columns in the post-tensioning frame the modulus of the Dywidag bars as well as the spring constants were measured in order to calculate stresses based on displacements of either springs or bars.

6.2 Instrumentation for Expansion Measurements

6.2.1 Internal Instrumentation

The primary strain gauge being used to measure the internal expansion of the concrete is a vibrating wire gauge (VWG) with a gauge length of about 6.75". Figure 6.2 illustrates the layout of the VWG's. At the center of the block where the central stirrup is located, four vibrating gauges have been placed. Two of the gauges, labeled 1.A and 2.A, have been securely attached to the stirrup with a high strength epoxy. The purpose of these gauges is to measure the actual strain in the rebar. The intermediate gauges, labeled 3.A and 4.A have been placed at the center of the block with gauge 3.A located just inside the stirrup and gauge 4.A extending out past the stirrup to the edge of the cover. The purpose of these two gauges is to determine if there is a significant strain differential between the concrete located within the stirrups versus the cover concrete. At section B-B a set of VWG's has been placed that mirror the gauges at section A-A but are located between stirrups to determine how DEF induced strains might differ away from the transverse rebar. A fifth VWG, 5.A, is located at the center of the block and oriented with the longitudinal axis of the block to measure axial strains.

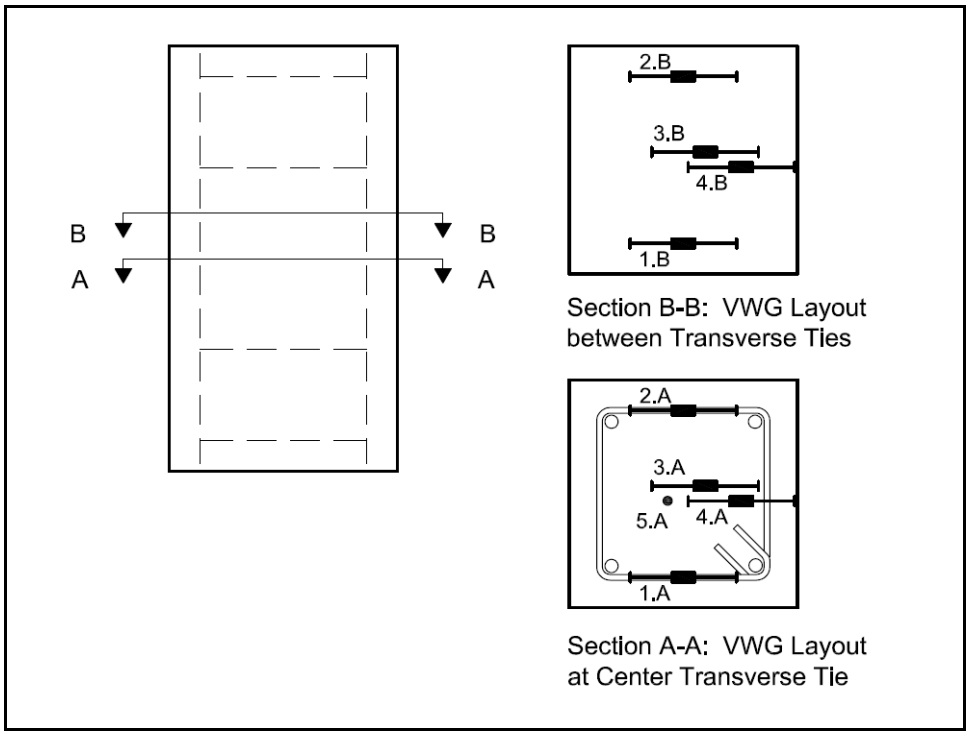

Figure 6.2: Vibrating Wire Gauge Layout

In addition to the vibrating wire gauges, foil strain gauges were mounted to the stirrup located just above the middle stirrup, as illustrated by Figure 6.3.

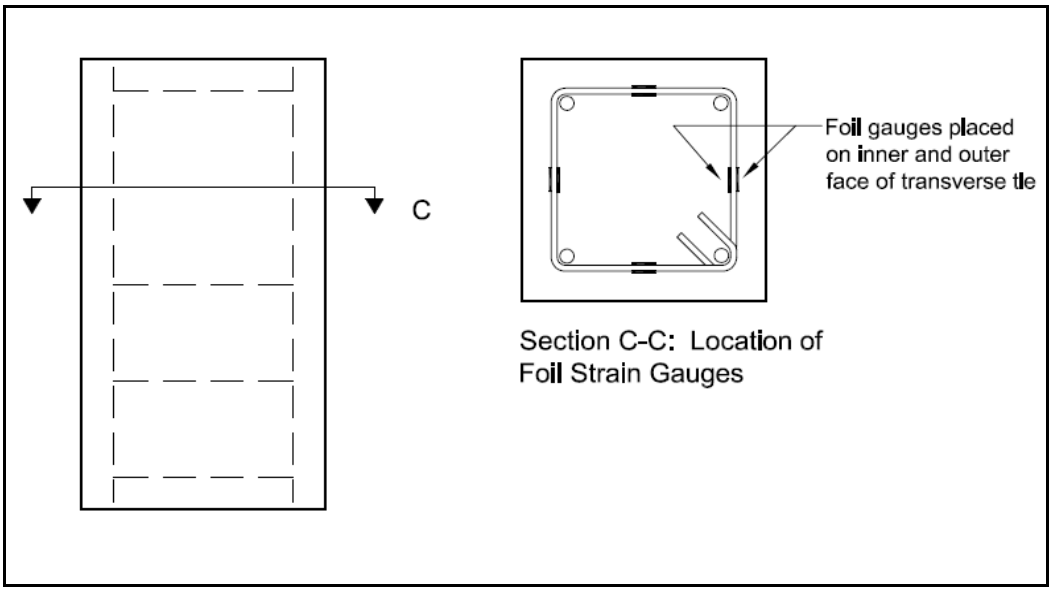

Figure 6.3: Foil Strain Gauge Arrangement. The foil gauges are mounted to the inner and outer surface of the stirrup on all four sides.

6.2.2 External Instrumentation

To measure the vertical and transverse expansion demec points, identical to the ones used on the model columns mentioned in section 5.3.1, were directly adhered to the surface of the reinforced columns with a ceramic epoxy. Mayes gauges were used to measure the changes in length of the demec points and the expansion between each gauge length was calculated. Figure 6.4 illustrates the placement of the demec points on the surface of each reinforced column. Figure 6.4 not only shows the placement of the demec points with respect to transverse reinforcing ties, but also shows the lines of measurement for both the vertical and transverse directions. Each reinforced column has 9 transverse and 3 vertical measurements; each transverse and vertical measurement is comprised of two measurement lengths that were averaged to get the expansion across the column. The same procedure in section 3.2 was used to replace demecs that had fallen off or had surpassed the range of the Mayes gauge to obtain continuous data.

Crackmeters were also used to measure the displacement at the surface of the cracked elements. Figure 6.5 shows the placement of the Crackmeters on the reinforced blocks.

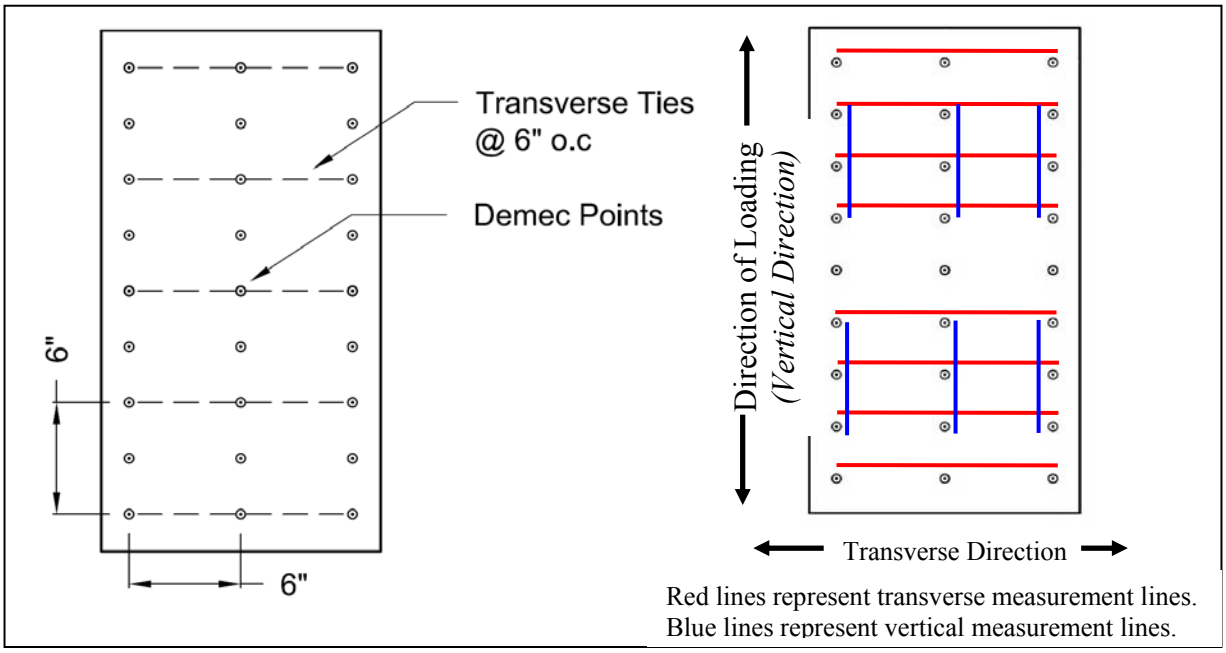

Figure 6.4: Placement of demec points and measurement lines.

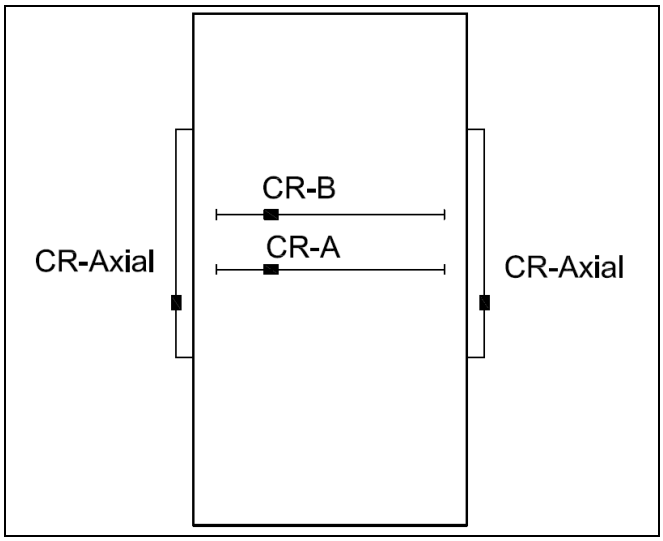

Figure 6.5: Placement of Crackmeters on the reinforced Columns.

6.3 Results of Reinforced Column Testing

The following data is from the testing of the reinforced column to date. The reinforced columns have been in the water storage environment for over 300 days. The reinforced column will remain submerged in the water trough indefinitely and monitoring will continue, followed by forensic evaluations.

6.3.1 External Expansion Measurements: Column A

Figure 6.6 and 6.7 show the transverse and vertical expansion to date of Column A in increments of 50 days respectively. Column A expanded significantly in both directions, more so in the transverse direction mostly due to the fact that this direction is perpendicular to the direction of loading. In Figure 6.6 the zero inch measurement is the contact point between the reinforced column and the post-tensioning system, the 28 inch measurement is the contact point between Column A and the bearing pad separating both Columns A and B. Figure 6.6 also shows the restraining effect that the post-tensioning system has on the column as the side nearest the loading bars has the smallest observed expansion. What is also important to note is that transverse demec lines 1, 3, 5, 7, and 9 are located above the transverse ties as mentioned before. Theoretically these demec lines should expand less than the others due to the fact that the transverse ties beneath them provide greater restraint to expansion. Demec line 7 in Figure 6.6 shows more expansion than the demec lines 6 and 8, which are not located above transverse reinforcement.

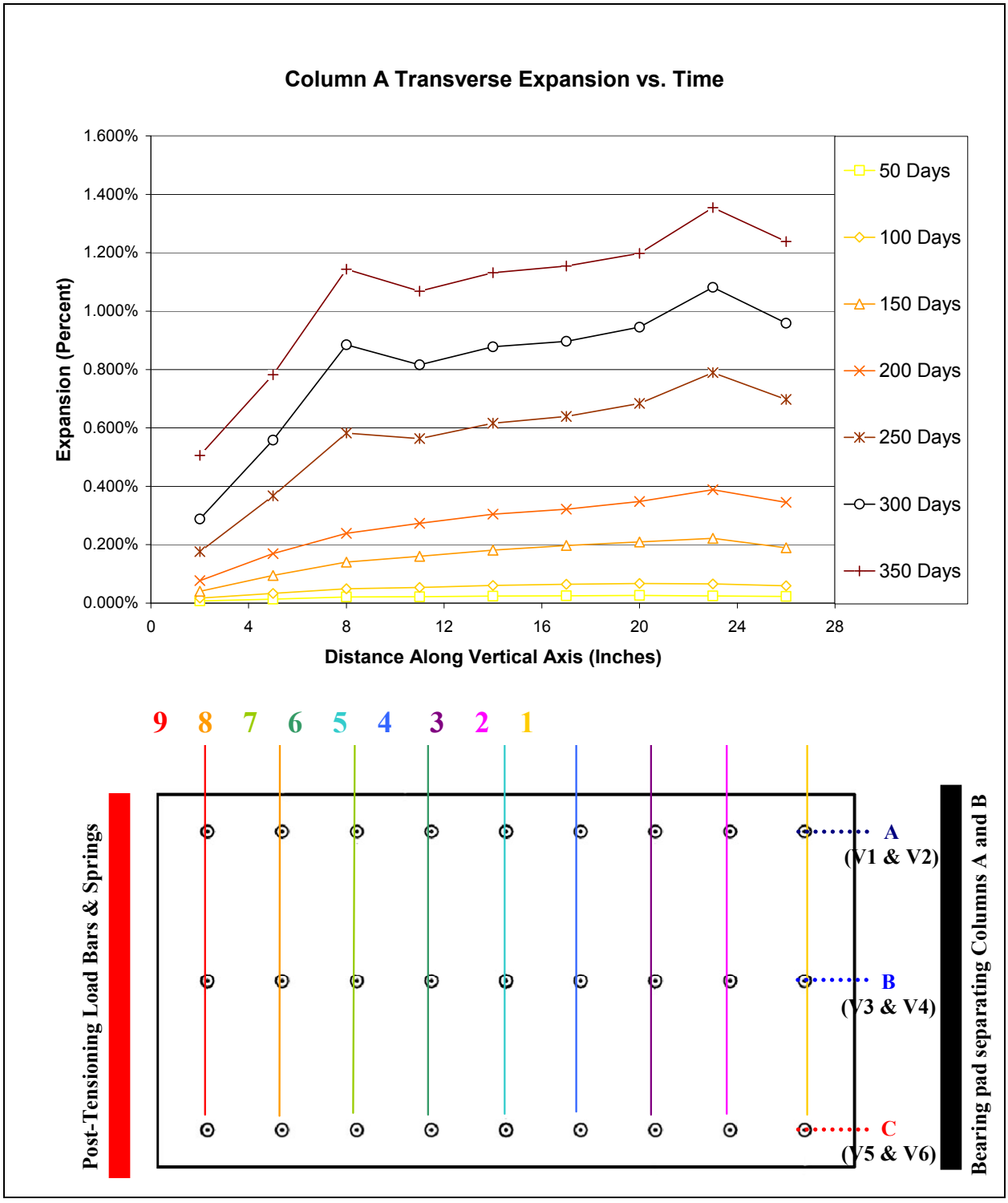

Figure 6.6: Profile plot of transverse expansion of Column A versus time.

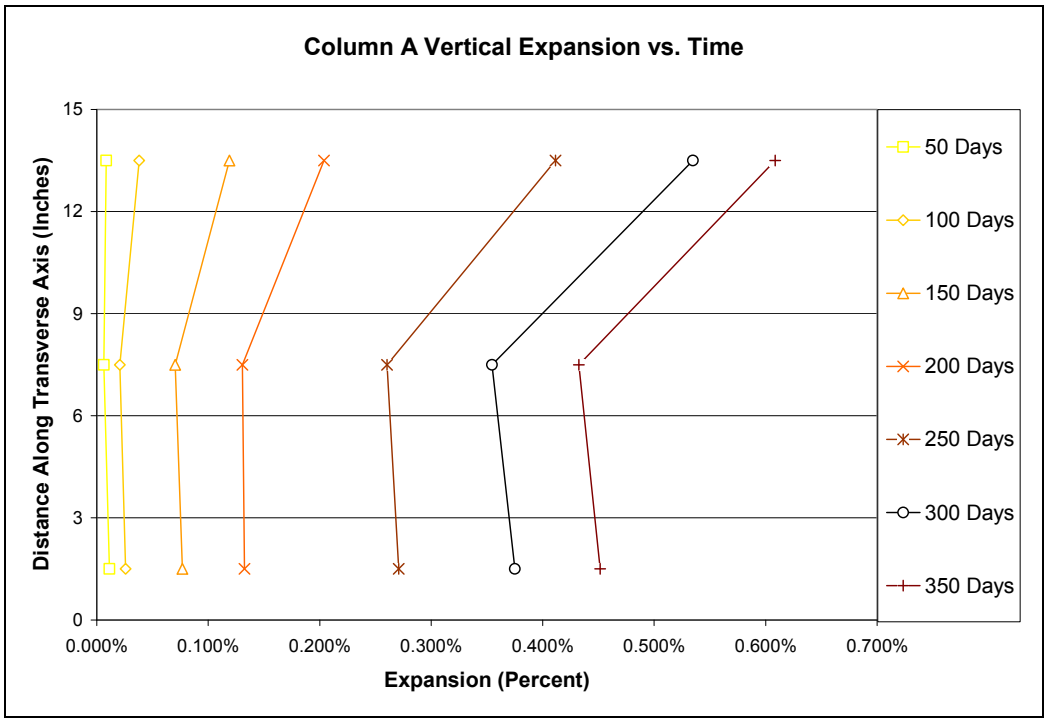

Figure 6.7: Profile plot of vertical expansion of Column A versus time.

Figure 6.7 shows the vertical expansion of Column A in increments of 50 days to date. Column A did not expand nearly as much in the vertical direction as it did in the transverse direction. This is attributed to the fact that the column is loaded in the vertical direction and therefore is restrained from expansion by internal reinforcement as well as the exterior post-tensioning system. Although Column A is loaded with a 400 psi load it still manages to expand beyond 0.60% in some areas despite the efforts of the internal reinforcing cage and the post-tensioning system.

Figures 6.8 and 6.9 show the rates of expansion of the various lines of demec points in both the transverse and vertical direction respectively. As observed from Figure 6.7 the transverse expansions measured nearest the post-tensioning system loading bars have the smallest observed expansion as well as the smallest expansion rates as shown in Figure 6.8 (line #8 and #9). As stated above the smaller expansion is due to the compound restraining effect of the internal reinforcement as well as the external post-tensioning system. In general all the transverse expansion lines follow the same trends as unreinforced DEF cylinders stored in or above water, however, more time is needed to realize the final expansions of each line.

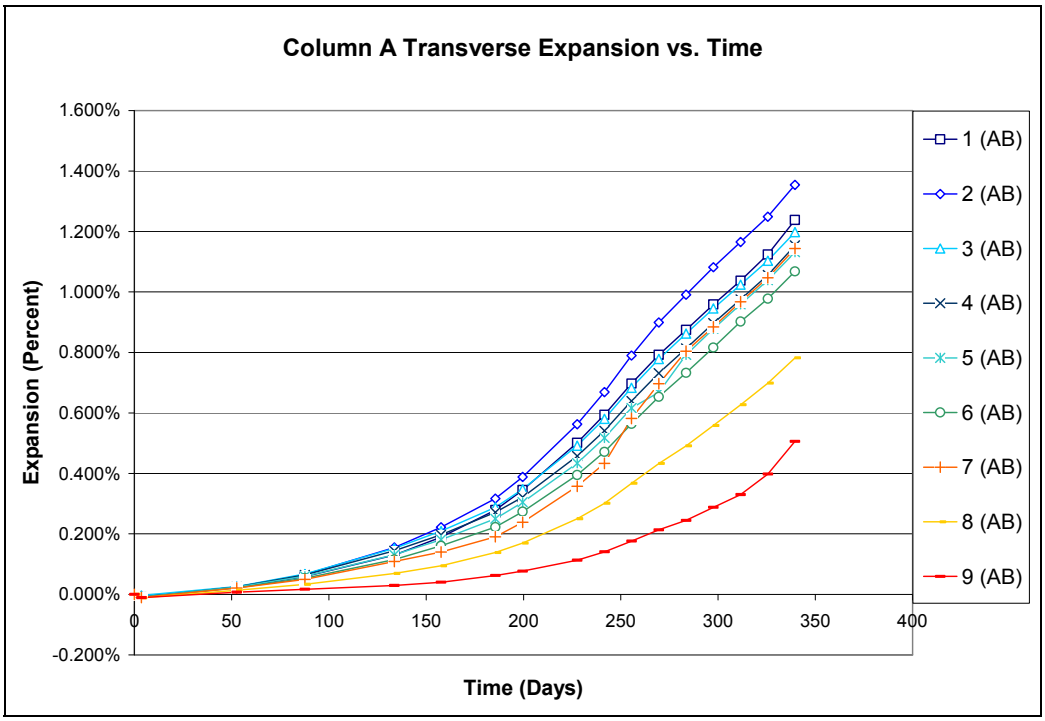

Figure 6.8: Transverse expansion of Column A versus time.

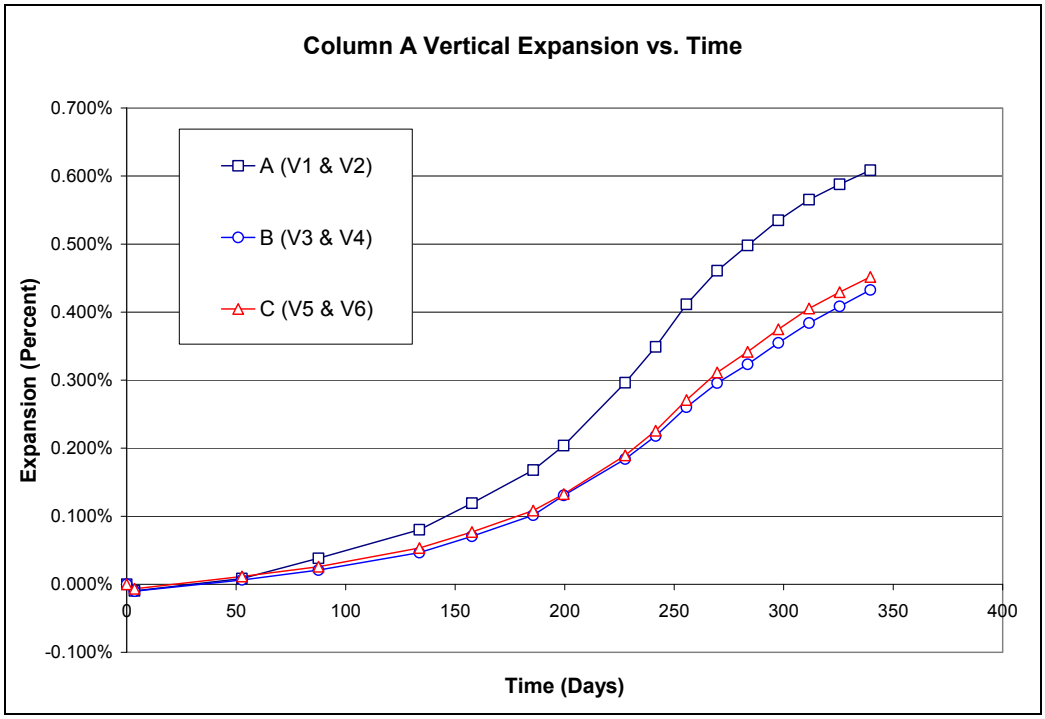

Figure 6.9: Vertical expansion of Column A versus time.

6.3.2 External Expansion Measurements: Column B

Figure 6.10 and 6.11 show the transverse and vertical expansion to date of Column B in increments of 50 days respectively. Column B expanded significantly in both directions, more so in the transverse direction mostly due to the fact that this direction is perpendicular to the direction of loading. In Figure 6.10 the zero inch measurement is the contact point between Column B and the bearing pad separating both Columns A and B. The 28 inch measurement is the contact point between Column B and the post-tensioning system. Figure 6.10 also shows the restraining effect that the post-tensioning system has on the column as the side nearest the loading bars has the smallest observed expansion. What is also important to note is that transverse demec lines 1, 3, 5, 7, and 9 are located above the transverse ties as mentioned before. Theoretically these demec lines should expand less than the others due to the fact that the transverse ties beneath them provide greater restraint to expansion. Demec line 3 in Figure 6.10 shows more expansion than the demec lines 2 and 4, which are not located above transverse reinforcement. This confirms the observations in Column A that the demecs located directly above transverse ties experience just as much if not more expansion than the demecs located between reinforcement.

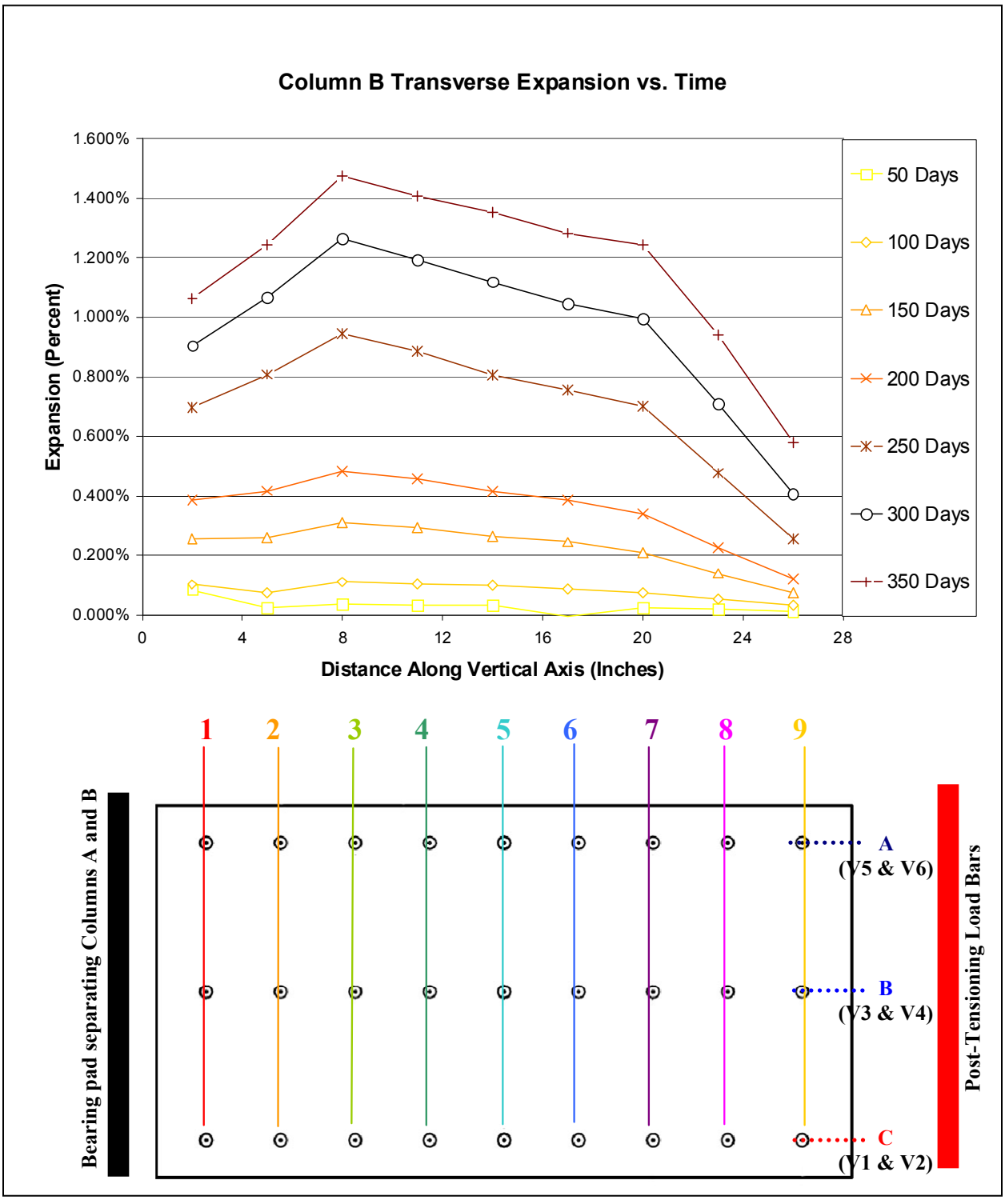

Figure 6.10: Profile plot of transverse expansion of Column B versus time.

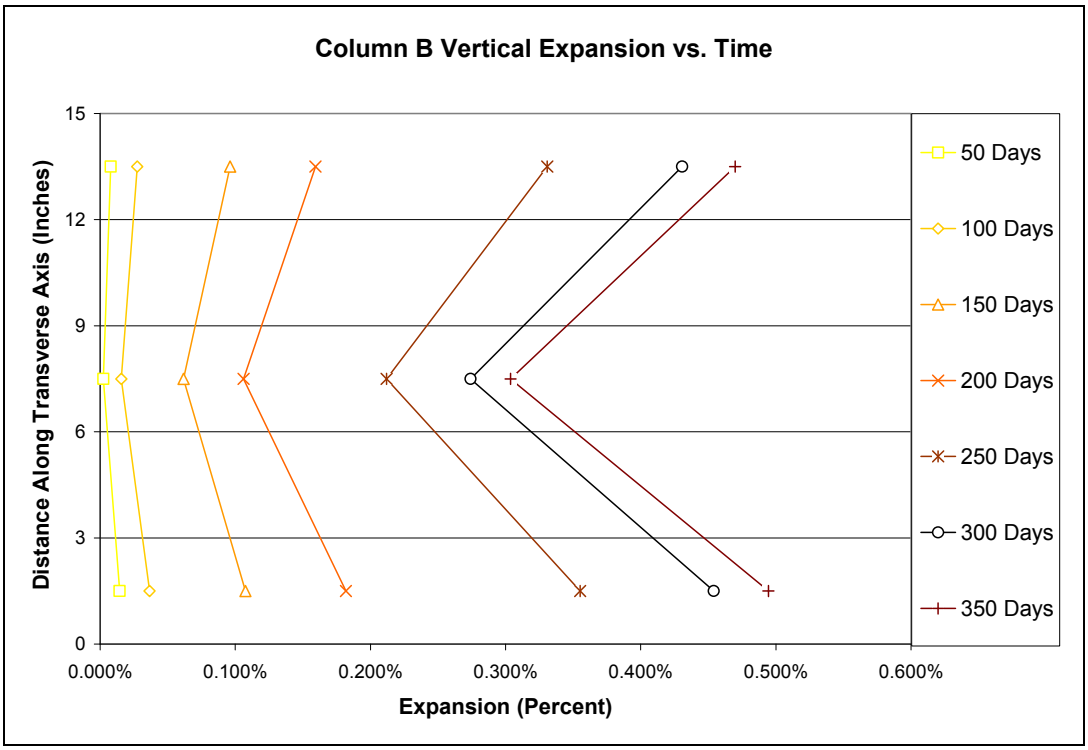

Figure 6.11: Profile plot of vertical expansion of Column B versus time.

Figure 6.11 shows the vertical expansion of Column B in increments of 50 days to date. Column B did not expand nearly as much in the vertical direction as it did in the transverse direction. As stated before this is attributed to the fact that the column is loaded in the vertical direction and therefore is restrained by loading as well as the internal reinforcement. Although Column B is loaded with a 400 psi load it still manages to expand beyond 0.50% in some areas despite the efforts of the internal reinforcing cage and the post-tensioning system.

Figures 6.12 and 6.13 show the rates of expansion of the various lines of demec points in both the transverse and vertical directions respectively. As observed from Figure 6.10 the transverse expansions measured nearest the post-tensioning system loading bars have the smallest observed expansion as well as the smallest expansion rates as shown in Figure 6.12 (lines #8 and #9). As stated above the smaller expansion is due to the compound restraining effect of the internal reinforcement as well as the external post-tensioning system. In general all the transverse expansion lines follow the same trends as unreinforced DEF cylinders stored in or above water, however, more time is needed to realize the final expansions of each line.

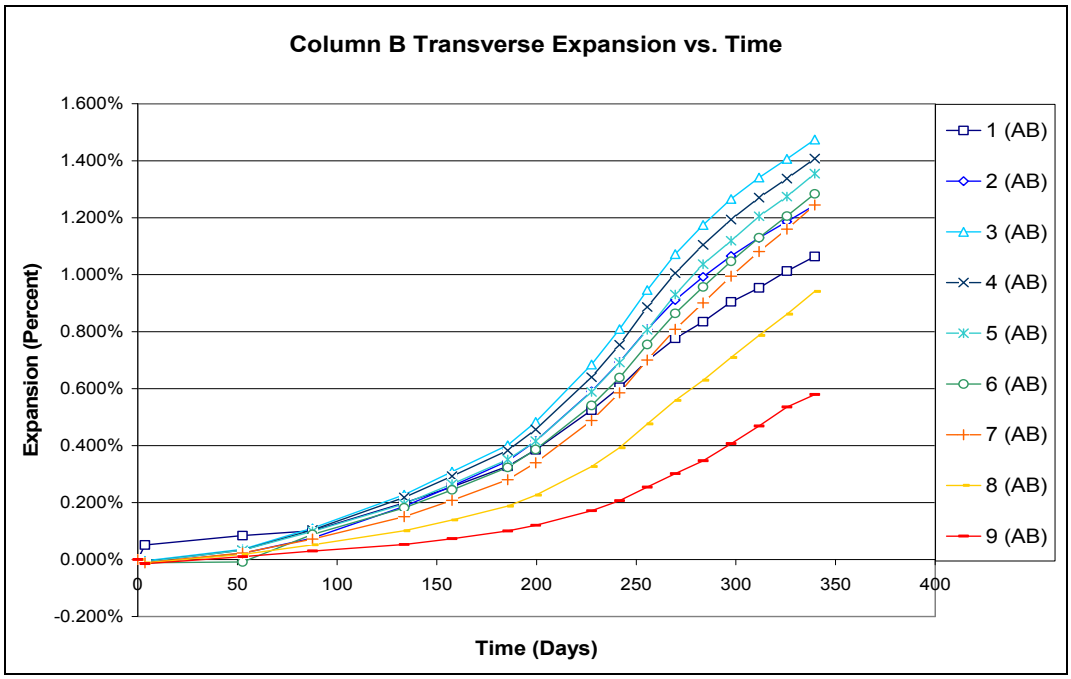

Figure 6.12: Transverse expansion of Column B versus time.

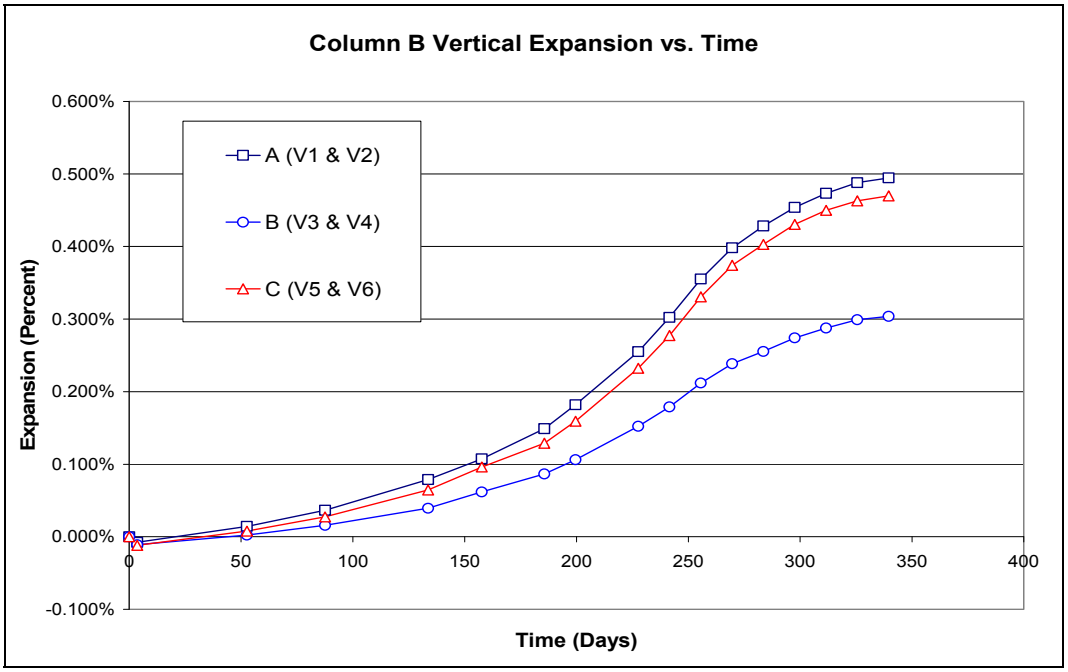

Figure 6.13: Vertical expansion of Column B versus time.

6.3.3 External Post Tensioning Loads

As mentioned before in section 6.1.6 the springs and the Dywidag bars of the post-tensioning system had demec points placed on them to measure any displacements resulting from

the expansion of the reinforced columns within the system. As stated before a 400 psi load was applied to the columns by the post-tensioning system to simulate a nominal service load. Figure 6.14 shows the development of load and stress over time in the Dywidag bars both in kips and psi respectively. What is important to note is that there was an initial relaxation period immediately following the placement of the columns within the post-tensioning system. After this initial relaxation period and subsequent expansion of the columns, the load exerted on the Dywidag bars increased by a maximum of 36 kips or 46 ksi. This shows that significant stresses are developed even in small sized elements that are exhibiting DEF.

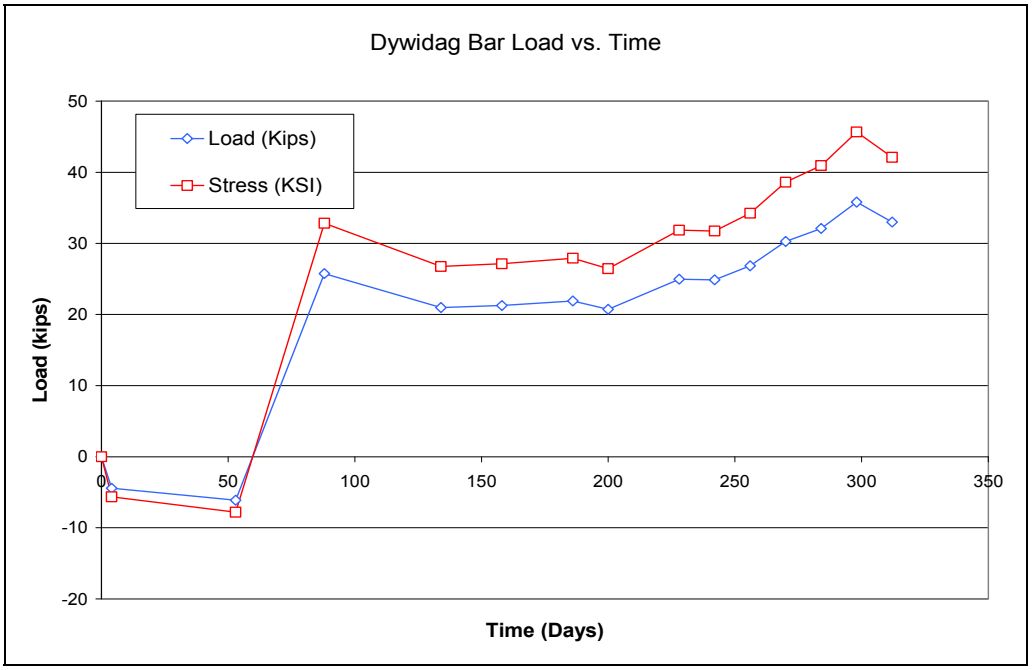

Figure 6.14: Dywidag bar load versus time.

Figures 6.15 and 6.16 show the force exerted on the springs versus time. Figure 6.15 shows the force exerted directly on the springs and Figure 6.18 shows the resolved stress and thus net stress that the columns are subjected to. As mentioned before with the Dywidag bars there is an initial period of relaxation of the post-tensioning system and thus the negative stress observed in the figures is a decrease in stress from the original 400 psi that was applied to the system. After this initial period, with additional expansion of the columns, the columns force the post-tensioning system beyond the initial 400 psi loading to 409 psi.

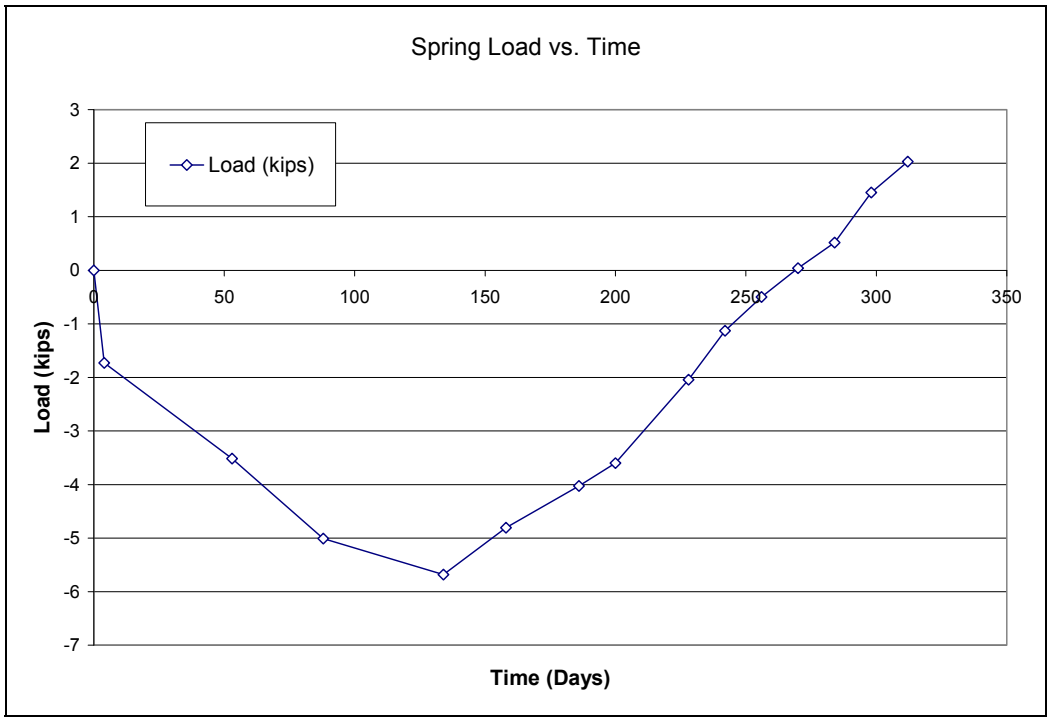

Figure 6.15: Spring load in kips versus time.

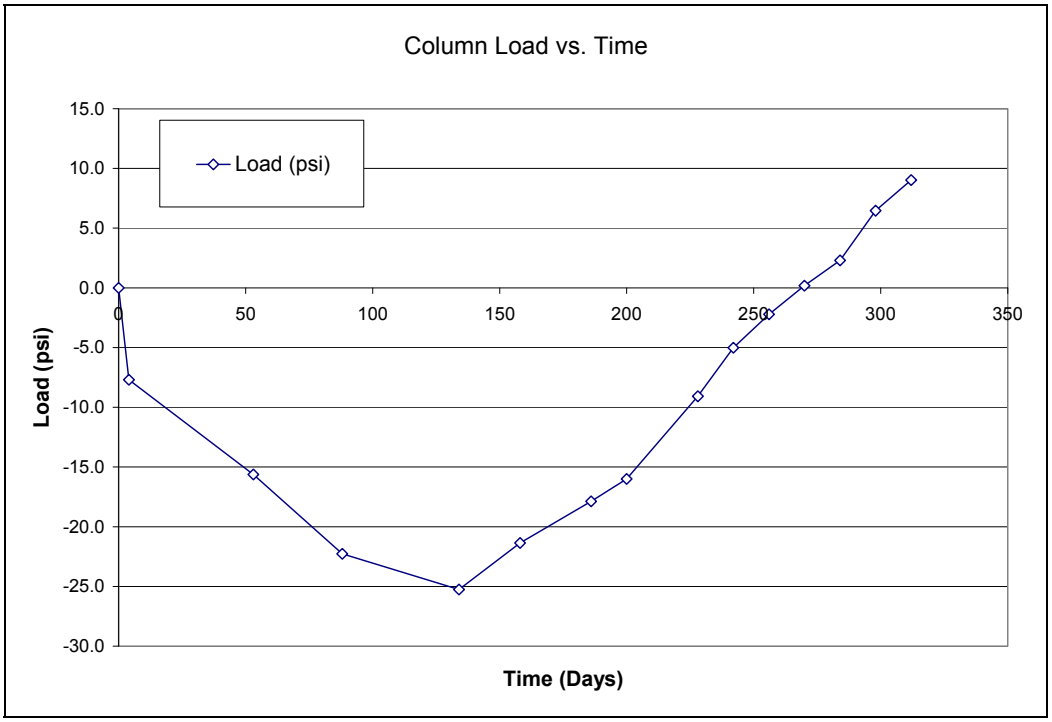

Figure 6.16: Column load in psi versus time.

6.3.4 Internal Expansion Measurements

Figure 6.17 and 6.18 show the expansion of the crackmeters for both Column A and B respectively. The reinforced columns expand beyond the range of the crackmeters and therefore the instantaneous jumps in measurements towards the end of testing occurred. Similar to the load figures of the post-tensioning system in section 6.3.3 there is an initial relaxation period followed by a subsequent increase due to the expansion of the concrete in the reinforced columns. Figures 6.19 and 6.20 show the expansion of the VWG for both Column A and B respectively. The VWG for both columns follows the same general trends as the external surface laid demec point measurements; however, the expansion of the column goes beyond the range of the VWG's.

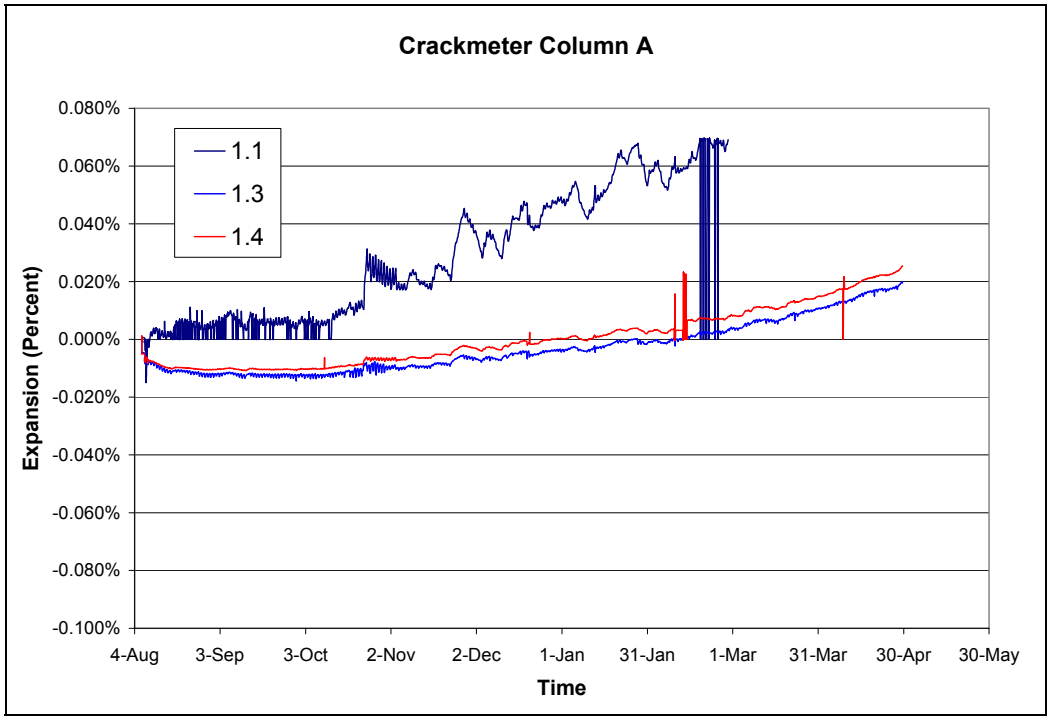

Figure 6.17: Internal expansion measured by the crackmeter in Column A versus time.

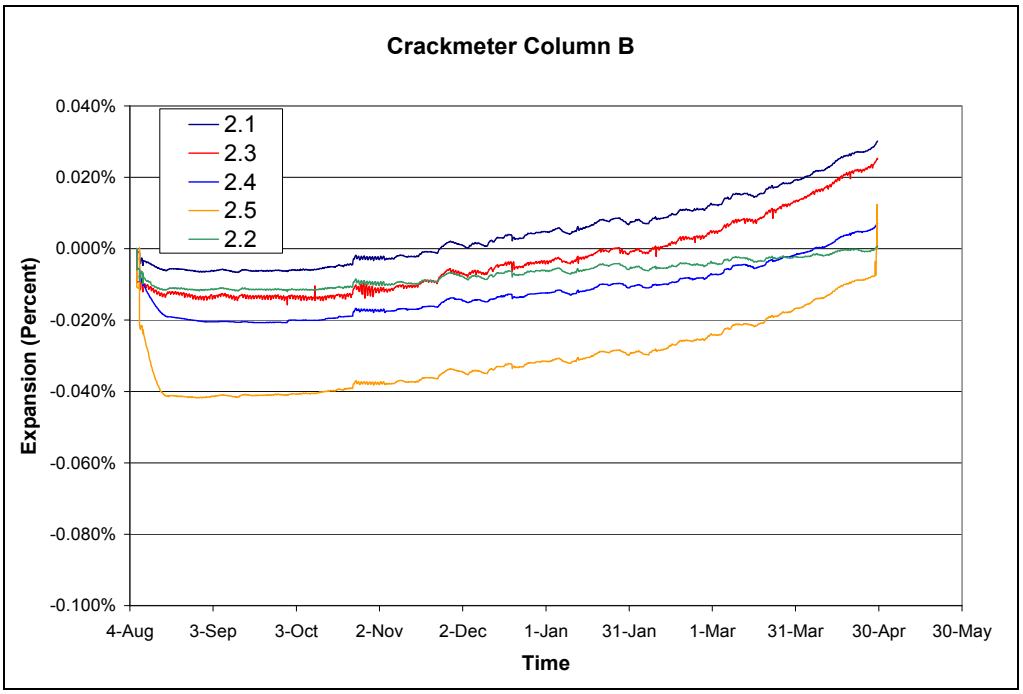

Figure 6.18: Internal expansion measured by the crackmeter in Column B versus time.

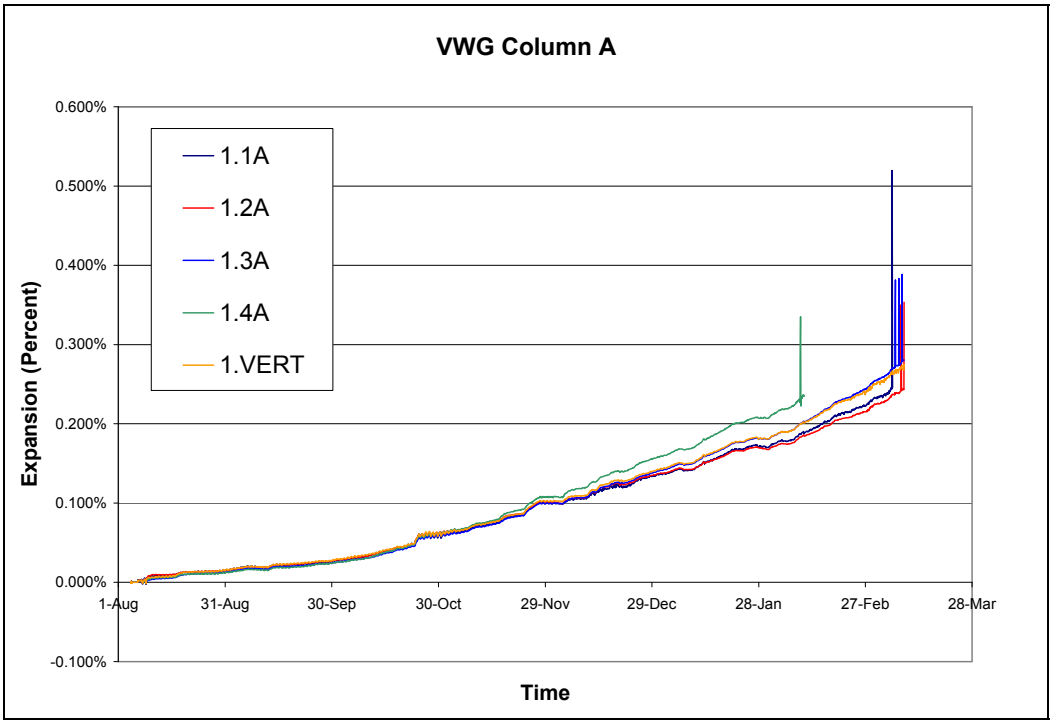

Figure 6.19: VWG expansion for Column A versus time.

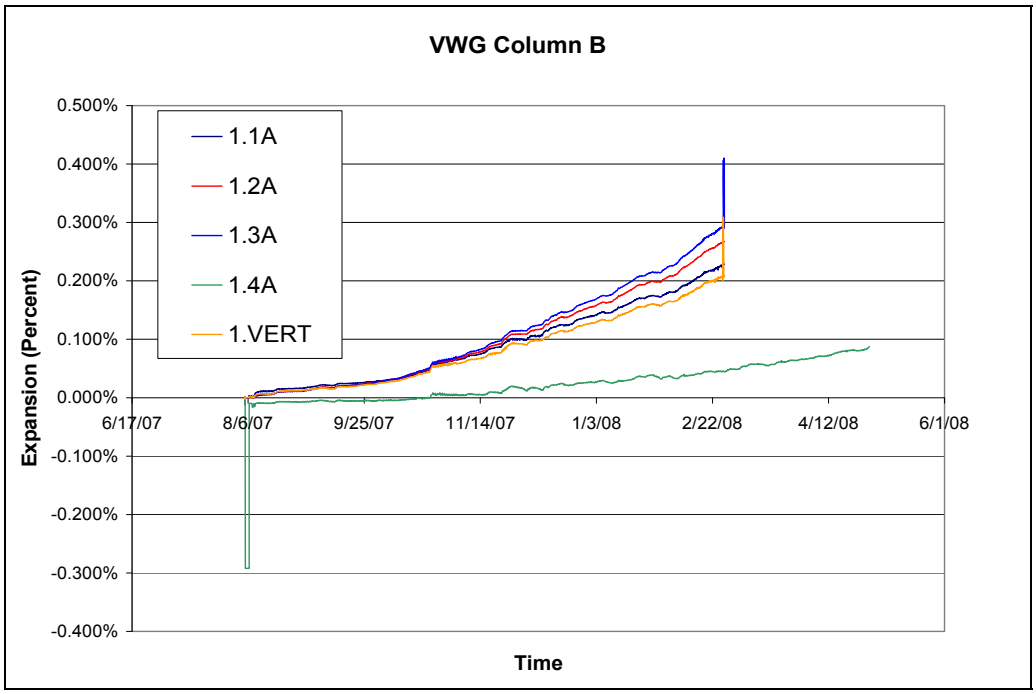

Figure 6.20: VWG expansion for Column B versus time.

6.4 Summary

This chapter described an ongoing test that focused specifically on internal strain distribution in reinforced elements and the impact of external, longitudinal restraint on behavior. This study was the first in Texas to specifically attempt to quantify the effects of reinforcement and axial load on subsequent DEF-induced stresses and strains and similar approaches have since been applied in other TxDOT-funded projects. Although the current project has reached its conclusion, these specimens will continue to be monitored and the long-term results will allow for technical conclusions to be drawn, helping to shed light on this complex topic.

Chapter 7. Testing at University of New Brunswick (UNB) to Determine the Level of Confinement Required to Prevent Expansion due to DEF in Concrete

7.1 Introduction

This chapter presents the results of a series of tests conducted at UNB to determine the level of stress required to restrain the expansion caused by delayed ettringite formation (DEF) in concrete. The following tests have been conducted since the project began in 2005:

- Effect of dead load on the expansion of heat-cured mortars (using soil oedometer cells)
- Effect of carbon-fiber reinforced plastic wraps on the expansion of heat-cured concrete cylinders
- Effect of reinforcement ratio on the expansion of heat-cured concrete cylinders
- Three-dimensional stresses developed by heat-cured concrete confined in Hoek cells

All testing was carried out using a high-early strength portland cement from a local source. The cement meets the requirements of ASTM C 150 Type III. This cement has been used in previous studies and is known to be highly susceptible to DEF expansion when heat-cured at or above a temperature of 176ºF (80ºC). Quartz sand from Ottawa, IL, meeting the requirements of ASTM C 778 for sand type 20/30 was used for the mortar tests. The siliceous sand and gravel used to manufacture the concrete specimens meets the requirements of ASTM C 33 and is non-deleteriously-reactive when tested in accordance with ASTM C 1293.

7.2 Effect of Dead Load on the Expansion of Heat-Cured Mortars

Mortar samples 2 in. diameter x 2.75 in. long (50 x 70 mm) were compacted into rigid stainless steel tubes with a wall thickness of ¾ in. (19 mm). The assembly was then cured over water at 203ºF (95^{o}C) for 12 hours, soaked in water at room temperature for 6 hours, and then dried in an oven at 185ºF (85^{o}C) for 24 hours. This curing regime has been found to rapidly promote DEF expansion in mortars[1]. After drying specimens were then immersed in limewater at room temperature until they reached constant mass. At an age of 7 days, porous plates were placed at the top and bottom of each specimen, and the specimens were immersed in a container of limewater. The containers and specimens were placed in large-scale test rigs for measuring the consolidation of soils. A surcharge was placed on each specimen and dial gauge fitted to measure vertical expansion. The test set up is shown Figure 7.1.

The surcharge was varied to supply a vertical stress of 0, 300, 450, and 600 psi (0, 2, 3, and 4 MPa) on four different specimens. The samples were cast on 13 February 2006. No significant expansion was observed during the first year. In February 2007, it was observed that

[1] Y. Fu, Delayed Ettringite Formation in Portland Cement Products, PhD thesis, Department of Civil Engineering, University of Ottawa, Ottawa, 1996.

there had been a significant loss of water from the containers, but that the bases of the samples were still damp. The loads were removed, the samples re-saturated, the loads re-applied and length-change measurements restarted at this time. The subsequent expansion of the samples is shown in Figure 7.2.

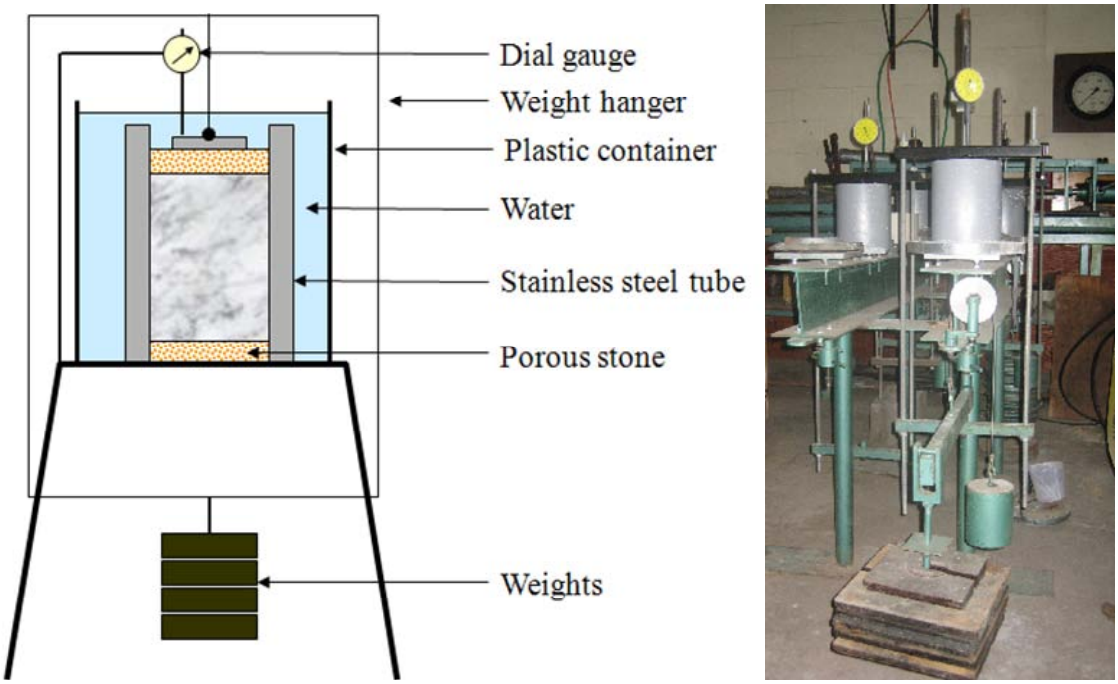

Figure 7.1: Set-Up for Mortar Tests Using Soil Oedometer Cells

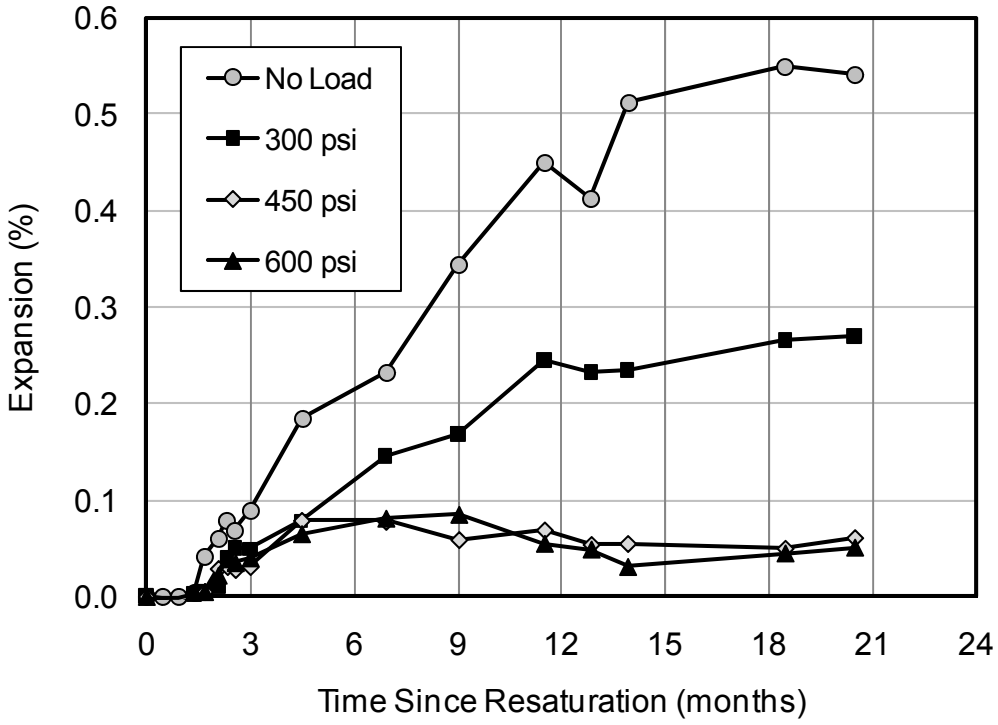

Figure 7.2: Expansion Results for Mortar Tests (from Feb 2007 when specimens were re-saturated)

The magnitude of the dead load clearly has an impact on the expansion of the mortar specimens. A surcharge equivalent to 300 psi reduced the "free expansion" by 50% and loads producing confining stresses of 450 or 600 psi effectively prevented significant expansion from occurring. It should be noted that the term "free expansion" is not valid as the friction between the mortar and the stainless steel ring is likely to provide some impediment to expansion in the vertical direction.

7.3 Effect of Carbon-Fiber Reinforced Plastic Wraps on the Expansion of Heat-Cured Concrete Cylinders

The concrete produced for this study contained 750 lb/yd^3 (450 kg/m^3) and W/CM = 0.35. A high-range water-reducing admixture was used to produce a slump of 6 to 8 in. (150 to 200 mm). Three cylinders 12 in. diameter x 12 in. long (300 x 300 mm) were cast with two embedded strain gauges (Vishay EGP series) placed in the center; one gauge was oriented vertically and the other horizontally. Eight #5 (16-mm) reinforcing bars were placed vertically with approximately 1 inch of clear cover. Figure 7.3 shows the specimen configuration.

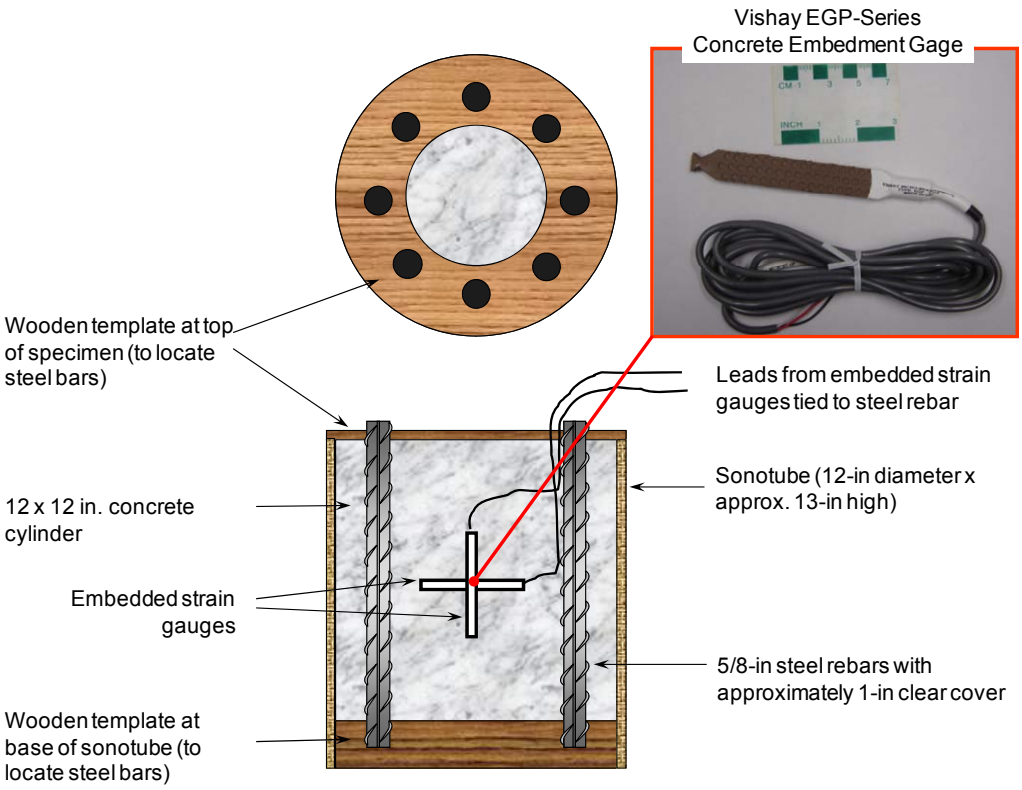

Figure 7.3: Test Set-Up for Cylinders Used in the Study on the Effect of Confinement by CFRP Wraps on DEF Expansion

Each concrete cylinder was placed in a large sealed aluminum pot containing water to a depth of 1 inch. The pot was placed in an oven and heat-cured at 203ºF (95^{o}C) for eighteen hours. After heat curing, the specimens were immersed in limewater and expansion monitored periodically. When the strain gauges indicated an expansion of approximately 0.10% and cracks were just visible at the surface, the concrete specimens were "repaired" as follows:

Curved surface wrapped with a bituminous waterproofing membrane (product name "Blueskin")

1. Curved surface wrapped with a single layer of carbon-fiber reinforced plastic (CFRP)
2. Curved surface wrapped with two layers of CFRP.

The CFRP system used was supplied by Fyfe and consisted of two products: Tyfo SCH-41 Composite and Tyfo S Epoxy. The fabric sheets contain carbon fibers in the primary direction and glass fibers in the transverse direction. According to the manufacturer the composite system has a tensile strength of 143,000 psi (986 MPa), tensile modulus of 13.9 x 10^{6} psi (95.8 GPa), elongation at failure of 1.0% and a laminate thickness of 0.04 in. (1 mm).

Prior to wrapping electrical foil strain gauges were attached to the surface of the cylinders to measure strain in both the longitudinal and horizontal directions. In addition, gauge points were fixed to the specimens after wrapping to allow vertical expansion measurements to be made

using a Demec-type gauge (8-inch, 200-mm gauge length) and horizontal expansion measurements to be made across the diameter using a digital caliper.

Photographs showing the repair and monitoring of these specimens are shown in Figure 7.4.

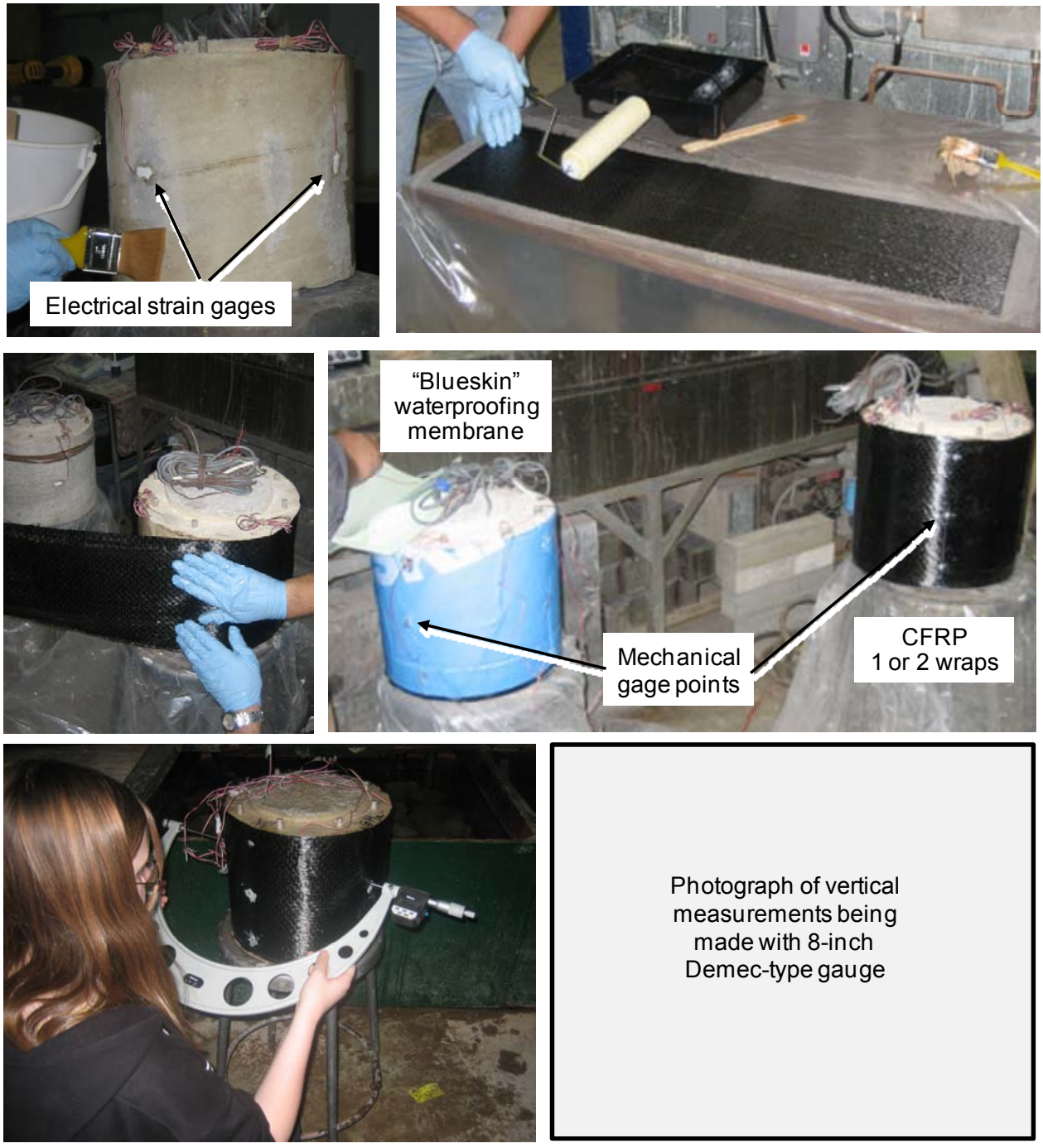

Figure 7.4: Wrapping and Monitoring Heat-Cured Cylinders

The specimens were repaired in January 2007 and post-repair expansion results are shown in Figure 7.5. The data clearly indicate that wrapping with CFRP is effective in reducing the expansion of the columns in the horizontal direction. Expansion in the vertical direction was approximately half the expansion in the horizontal direction for cylinders that were wrapped with the waterproofing membrane. The CFRP wraps had little effect on the magnitude of expansion in this direction. The reduced expansion in the vertical direction is likely the result of the longitudinal reinforcement even though the there is insufficient bond-development length. The CFRP does not have significant strength perpendicular to the direction of the primary fibers and thus has little impact on the vertical expansion.

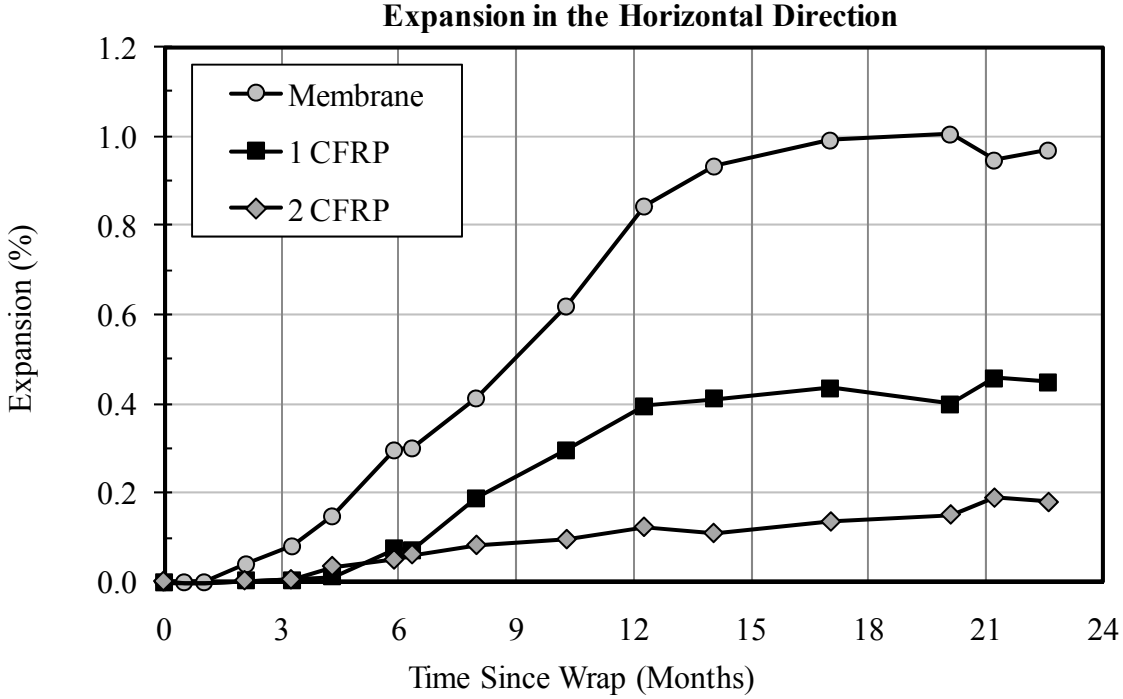

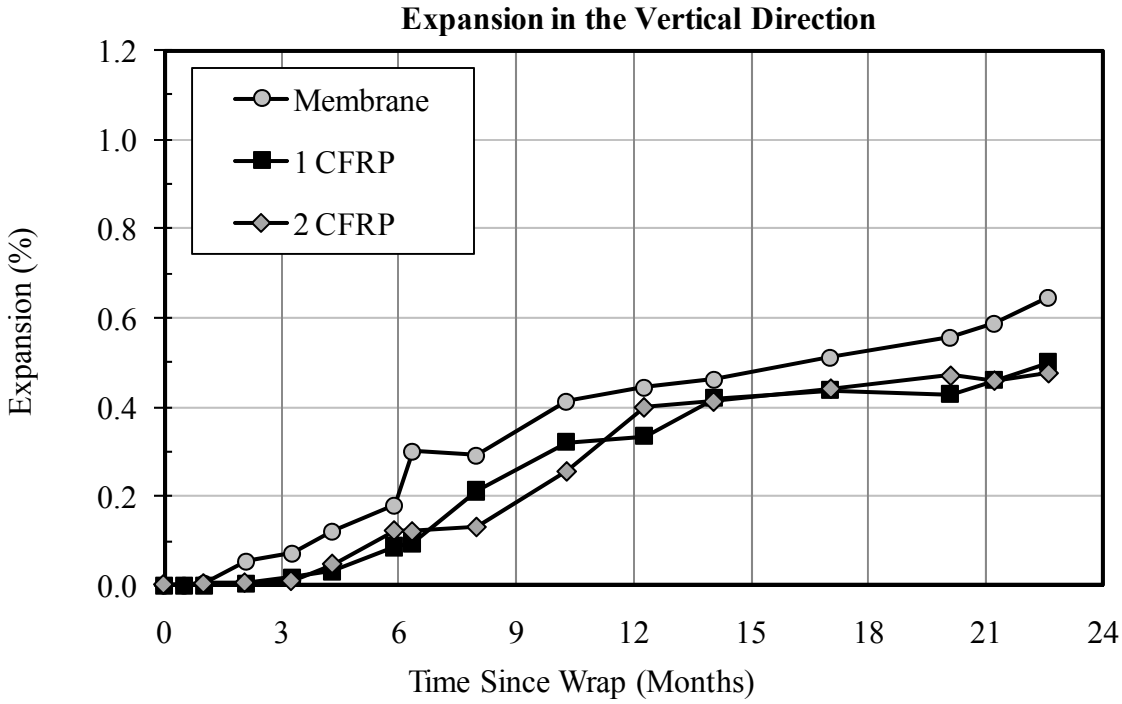

Figure 7.5: Post-Repair Expansion Results for Wrapped Cylinders

The compressive stress in the concrete resulting from the confinement provided by the wrap can be calculated by considering equilibrium as follows:

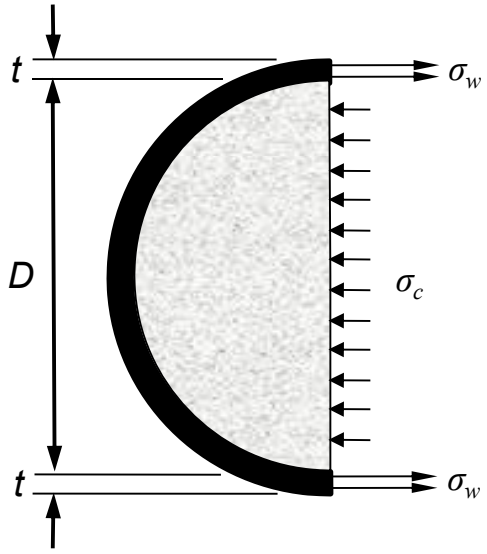

For equilibrium:

$$D\sigma_c = 2t\sigma_w$$

$$\sigma_c = \frac{2t}{D} \cdot \sigma_w$$

$$\sigma_c = \frac{2t}{D} \cdot \varepsilon_w E_w$$

Where σ_c and σ_w are the stress in the concrete and the wrap, respectively, ε_w and E_w are the strain and the modulus of the wrap, t is the thickness of the wrap and D is the diameter of the concrete cylinder

The compressive stress here is the confinement pressure, which can be verified by the equation (12-4) in ACI 440-2R-08, "Guide for the Design and Construction of Externally Bonded FRP Systems for Strengthening Concrete Structures.

The cylinder with a single layer of CFRP expanded by approximately 0.42% after wrapping. Assuming a similar strain in the wrap (ε_w = 0.004) and that D = 12", t = 0.04" and E_w = 13,900 ksi, the stress in the concrete is σ_c = 389 psi.

Performing a similar calculation for the column that is wrapped with two layers of CFRP and expanded by approximately 0.22% after wrapping, thus ε_w = 0.0018 and t = 0.08", and the stress in the concrete is σ_c = 408 psi.

7.4 Effect of Reinforcement Ratio on the Expansion of Heat-Cured Concrete Cylinders

The concrete produced for this study contained 750 lb/yd^3 (450 kg/m^3) and W/CM = 0.35. A high-range water-reducing admixture was used to produce a slump of 6 to 8 in. (150 to 200 mm). Three cylinders 12 in. diameter x 18 in. long (300 x 450 mm) were cast with two embedded strain gauges (Vishay EGP series) placed in the center; one gauge was oriented vertically and the other horizontally. One specimen was not reinforced. For the other two specimens, eight #5 (16-mm) reinforcing bars were placed vertically with plates welded top and bottom to fully develop tension in the steel. A spiral cage was wound around the vertical reinforcement using either 0.2-inch (5-mm) wire with a 2-inch (50-mm) pitch or 0.4-inch (10-mm) rebar with a 4-inch (100-mm) pitch. The cover to the steel spiral was approximately ¾ inch (19 mm). Figure 7.6 shows the specimen configuration.

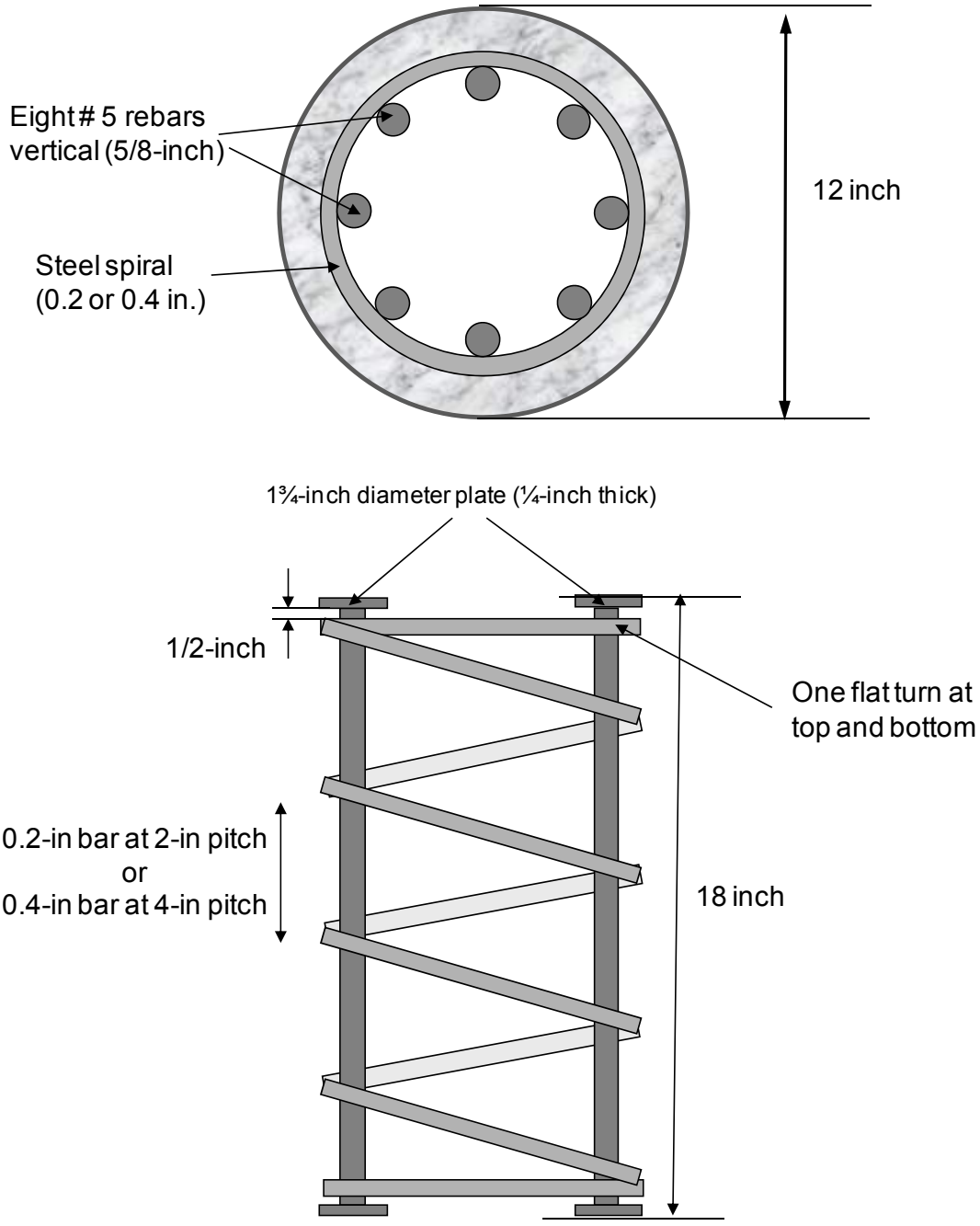

- Electrical stain gages on spiral and longitudinal steel
- Embedded gages – 1 longitudinal and 1 horizontal at center of specimen

Figure 7.6: Details of Reinforced Concrete Cylinders

Each concrete cylinder was placed in a large sealed aluminum pot containing water to a depth of 1 inch. The pot was placed in an oven and heat-cured at 203ºF (95^{o}C) for eighteen hours. After heat curing, the specimens were immersed in limewater and expansion monitored periodically.

The specimens were cast in May 2007 and expansion results are shown in Figure 7.7.

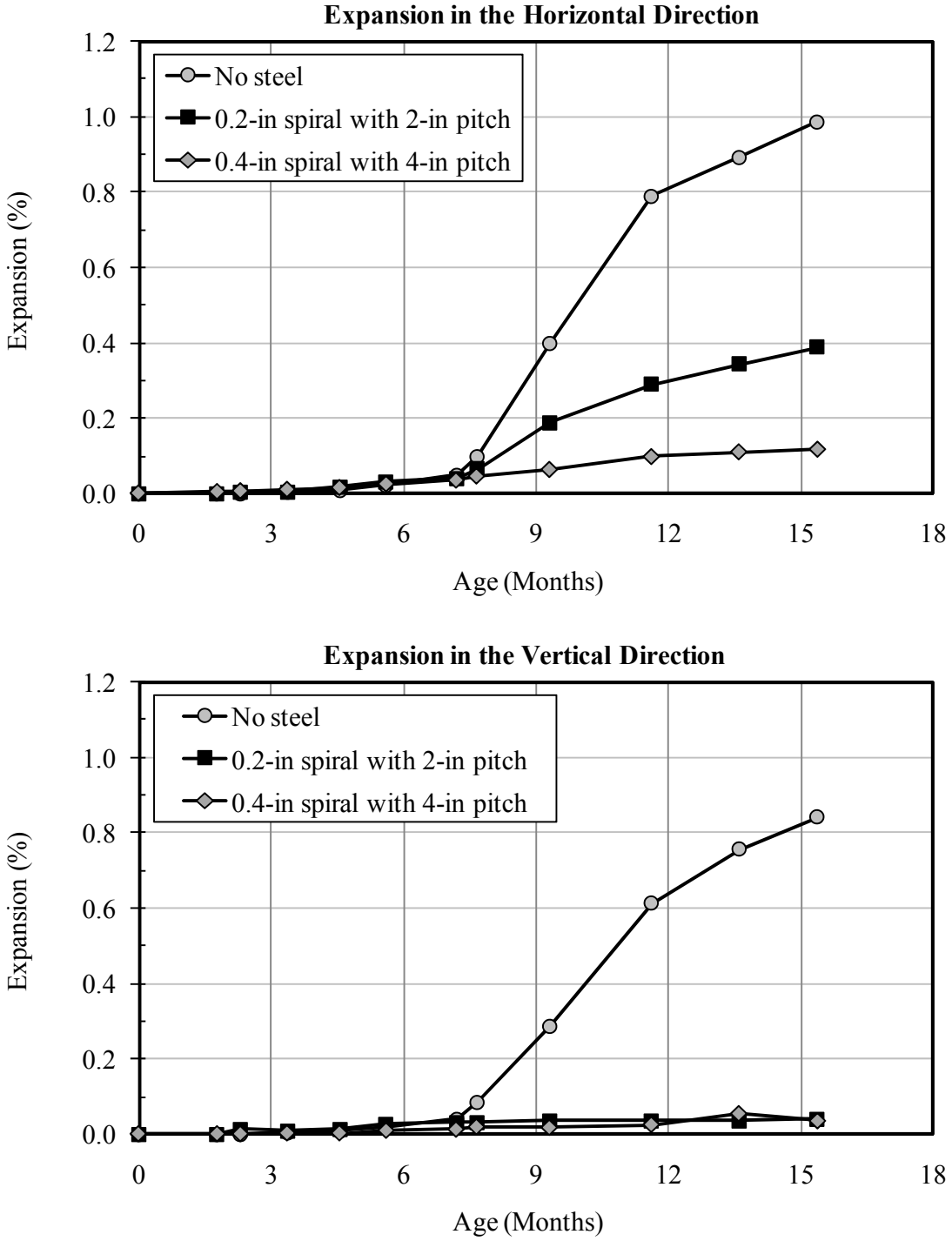

Figure 7.7: Expansion Data for Reinforced Cylinders

As expected, reinforced concrete specimens showed considerably less expansion in the horizontal direction, but somewhat surprisingly no significant expansion in the vertical direction. The confinement pressure in the concrete resulting from the confinement provided by the spiral can be calculated by considering equilibrium as follows:

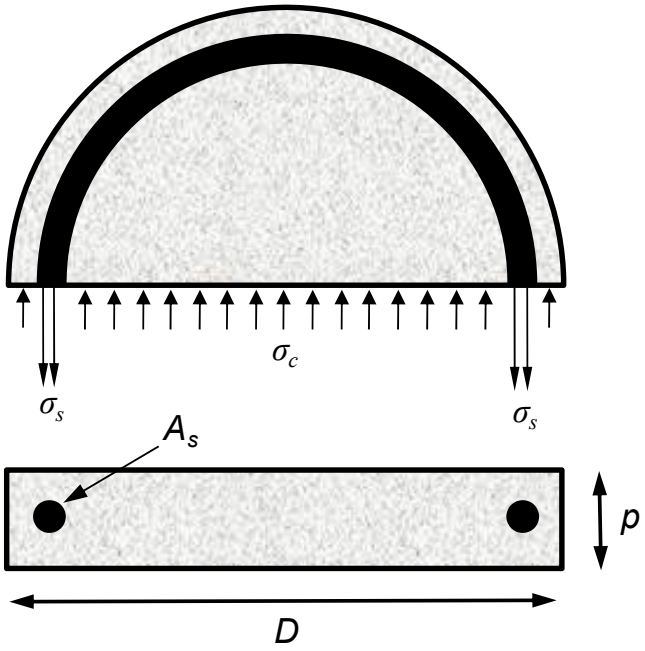

For equilibrium:

$$(Dp - 2A_s)\sigma_c = 2A_s\sigma_s$$

$$\sigma_c = \frac{2A_s}{(Dp - 2A_s)} \cdot \sigma_s$$

$$\sigma_c = \frac{2A_s}{(Dp - 2A_s)} \cdot \varepsilon_s E_s$$

Where σ_c and σ_s are the stress in the concrete and the steel, respectively, ε_s and E_s are the strain and the modulus of the steel, p is the pitch of the spiral, A_s is the cross-sectional area of the spiral, and D is the diameter of the concrete cylinder

The compressive stress here is the confinement pressure, which can be verified by the equation (12-4) in ACI 440-2R-08, "Guide for the Design and Construction of Externally Bonded FRP Systems for Strengthening Concrete Structures.

The cylinder with the 0.4-inch (10-mm) Ø spiral and 4-inch (100-mm) pitch showed a maximum horizontal expansion of 0.12%. Assuming a similar strain in the steel[2] (ε_s = 0.0012) and that D = 12 in., p = 4 in., A_s = 0.126 sq. in., and E_s = 30,000 ksi, the stress in the concrete is σ_c = 190 psi.

The cylinder with the 0.2-inch (5-mm) Ø spiral and 2-inch (50-mm) pitch showed a maximum horizontal expansion of 0.4%. Assuming a similar strain in the steel (ε_s = 0.004) means that the steel yielded. Unfortunately, the yield stress of the steel wire is not known[3] but assuming a value[4] of σ_y (= σ_s) = 36,000 psi results in a concrete stress of σ_c = 95 psi.

The compressive stress in the concrete resulting from the confinement provided by the vertical steel can be calculated by considering equilibrium as follows:

[2] The foil strain gauges attached to the reinforcing steel did not function properly after heat curing and the steel strains have to be inferred from the concrete strain.
[3] Attempts are being made to determine this value.
[4] ASTM A 36 carbon steel

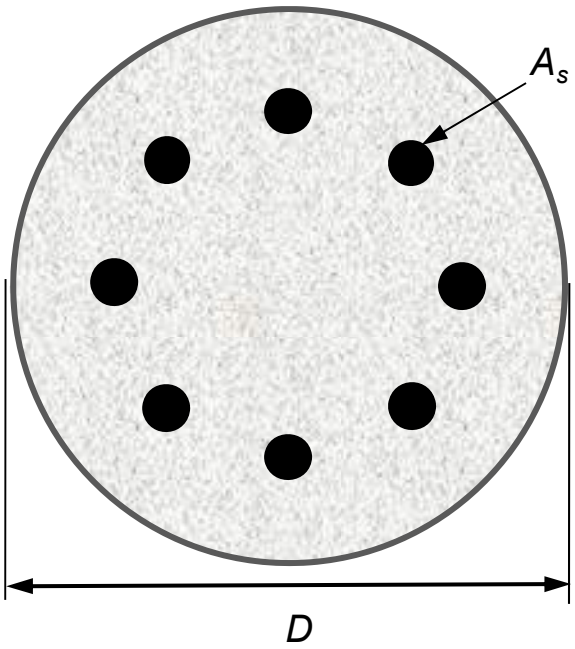

For equilibrium:

$$\left(\frac{\pi D^2}{4} - 8A_s\right)\sigma_c = 8A_s\sigma_s$$

$$\sigma_c = \frac{8A_s}{\left(\frac{\pi D^2}{4} - 8A_s\right)} \cdot \sigma_s$$

$$\sigma_c = \frac{8A_s}{\left(\frac{\pi D^2}{4} - 8A_s\right)} \cdot \varepsilon_s E_s$$

The compressive stress here is the confinement pressure, which can be verified by the equation (12-4) in ACI 440-2R-08, "Guide for the Design and Construction of Externally Bonded FRP Systems for Strengthening Concrete Structures.

The maximum expansion in the vertical direction for either of the reinforced concrete cylinders was 0.041%. Assuming a similar strain in the steel (ε_s = 0.004) results in a concrete stress of σ_c = 267 psi.

7.5 Three-Dimensional Stresses Developed by Heat-Cured Concrete Confined in Hoek Cells

Five Hoek cells were manufactured. Two of these were sent to the University of Texas and the remaining three have been used for testing at UNB. Three test frames were also built at UNB to accommodate the Hoek cells. The frames have a mechanical screw-jack loading system for applying vertical load to the cell. A photograph of one of the cells in a test frame is shown in Figure 7.8. Concrete specimens were received from the University of Texas. These specimens were heat-treated and stored in water until they started to exhibit expansion at which point they were wrapped to minimize drying and shipped to UNB. On arrival at UNB the cores were frozen until they were ready for testing. Specimens were loaded into the cells and an initial axial stress and lateral confining pressure of 145 psi (1 MPa) applied. The vertical load and lateral pressure are continuously monitored using, respectively, a load cell and pressure transducer. Unfortunately, the cells do not seem to be able to maintain the lateral pressure for more than a few days and it slowly dissipates. The loss of pressure is sometimes, but not always, accompanied by a loss of hydraulic fluid indicating leakage. When leakage does occur, it appears to take place at the seal between the neoprene membrane and the wall of the cell and not at the inlet for the hydraulic pump or the pressure transducer. Currently, various alternatives are being explored to improve the seal. One cell has been left “on test” with the lateral pressure being maintained in the range between 73 to 145 psi (0.5 to 1.0 MPa) by recharging the hydraulic

pressure to 145 psi (1 MPa) when it falls to 73 psi (0.5 MPa); the change in vertical load is being monitored. To date there has been no significant or consistent change in the vertical load.

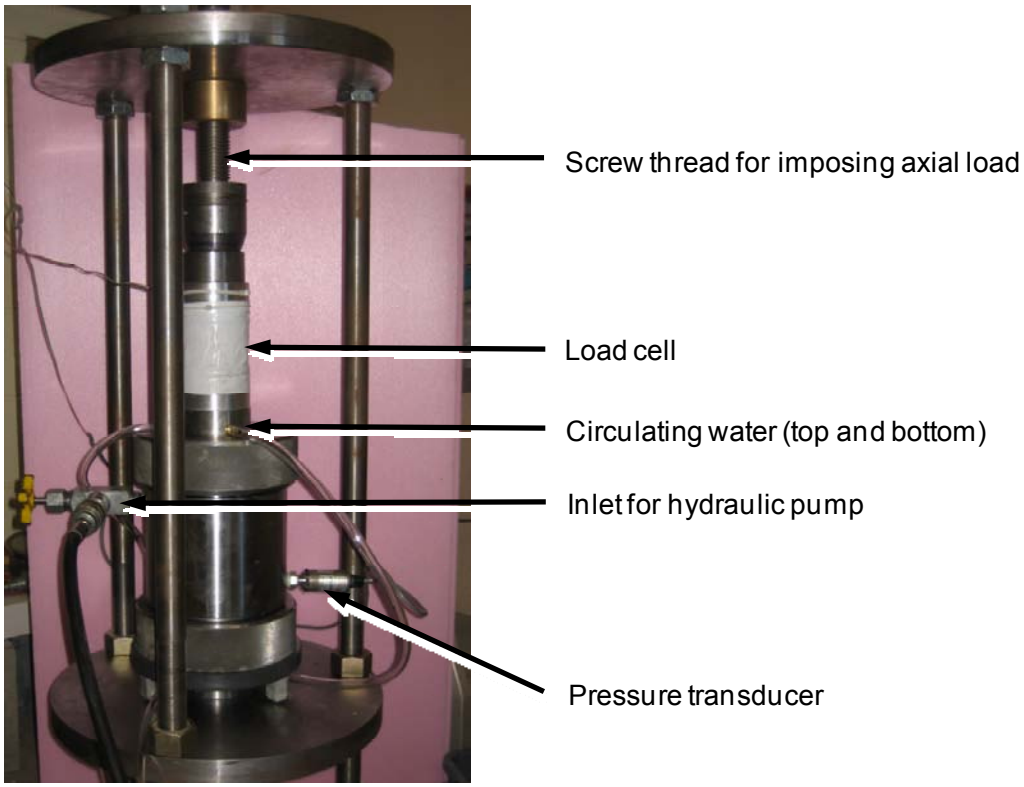

Figure 7.8: Experimental Set-Up for Hoek-Cell Tests

7.6 Summary

Four different approaches were used to determine the effect of confinement on the expansion due to delayed ettringite formation. Of these, three generated data that warrant further consideration. The approach using the Hoek cell has yet to generate any reliable data but efforts will continue in the form of modifications to enable a constant confining pressure to be maintained.

Figure 7.9 shows the normalized expansion plotted as a function of the confining pressure. The normalized expansion is the ratio of the maximum expansion measured for the mortars with dead load, the wrapped columns, and the reinforced columns to the maximum expansion measured for unloaded or unconfined specimens from the same study. In the case of the mortars the confining pressure is simply calculated from the applied dead load, whereas for the wrapped and reinforced concretes the confinement was calculated by equilibrium assuming that the CFRP wrap and the reinforcing steel expanded by the same amount as the concrete.

The data in Figure 7.9 show, not surprisingly, that the expansion decreases as the level of confinement increases. However, there is a wide range in the calculated level of confinement required to suppress expansion. Of course, it is not possible to achieve zero expansion in the

CFRP wrapped and reinforced concrete as the confining pressure is activated by the strain in the wrap or the steel. If a normalized expansion of 0.1 is taken as a measure of effective confinement, then the different approaches used here indicate that the confining pressure required to suppress DEF expansion ranges from approximately 200 psi in the reinforced concrete to 400 psi in the mortars or the CFRP wrapped concrete.

Figure 10 shows the absolute expansion plotted against the confining pressure. Also shown are horizontal lines drawn to represent and expansion of 0.04% and 0.10% as these values are used in some concrete and mortar tests, respectively, as limits of acceptable expansion. Using these values it would appear that confining pressures in the region of 300 to 450 psi are required to suppress the expansion of mortar or concrete due to DEF.

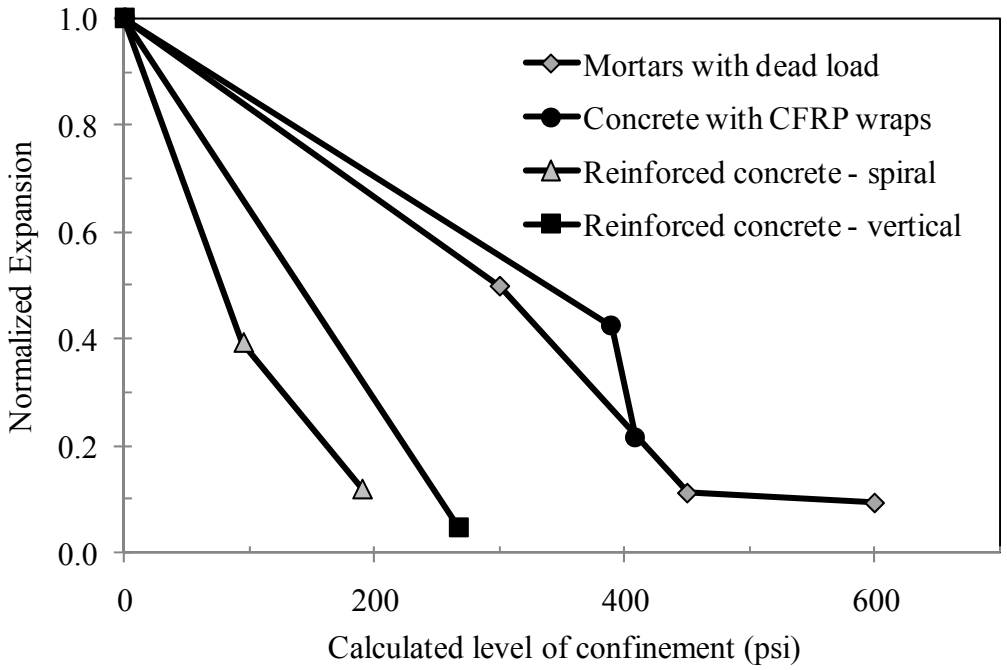

Figure 7.9: Effect of Confinement on the Normalized Expansion due to DEF

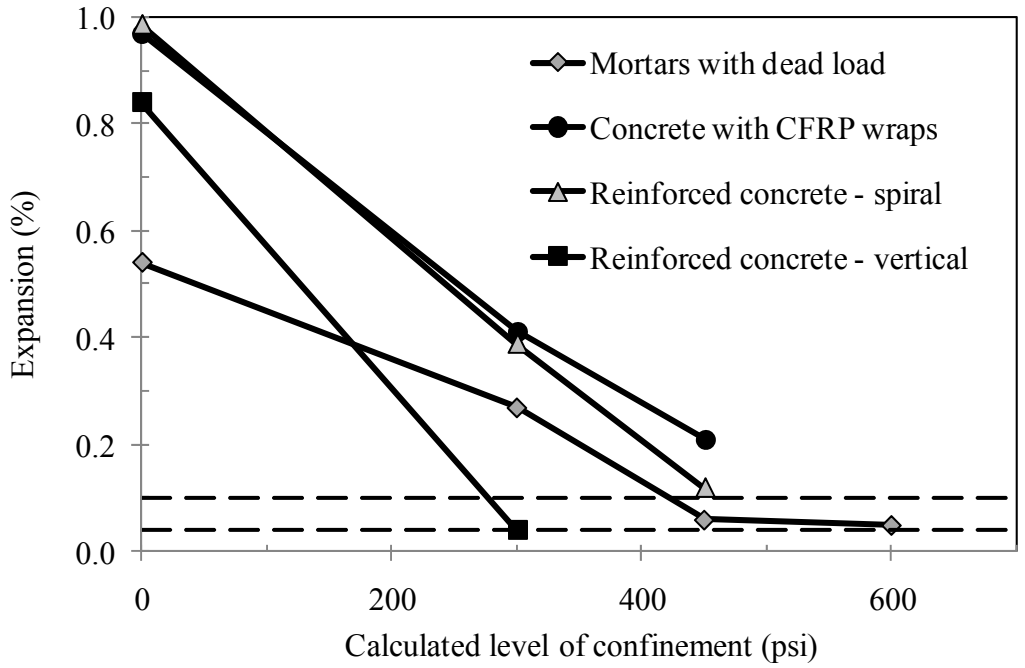

Figure 7.10: Effect of Confinement on the Absolute Expansion Measured on Heat-Treated Mortars and Concretes

Based on the work performed at UNB, recommendations for further research include the following:

- Improve the Hoek cell set up to minimize the loss of confining pressure during test
- Repeat tests with CFRP using larger columns and varying the number of wraps. The columns should be fully restrained in the axial direction. Instrument the wraps to determine strain directly and verify stress-strain relationship for the composite material when fabricated in the same manner as it is for a wrap. For example the CFRP could be laid up using a varying number of layers on a flat surface with a bond breaker between the CFRP and the surface, and coupons could be cut from the cured material to determine σ-ε relationships for different numbers of layers.
- Repeat tests on reinforced columns using larger columns and varying amounts of reinforcement. The steel should be strain gauged using materials that can survive the heat-curing process.

Chapter 8. Conclusion

This research project has focused on various aspects related to structures affected by ASR and/or DEF. Much of the research performed under this project has already been disseminated through various publications and technical memos, including perhaps the most important product of this research – a protocol for evaluating materials-related distress, which is already being used by various research groups and practitioners in Texas and throughout the United States. This specific report focused on a key point of emphasis of this project – specifically an attempt to quantify stresses and strains generated by DEF and an attempt to shed some light on the levels of confinement needed to suppress DEF-induced strains in field elements. To this end, this project has been quite successful. Through a variety of different approaches (steel fiber-reinforced concrete, Hoek cells, oedometers, FRP wraps, etc.), the researchers have been able to provide estimates for the levels of confinement needed to control DEF (see Chapter 7, in particular for a synopsis). The general conclusion is that although DEF can lead to significant levels of expansion, it appears to be possible and feasible to confine DEF in affected structures, and interestingly, the levels of confinement tend to be on the order of those needed to confine ASR, or even less. In separate, TxDOT-funded research, it has also been shown that it is actually easier to suppress DEF than ASR when drying out concrete through the use of sealers/coatings (DEF can be suppressed at relative humidities below 90 percent, whereas ASR may require relative humidities as low as 80 percent to reduce expansion). Of course, a great deal more work is needed on this topic, and this project was just one of several past and ongoing studies evaluating the structural effects of DEF (and/or ASR for that matter). It is hoped that this study, coupled with the other efforts, will provide TxDOT with guidance on how best to manage structures affected by ASR and/or DEF.

References

Thomas, M.D.A., Folliard, K.J., Drimalas, T., and Ramlochan, T., (2008) "Diagnosing Delayed Ettringite Formation in Concrete Structures," *Cement and Concrete Research*, Volume 38, Issue 6, June 2008, pp. 841-847.

Folliard, K.J., Barborak, R., Drimalas, T., Du, L., Garber, S., Ideker, J., Ley, T., Williams, S., Juenger, M., Thomas, M.D.A., and Fournier, B., "Preventing ASR/DEF in New Concrete: Final Report," The University of Texas at Austin, Center for Transportation Research (CTR), CTR 4085-5, 2006.

Taylor, H.F.W., Famy, C., Scrivener, K.L., 'Delayed Ettringite Formation,' *Cement and Concrete Research,* 31, 2001, pp. 683-693.

Diamond, S., 'Delayed Ettringite Formation – Processes and Problems,' *Cement and Concrete Composites*, 18, 1996, pp. 205-215.

Riding, K., 'Early Age Concrete Thermal Stress Measurement and Modeling,' Diss. The University of Texas at Austin (2007) Austin, Texas.

Poole, J., 'Modeling Temperature Sensitivity and Heat Evolution of Concrete,' Diss. The University of Texas at Austin (2007) Austin, Texas.

Turanli, L., Shomglin, K., Ostertag, C.P., Monteiro, P.J.M., 'Reduction in Alkali-Silica Expansion due to Steel Microfibers,' *Cement and Concrete Research*, 31, 2001, pp. 825-827.

Multon, S., Toutlemonde, F., 'Effect of Applied Stresses on Alkali-Silica Reaction-Induced Expansions,' *Cement and Concrete Research*, 36, 2006, pp. 912-920.

Sahu, S., Thaulow, N., 'Delayed Ettringite Formation in Swedish Concrete Railroad Ties,' *Cement and Concrete Research*, 34, 2004, pp. 1675-1681.

Drimalas, T., 'Laboratory Testing and Investigations of Delayed Ettringite Formation,' Thesis. The University of Texas at Austin (2004) Austin, Texas.

Kapitan, J., 'Structural Assessment of Bridge Piers with Damage Similar to Alkali Silica Reaction and/or Delayed Ettringite Formation,' Thesis. The University of Texas at Austin (2006) Austin, Texas.

ASTM C 1260. 'Standard Test Method for Potential Alkali Reactivity of Aggregates (Mortar-Bar Method),' ASTM International, West Conshohocken, PA, Doc. Date: 8/10/2001.

ASTM C 1293. 'Standard Test Method for Determination of Length Change of Concrete Due to Alkali-Silica Reaction,' ASTM International, West Conshohocken, PA, Doc. Date: 02/10/2001.

Appendix A: Hoek Cell Set Up Procedures

The following procedures outline the steps needed in order to successfully place a concrete specimen in the Hoek Cell and commence testing.

1. Make sure that all components are clean, free of dust, in good condition with no cracks or holes.
2. Make sure to have two rubber gaskets for the top and bottom seal (70 or 90 durometer, 1/8" thick, 6 3/16" O.D., 3 1/2" I.D.)
3. If not already, place the confining sleeve inside the Hoek Cell body.
4. Place the concrete specimen inside the sleeve within the Hoek Cell. It should be a tight fit, so a RUBBER mallet may be needed to GENTLY hammer the specimen into the sleeve. BE SURE THAT THE BOTTOM OF THE SLEEVE DOES NOT PUSH OUT THE BOTTOM END OF THE HOEK CELL BODY.
5. Apply copper anti-seize lubricant generously to the top and bottom threads of the Hoek Cell body. MAKE SURE TO PERFORM THIS STEP, IF NOT IT WILL BE VERY HARD TO REMOVE THE TOP AND BOTTOM CAPS FROM THE CELL ONCE THE TEST IS COMPLETED.
6. Place a rubber gasket into the cell cap and screw the cap onto the Hoek Cell body. Repeat the procedure for the second cap. This procedure needs a push bar and loading strap to ensure the cell caps are on tight. The push bar will provide a greater moment arm so that the caps may be screwed on with greater force.
7. Place the cell assembly HORIZONTALLY onto an elevated platform to fill the cell with hydraulic oil. MAKE SURE THAT THE CONCRETE CYLINDER IS CENTERED INSIDE THE CELL. MAKE SURE THE AIR OUTLET IS OPEN AND THAT THE OUTLET IS POINTING IN THE UPWARDS DIRECTION. Be sure to fill the confinement space SLOWLY because oil will flow out the air outlet. Upon filling the confinement space with hydraulic oil, screw the air outlet cap back on.
8. Place the cell assembly vertically and with a utility knife cut the excess of the rubber gaskets that is protruding. It is VERY IMPORTANT TO PERFORM THIS STEP because any protrusion of rubber will inhibit a good seal from forming between the rubber sleeve and the loading platens.
9. Place the Hoek Cell assembly inside the loading assembly. Make sure that the Hoek cell assembly is standing vertically inside the cell and is not leaning in any direction.
10. Place the top loading platens into the Hoek Cell assembly and lower the top loading plate onto the cell, DO NOT TIGHTEN THE TOP LOADING PLATE YET.
11. Increase the confining pressure to 100+ psi. The first few days the cell will lose confining pressure until the cell reaches an initial equilibrium. If the cell loses too much pressure, the confining pressure may need to be increased again. This initial pressure will ensure a good seal between the loading platens and the confinement sleeve ensuring no leaks.

12. The axial pressure may now be put on the cell. Tighten the top bolts to achieve the desired pressure as read by the gauges. An initial axial pressure of 400 psi +/- 25 psi should be placed on the cell. This initial pressure should err to the high side, 425 psi, because some initial pressure loss may be observed.
13. With both the axial and confining pressure applied to the cell, turn on the water source that circulates water through the Hoek Cell.
14. The Hoek Cell is now in operation and should be monitored daily for the duration of the test. If the water source needs to be replenished, make sure that the water that is being added to the system has sat in the testing room for at least 48 hours or more prior to circulation.

Appendix B: Custom Molds

The following procedure outlines a method to make custom size mold for cylindrically shaped concrete specimens.

Materials:

Light gauge metal sheet
½" plywood
Hose clamps
Pipe with desired O.D. of concrete cylinder

Equipment:

Angle
Ruler
Markers
Steel Cutting Scissors

1. Calculate the circumference of the desired O.D. of the cylinder. Add an additional 1-2" for overlap when rolling the metal.
2. Mark a square on the metal sheet that measures the length of the desired cylinder +1/2" and width, the circumference of the cylinder +1-2".
3. Cut two circular end caps with the desired O.D. from the plywood sheet.
4. Prepare three hose clamps but make sure they are loose.
5. Put the sheet metal on a flat surface and put the pipe on the sheet.
6. IN ONE SMOOTH MOTION roll the sheet around the pipe and secure the sheet loosely to the pipe with the hose clamps.
7. Place one of the end caps on one side of the rolled mold and make sure it is ¼" into the mold. Move one of the hose clamps over that end and secure it tightly. As you pull out the pipe secure the hose clamps so that they are snug, not tight around the pipe to ensure the correct diameter. The other end cap does not need to be tight due to the fact that the other plywood cap will ensure the proper diameter of the mold.
8. The mold is now ready to use. After concrete has been poured into the mold, place the last end cap on the cylinder and secure it tightly with the third hose clamp. If the concrete is to be heat treated silicone may be used to ensure no moisture is lost.